Technical Report No. 24

INDICATORS FOR DROUGHT CHARACTERIZATION ON A GLOBAL SCALE

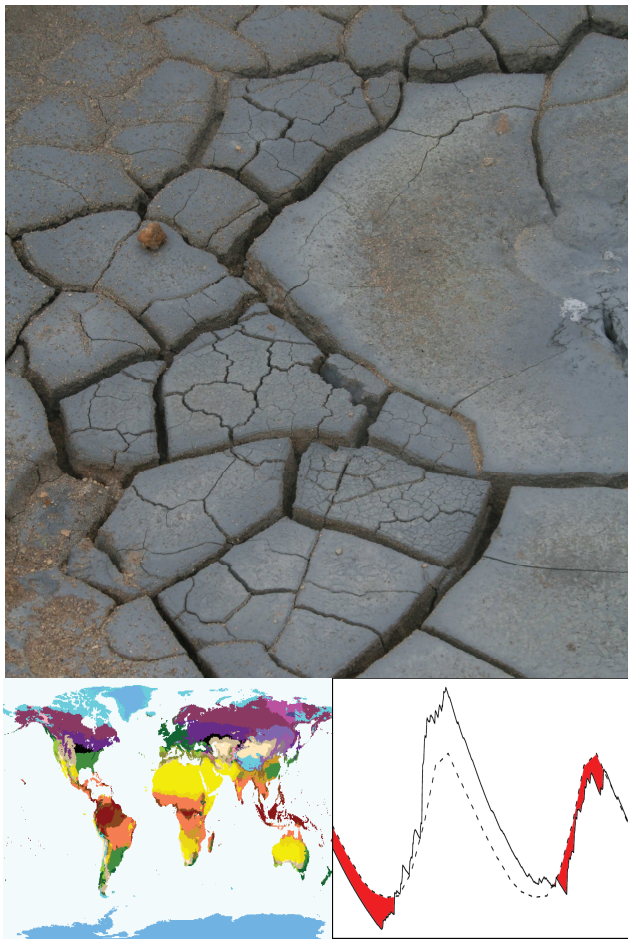

Author names: Niko Wanders, Henny A.J. van Lanen, Anne F. van Loon

Date: 15 October 2010

WATCH is an Integrated Project Funded by the European Commission under the Sixth Framework Programme, Global Change and Ecosystems Thematic Priority Area (contract number: 036946).
The WACH project started 01/02/2007 and will continue for 4 years.

Title:	Indicators for drought characterization on a global scale
Authors:	Niko Wanders, Henny A.J. van Lanen & Anne F. van Loon
Organisations:	Wageningen University - Hydrology and Quantitative Water Management Group (WUR)
Submission date:	15 October 2010
Function:	This report is an output from Work Block 4; Task 4.2.1 Drought and flood indices at different scales
Deliverable	WATCH deliverables D 4.2.1 Report on indices for different type of droughts and floods at different scales.

Preface

This study is based on research done by Niko Wanders for his MSc thesis Hydrology and Quantitative Water Management (HWM-80436) at the Wageningen University, the Netherlands to obtain the MSc degree of Hydrology and Water Quality. He received input from his supervisors Anne F. van Loon and Henny A.J. van Lanen. In the context of his MSc research, the first author participated in the International Workshop on Hydrological Extremes and Large-Scale Data, Oslo (Norway), 15-17 February 2010. He gave a presentation on the revision of the Köppen-Geiger map that has been used to illustrate performance of indicators for various hydroclimatic regions across the world. The visit to Oslo was supported by the EU-FP6 project WATCH (WATer and global Change).

Henny A.J. van Lanen, Wageningen, September 2010.

Abstract

Droughts are caused by a situation with less than normal water availability due to climate variability. They occur in every hydroclimatic region and in all components of the hydrological cycle. Droughts can be classified either as meteorological, soil moisture or hydrological drought. Identification of droughts on a global scale has been done in recent studies. Different drought indicators were used for the identification of droughts on a global scale. However, the effect of the choice for a certain indicator on the drought characterization (e.g. severity, frequency and duration of droughts) is not fully understood, as is the impact of hydroclimate and physical catchment structure. The objective of this study is to examine the characterization of drought with different drought indicators across the world. It also includes the impact of climate and physical catchment structure on the performance of the drought indicators. Time series of meteorological variables were retrieved from or calculated with the WATCH Forcing Data (WFD) at a daily time step, for cells with a resolution of 0.5° by 0.5°. The NUT_DAY model was applied to generate time series of hydrological variables (e.g. soil moisture storage, discharge). NUT_DAY is a synthetic rainfall-runoff model which uses precipitation, temperature and potential evapotranspiration time series from WFD as input. Three different soil types (low, medium and high soil moisture storage capacity) and groundwater systems types (fast, medium and slow responding) have been used in the model simulations, to explore the effect of changes in the physical catchment structure. climatic regions were defined with the Köppen-Geiger classification. For all climatic regions drought analyses were done. Per cell, drought events for each drought indicator were identified by applying the threshold method to the time series of meteorological, soil moisture and hydrological variables. The threshold is either variable or fixed, depending on the indicator. In this study 14 indicators were selected, of which 2 were newly developed (Moving Average Precipitation, Standardized Streamflow Index). All 14 indicators were applied to the 5 major climates; performances were tested and evaluated with expert knowledge mainly from literature. From this 14 indicators finally 6 have been selected, for a more detailed analysis. In total 961 cells were randomly selected for that purpose ensuring that all Köpen-Geiger climate regions are adequately represented. The 6 selected indicators are: the Standardized Precipitation Index (SPI), Effective Drought Index (EDI), Total Storage Deficit Index (TSDI), Moving Average Precipitation with Variable Threshold (MAPVT), Soil moisture with Variable Threshold (SVT), Discharge with Variable Threshold (QVT). These indicators were used to study the effects of hydroclimate and physical catchment structure on drought characterization and subsequently to assess their performance. It was found that the hydroclimate has a profound impact on the average drought durations and deficit volumes as identified by all indicators. The SPI, EDI and MAPVT are not influenced by the physical catchment structure, because they only depend on precipitation. Average drought durations and deficit volumes determined by the TSDI and QVT increase for slower responding groundwater systems. In general, a higher soil water storage capacity increases the average drought durations as identified by the TSDI, SVT and QVT. Overall, the effects of hydroclimate and of properties of the groundwater system are more profound than changes in soil type. The MAPVT and QVT seem to be the most promising indicators for drought analysis on a global scale. Both indicators had a very constant performance for different hydroclimates and physical catchment structures and are rather straight forward to calculate.

Keywords: Drought, Hydrology, Drought indicators, Global scale, Hydroclimate, Physical catchment structure

Contents

List of Figures

List of Tables

1 Introduction

Background

Droughts are caused by situations with temporarily less than normal water availability. They are present in every hydroclimatic region and appear in different components of the hydrological cycle (Wilhite, 2000). One thing all droughts have in common, is that they are caused by a deviation from normal conditions (Tallaksen & van Lanen, 2004). These deviations can be in precipitation, soil moisture, streamflow or groundwater. Droughts can be classified into meteorological, soil moisture and hydrological droughts (Hisdal *et al.*, 2001). Meteorological droughts are characterized by a lack of precipitation, often combined with higher than normal potential evapotranspiration, for a long period of time and over a large area (Tallaksen & van Lanen, 2004). Soil moisture droughts are caused by a deficit in soil moisture created by a high potential evapotranspiration and low precipitation. Hydrological drought can occur in both groundwater and streamflow. Groundwater droughts can be the result of long periods with below average precipitation. While streamflow droughts can be caused by shorter periods with no precipitation, due to the fact that surface runoff or other quick flows can be a large component of the streamflow (Peters *et al.*, 2003). Propagation of drought is a process in which a deficit in precipitation subsequently results in a below normal deficit in soil moisture, groundwater and/or streamflow (Van Lanen *et al.*, 2004). Droughts occur in all hydroclimatic regions and differ in duration, frequency and severity (Stahl & Hisdal, 2004). This makes the intercomparison of droughts on a global scale very difficult. For example, areas in a semi-arid or arid climate often have ephemeral streams with very low or even no discharge for long periods of time (Hisdal *et al.*, 2004), which makes comparison with rivers in humid areas with high discharges difficult (Simmers, 2003; Hisdal *et al.*, 2004). The same is true for rivers in locations where no streamflow is present for the entire or part of the year due to snow accumulation. Research done by Fleig *et al.* (2006); Van Lanen & Tallaksen (2007); Sheffield *et al.* (2009) show the difficulties in using one single drought indicator on global scale. Further research using a wider set of drought indicators on a global scale, could provide more knowledge on the performance of drought indicators. The characterization of droughts for different hydroclimatic regions can be difficult when only a single variable is used (Hisdal *et al.*, 2004). Several studies by Dai *et al.* (2004); Sheffield & Wood (2007); Sheffield *et al.* (2009) tried to identify global droughts based on one variable, namely soil moisture. Problems occurred in defining droughts in arid regions, but overall, results were encouraging. However, the effects of different hydroclimatic conditions on the severity, frequency, and duration of droughts is not fully understood. Moreover, the effect of different physical catchment structures on the drought characteristic is poorly understood. Research done by Van Lanen & Tallaksen (2007) using CRU climate forcing data (Mitchell & Jones, 2005) showed clear differences in drought characteristics between hydroclimatic regions and physical catchment structures. Using a synthetic model they examined the effects of different physical catchment structures (i.e soil types and groundwater systems) on the frequency of droughts in groundwater discharge. However, the study was limited to two different locations in different hydroclimatic regions, one in Guinea (Africa) and one in Missouri (USA). The authors identified two soils: one with high and one with low soil moisture supply capacity. The synthetic model was used for the simulation of a slow and a fast responding groundwater system. The effect of the groundwater system on the frequency and duration of droughts was larger than the effect of different soil types. Additional research by Van Lanen & Tallaksen (2008) following the same procedure for two synthetic catchments in Europe, showed that the groundwater system has large influence on the propagation of droughts through the hydrological cycle and hence on drought characterization. The research on the four locations investigated by Van Lanen & Tallaksen (2007; 2008) showed interesting results, however it needs to be further extended to a more global coverage. Increasing the number of study areas could lead to a better quantification of the impact of climate variability and physical catchment structure on droughts characterization. Only one drought indicator (streamflow) was included in the studies of Van Lanen & Tallaksen (2007; 2008). For a better understanding of droughts on a global scale more drought indicators have to be investigated. Further research is needed to get better insights in the effect of hydroclimatic conditions and physical catchment structures on different types of drought indicators, including how they characterize the severity, frequency, and duration of droughts across the globe.

Objectives

The objective of this study is to examine the characterization of drought using different drought indicators across the world. It includes the impact of climate and physical catchment structure on the performance of the drought indicators.

This leads to the following research questions:

- Which methods are available to characterize different types of drought (e.g. meteorological, soil moisture and hydrological) on a global scale?
- Which method is most suitable for characterizing droughts on a global scale, what are the advantages and disadvantages when used at global scale?
- What is the effect of different hydroclimatic conditions on drought characterization using different drought indicators?
- What is the effect of different physical catchment structures on drought characterization using different drought indicators?
- How large is the combined effect of hydroclimatic conditions and physical catchment structures on drought characterization using different drought indicators?

Outline

First the drought indicators which to our knowledge are currently used in research and operational management are identified. From all these drought indicators, a number have been selected and described in more detailed in Chapter 2. To study the performance of the selected drought indicators, time series of hydrometeorological variables (e.g. precipitation, soil moisture, streamflow) are required from across the globe. The meteorological variables are from a global dataset, whereas the hydrological variables are simulated with a hydrological model. Chapter 3 describes the hydrological model and data used for the analysis of each drought indicator. Chapter 4 explains the effect of major hydroclimatic conditions on the performance of each selected drought indicator (i.e. covering precipitation, soil moisture and hydrological droughts). Based upon this evaluation, a smal selection of promosing indicators is used to study a wider range of climate conditions and the effect of the physical catchment structures (i.e. the response time of the groundwater system and the soil type) (Chapter 5). The report conludes with a discussion (Chapter 6) and conclusions and recommendations (Chapter 7).

2 Review of frequently-used drought indicators

In this chapter a variety of drought indices will be discussed with their advantages and disadvantages for characterization of drought on a global scale. First, indicators which are classified as meteorologic drought indicators are discussed. These indicators use precipitation (rain and snow) data. The second group of indicators is the soil moisture indicators, which use soil moisture observed or simulated soil moisture as input. Hydrological drought indicators use observed or simulated streamflow, groundwater storage or groundwater levels to characterize droughts. The last group are combined drought indicators, which use a combination of precipitation, observerd or simulated soil moisture, streamflow or groundwater storage data.
A full list of indices that were found in literature is included in Annex I. All indicators were assessed, based on climate independency, physical meaning, and the time scale. This assessment led to a first selection of 18 drought indicators. In this Chapter the origin and properties of every indicator are described. The applicability of the indicator and the possibilities for use on a global scale are mentioned as well. Equations and a more detailed description of selected indicators will be presented in Section 3.5.

2.1 Meteorological drought indicators

Meteorological drought indicators use precipitation (rain and snow) data to determine meteorological droughts. Indicators which use precipitation in combination with observed or simulated soil moisture content are also often classified as meteorological drought index (Hisdal *et al.*, 2004). However, in this research they are classified as soil moisture drought indicators, because of the use of soil moisture which is not according to the definition of a meterological drought indicator. Meteorological indicators can be used for drought analysis, without the need for the physical properties of the site. A challenge for all indicators based on precipitation is the high variety in temporal and spatial distribution of precipitation (Steinemann *et al.*, 2005). To deal with this problem, often monthly values or moving average values are taken. The most common meteorological drought indicators are described in this section. Equations and a more detailed description of a selection of indicators can be found in Section 3.5.

Rainfall deciles

The theory of rainfall deciles was first introduced by Gibbs & Maher (1967). Monthly aggregated data of precipitation (rain and snow) are compared with average values extracted from long term observations. The method uses precipitation deciles, which are created with ranked observed precipitation. A site will be drought affected when the precipitation is below the 90% percentile for 3 months in a row (Kinninmonth *et al.*, 2000). The site will no longer be drought affected when the precipitation of the past 3 months is above the 80% percentile or in previous month is above the 40% percentile (Keyantash & Dracup, 2002). The rainfall decile method is used by the Australian Drought Watch System, because it is easy to calculate and requires less data than many other indices (Hayes, 1999). Downside of this method is the need for long-term time series of meteorological data. Keyantash & Dracup (2002) also indicate that the rainfall deciles method may be less suited for climates with a strong seasonality or (very) dry climates in which the 90% is exceeded by large numbers of zero values.

Standardized Precipitation Index

The Standardized Precipitation Index (SPI) was developed by McKee *et al.* (1993). The SPI calculation is done with monthly precipitation, which is fitted to a two parameter gamma probability distribution. This distribution is then transformed into a normal distribution (Hayes, 1999; Redmond, 2000; Keyantash & Dracup, 2002; Naresh Kumar *et al.*, 2009). The equations of the SPI will be discussed in Section 3.5.1. The SPI is designed to quantify the precipitation deficits for multiple timescales (Keyantash & Dracup, 2002). McKee *et al.* (1993) suggest to calculate the SPI for 3-, 6-, 12-, 24-, and 48 month time scales. The longer timescale are sometimes used as an approximation of streamflow and groundwater droughts (Hayes, 1999). Because of the normalized distribution, wetter and drier climates can be represented and compared in the same way. A disadvantage of the SPI is the need for a long time series of observed data, and the possibility of trends in precipitation during this period (Hayes, 1999). In the United Kingdom

the University College London[1], uses the SPI to create monthly maps for drought monitoring on a global scale. The National Drought Mitigation Centre[2] in the United States has daily updates of the SPI for the United States. SPI has gained importance in recent years as a potential drought indicator and is being used more frequently for assessment of drought intensity in many countries (e.g United States, Korea, and Australia) as mentioned by Vincente-Serrano *et al.* (2004); Wilhite *et al.* (2005); Wu *et al.* (2006). The World Meteorological Organization (2009) has indicated that the SPI is the best suitable indicator for meteorological droughts.

Cumulative Precipitation Anomaly

The Cumulative Precipitation Anomaly (CPA) measures the shortage of precipitation compared to the long-term mean (Hayes, 1999; Keyantash & Dracup, 2002; Hayes, 2007). The CPA was first suggested by Foley (1957) as the precipitation anomaly. Later, the cumulative function was preferred because the effect of several months in a row with below average precipitation could be assessed (Keyantash & Dracup, 2002). The timescale of this method is not fixed and can vary from monthly to annual precipitation. A disadvantage of the CPA is that the mean precipitation is often not the same as the median. Using the mean, indicates a normal distribution, while precipitation is often not normal distributed (Hayes, 2007). Another disadvantage is that the begin of a dry spell is not clearly indicated. Therefore the drought initiation time is usually the point when the precipitation anomaly is declining. The CPA is used as an additional index to indicate drought situations (Willeke *et al.*, 1994).

Effective Drought Index

A method to calculate drought on a daily time scale is the Effective Drought Index (EDI). It was developed by Byun & Wilhite (1999) to calculate daily water accumulation with a weighting function of time passage. The equations to calculate the EDI can be found in Section 3.5.1. Daily rain,- and snowfall data from time series of 30 years or more are used for the calculation of the EDI. These long series are needed to transform the EDI values into a reliable normal distribution (Kim *et al.*, 2009). Most drought indices have their limitations because they are based on a monthly time step (Byun & Wilhite, 1999; Kim *et al.*, 2009), while the EDI has a daily time step. The EDI is a standardized index, which makes it possible to compare EDI's from different climatic regions. The use of the EDI has been tested in several drought studies (Byun & Wilhite, 1999; Smakhtin & Hughes, 2007; Kim *et al.*, 2009).

Number of consecutive dry days

The number of consecutive dry days is defined as the maximum number of consecutive dry days, with no measurable precipitation during a year (Deni & Jemain, 2009). This method gives one number for every year, which indicates the relative dryness of the location in that year, which can be compared with historic values for a drought assessment. Therefore, long-term records are needed to have an estimate of the range of values that can be expected (Mekis & Vincent, 2005). The method can also be used as the number of consecutive dry days until the current moment. The number of consecutive dry days method is used by the National Drought Mitigation Center of the United States. The method is also applied in research on climate changes, as a measure for changes in precipitation patterns (Deni & Jemain, 2009).

Rainfall Anomaly Index

The Rainfall Anomaly Index (RAI) was developed by Van Rooy (1965). The RAI is calculated on weekly, monthly or annual time scale. The choice of time scale is done based on the distribution of precipitation. In areas with long dry periods a larger time scale is used, than in areas with (very) short dry periods. The average precipitation of a week, month, or year is used to calculate relative drought. Ranking is done based on the 10 most extreme drought events of the long term records (Oladipo, 1985; Keyantash & Dracup, 2002). Oladipo (1985) has compared the RAI with the PDSI (Section 2.2) and found no major differences in the results.

[1] http://drought.mssl.ucl.ac.uk/
[2] http://drought.unl.edu/monitor/monitor.htm

2.2 Soil moisture drought indicators

Soil moisture drought indicators use observed or simulated soil moisture data, to indicate drought situations. Based on the amount of water stored in the unsaturated zone this indicator calculates drought situations. When observed soil moisture values are not available soil moisture can be simulated using soil water or hydrological models. For both simulated and observed soil moisture the soil moisture drought indicators focus on the abnormalities in soil moisture values with respect to the season and location. Precipitation is not directly taken into account for the drought analysis. A subset of soil moisture indicators presented in this section will be used for further analysis in this study. More details about these selected indicators can be found in Section 3.5.

Palmer drought severity index

The Palmer Drought Severity Index (PDSI) was developed by Palmer (1965) to provide a index based on drought severity, that allowed the comparison of droughts with different time and spatial scales. Palmer (1965) based his index on the supply-on-demand concept of the water balance. The PDSI takes into account precipitation, evapotranspiration, and soil moisture, although it is still classified by many authors as a meteorological drought indicator. For instance in the United States the PDSI is regarded the most prominent index for meteorological drought (Alley, 1984; Hayes, 1999; Keyantash & Dracup, 2002; Wells *et al.*, 2004). The PDSI is based on a generic two-layer soil model. For both layers soil moisture storage is calculated based on observed meteorological conditions. In this research the PDSI is considered a soil moisture drought indicator, because of the simulated soil moisture content. Several limitations of the PDSI have been reported by Alley (1984). The most important limitation is, that the beginning and end of a drought or wet spell are not clearly defined and only based on Palmer's study (Palmer, 1965). The two-layer approach is a simplification and may not be a accurate representation of the actual situation (Hayes, 1999). In colder climates, accumulation of snow and frozen ground are not represented by the index (Dai *et al.*, 2004).
The PDSI is used for drought research on a global scale in studies done by Dai *et al.* (2004); Sheffield & Wood (2007); Sheffield *et al.* (2009). In the United States the National Climatic Data Center has maps from 1895 till present of monthly PDSI values (National Drought Mitigation Centre, 2009).

Palmer Z-index

The Palmer Moisture Anomaly Z-index (Z-index) is used for the calculation of soil moisture droughts. The Z-index is derived from the calculation of the PDSI (Section 2.2). The soil moisture anomaly for the current month is calculated as the Z-index (Keyantash & Dracup, 2002). The Z-index suffers from the same advantages and disadvantages as the PDSI. The methods differ in the fact that the Z-index is time independent, while the PDSI is. Therefore the Z-index responds faster to changes in soil moisture values. The Z-index has been used for global scale drought analysis by Dai *et al.* (2004) and was recommended over the PDSI for drought analysis by Karl (1986).

Soil Moisture Deficit Index

The Soil Moisture Deficit Index (SMDI) has recently been developed by Narasimhan & Srinivasan (2005). They developed a drought index, which could detect short-term dry conditions, has no dependency on the season, and which has no reference to a climate region. The SMDI is used for the calculation of agricultural droughts and is used on a weekly time scale. The only variable used in the SMDI is the simulated or observed soil moisture content. Narasimhan & Srinivasan (2005) compared the SMDI with the SPI and PDSI. They found a high correlation between these three methods and state that the SMDI is a good indicator for the calculation of soil moisture droughts. The SMDI was originally developed for catchments in Texas (United States). However, no studies have been done on the use of the SMDI in other study areas or on a global scale.

Crop Moisture Index

The Crop Moisture Index (CMI) was developed by Palmer (1968) as a meteorological-driven drought indicator. The CMI monitors short-term soil moisture changes in observed or simulated data, and is

classified as a soil moisture drought indicator. The sum of the precipitation excess (with respect to normal conditions) and soil moisture infiltration are used for the calculation of the CMI on a weekly time scale. Because the focus is on soil moisture conditions, the CMI is classified as a soil moisture drought indicator, instead of a meteorological drought indicator.
One of the advantages of the CMI is that it is very suitable for the prediction of short-term droughts (Keyantash & Dracup, 2002; Hayes, 2007). However, it applicability for the prediction of long-term drought is very low (Hayes, 1999). Because the CMI can only be used in the growing season, it is not suitable for winter drought prediction (e.g. Van Loon *et al.* (2010)). However, it is more suited for summer drought predication than the related Palmer Z-index (Karl, 1986).

Soil Moisture Content

The soil moisture content can be used as a indicator for soil moisture droughts (Tallaksen & van Lanen, 2004). When soil moisture content is below a predefined threshold the site is in a drought. The threshold method (Section 3.4) can also be applied to soil moisture content. Simulated soil moisture content in combination with the threshold approach has been used on a global scale by Dai *et al.* (2004); Sheffield & Wood (2007); Sheffield *et al.* (2009).

2.3 Hydrological drought indicators

Hydrological drought indicators are related to groundwater levels, storage in the saturated zone or streamflow. These indicators use both observed and simulated data. The most common hydrological drought indicators are described in this section. A subset of hydrological indicators presented in this section will be used for further analysis in this study. Equations and more detailed description of a selection of these indicators can be found in Section 3.5.

Surface Water Supply Index

The Surface Water Supply Index (SWSI) was developed by Shafer & Dezman (1982) to deal with accummulation of snow, and the delayed runoff caused by this process. The Palmer indices are not meant for large topographic variations like mountains, and do not account for the accumulation of snow. Therefore the SWSI was developed (Hayes, 2007). The SWSI is suitable for the calculation of hydrological droughts, because incorporates climatologic and hydrological characteristics into a single index value, which has the same classification as the Palmer indices (Shafer & Dezman, 1982). The calculation of exceedance probabilities used in the SWSI, are based on historical data. An advantage is that the SWSI is unique for every catchment, which gives a good drought indication on that scale. However, this will be a disadvantage for interbasin comparison (Hayes, 1999) or drought analysis on a global scale. Only the weighting factors in the calculation of the SWSI, can be used as method for interbasin comparison (Garen, 1992).

Palmer Hydrological Drought Index

The Palmer Hydrological Drought Index (PHDI) has been developed by Palmer (1965). The PHDI is very similar to the PDSI, and is derived as an additional term of the PDSI calculation (Soul, 1992; Keyantash & Dracup, 2002; Cutore *et al.*, 2009). The PHDI is a method to calculate hydrological droughts based on precipitation and evaporation (Heim, 2002; Weber & Nkemdirim, 1998). The PHDI depends more on the value of the previous time step than the PDSI. This makes it more suitable for the calculation of hydrological droughts since they often have more memory (Weber & Nkemdirim, 1998). This is similar to the SPI for 24,- or 36-months (Section 2.1), where a longer memory was used for the simulation of soil moisture or hydrological droughts.

Groundwater Resource Index

For the calculation of groundwater droughts, the Groundwater Resource Index (GRI) can be used. This index, developed by Mendicino *et al.* (2008), was tested in Calabria, Italy. The GRI is based on a normal distribution of the simulated groundwater storage in at a site. Since the GRI is a very new drought indicator, the performance of the GRI has only been tested by Mendicino *et al.* (2008) with 40-years of

simulated data. The simulated data were generated by a hydrological model which used: precipitation, air temperature, and air pressure data as driving force. They compared the GRI with the SPI of 6-, 12-, and 24-months. They found that the GRI was a better indicator for droughts in the Mediterranean area than the SPI.

Base Flow Index

The Base Flow Index (BFI) was proposed by the Institute of Hydrology (1980) for a low flow study in the United Kingdom and is calculated on a daily time step. A large disadvantage of the BFI is that the base flow that need to separated from the total flow. The separation of base flow is full of difficulties (e.g. Peters & van Lanen (2005)). The BFI has not been used in drought analysis on a global scale. The BFI is closely related to other hydrological drought indices and therefore it is often used as a additional index for estimating droughts (Hisdal *et al.*, 2004).

Storage content

The amount of stored water in a hydrological system can be used as an indicator for hydrological droughts. Low recharge will cause lower storage, which will cause lower discharges (Peters *et al.*, 2003). This theory holds for systems which respond more or less like a linear reservoir, where discharge is directly related to the storage in the system. Droughts in storage can be determined with the threshold approach (Section 3.4).

Total Storage Deficit Index

The Total Storage Deficit Index (TSDI) was developed by Yirdaw *et al.* (2008) for drought characterization in the Canadian Prairie. In their study, they combined the TDSI with water storage anomalies from Gravity Recovery And Climate Experiment (GRACE) satellite observations and streamflow measurements. A study of Agboma *et al.* (2009) used the TSDI in combination with the Variable Infiltration Capacity (VIC) model. The TSDI uses precipitation, evapotranspiration, and discharge from the basin outlet. The anomalies in total amount of water stored in the catchment are an indicator for drought. Since, no further research has been done on the TSDI, only the experiences results from Yirdaw *et al.* (2008) and Agboma *et al.* (2009) are available. So far, the TSDI is not used on a global scale.

Discharge

The discharge can be used as a indicator for hydrological droughts (Tallaksen & van Lanen, 2004). When discharge is below a predefined threshold the site is in a drought. The possibilities to use discharge for drought drought analysis on a global scale are currently studied by Van Lanen *et al.* (2010a).

2.4 Combined drought indicator

A combined drought indicator uses a combination of precipitation, soil moisture, storage, or discharge. Therefore, it cannot be defined as meteorological, soil moisture or hydrological drought indicator. This indicator have the potential that it can describe the drought over the entire hydrological cycle with one index (Keyantash & Dracup, 2004).

Aggregate Drought Index

The Aggregate Drought Index (ADI) has been developed by Keyantash & Dracup (2004) and was tested in California, United States. The ADI considers all types of drought: meteorological, soil moisture, and hydrological droughts. The ADI consist of six different variables; one of the variables, snow can be excluded when it is not relevant for the selected climate type. The ADI performance was assessed for three different climates in California by Keyantash & Dracup (2004). A large advantage of the ADI is the integration of various types of droughts. A disadvantage is the need for observations of all five or six variables (depending on the snow). More detailed information about this indicator can be found in Section 3.5.

3 Material and methods

This chapter starts with a description of the data, models and techniques used for the assessment of the drought indicators on a global scale. Figure 3.1 gives a general overview of the methods used in this research. A synthetic hydrological model is applied to generate time series of hydrometeorological variables (Section 3.1). A global dataset is used as meteorological forcing data (Section 3.2). The Köpen-Geiger climate classification system will be applied to the global dataset with meteorological forcing data to find locations across the world with a specific climate type (Section 3.3). The threshold approach (Section 3.4) is used to classify the outcome from the selection of drought indicators, and to develop drought indicators (i.e. droughts in precipitation, soil moisture, discharge). In the previous chapter a number of drought indicators have been described. A subset of potential useful indicators has been identified and will be further described in Section 3.5. The performance of the selected drought indicators will be calculated using the time series of hydrometeorological variables, either from the global meteorological dataset or the outcome from the synthetic model.

3.1 Synthetic model

The program NUT_DAY that combines a soil water balance module and a simple conceptual hydrological module, was developed by Van Lanen *et al.* (1996) and is used in studies by Van Lanen & Tallaksen (2007; 2008). The basic set-up is given in this section, as well as some specific details used in the calculation with NUT_DAY for this research. A full description of the latest model version is given by Van Lanen *et al.* (2010b). The model is used for the simulation of time series of soil moisture content, actual evapotranspiration, and recharge for different locations across the globe. The calculations of NUT_DAY are done on a daily time step. A water balance equation is used in the calculation of NUT_DAY, which can be written as:

$$S(t) = S(t-1) - Q_{out}(t) + R_{ch}(t) \tag{1}$$

$$SS(t) = SS(t-1) + P_{ra}(t) + Q_{sm}(t) - ET_a(t) - R_{ch}(t) \tag{2}$$

$$S_{sn}(t) = S_{sn}(t-1) + P_{sn}(t) - Q_{sm}(t) \tag{3}$$

where S, SS and S_{sn} are respectively the storage in the groundwater, the soil and the snowpack (in mm). Q_{out} is the outflow from the groundwater and R_{ch} is the recharge from the soil into the groundwater. Precipitation can either fall as rain (P_{ra}) or snow (P_{sn}). Snow that melts (Q_{sm}) will enter the soil. Water disappears out of the soil through actual evapotranspiration (ET_a). All fluxes are given in $mm\ d^{-1}$, and calculations are done for a daily time step.
The hydrological module of NUT_DAY is simulated like an linear reservoir. The storage in the reservoir determinates the rate of outflow (Q_{out}). This outflow rate is defined by:

$$Q_{out}(t) = Q_{out}(t-1) * e^{-1/j} + R_{ch}(t) * (1 - e^{-1/j}) \tag{4}$$

which is the original de Zeeuw-Helling equation (Ritzema, 1994) and where j is descriped as:

$$j = \frac{\pi^2 * kD}{\mu * L^2} \tag{5}$$

where kD is the transmissivity (in $m^2 d{-}1$), μ is the storage coefficient and L is the distance between streams (in m).

3.1.1 Precipitation

The synthetic model is fed by meteorological variables from a global dataset (Section 3.2). The precipitation is divided in snow and rain following the concept of the HBV snow routine (Seibert, 2005), which is incorporated into NUT_DAY. For a given precipitation, HBV calculates, whether this precipitation will be snow or rain based on the temperature. Snow accumulation is handled by the same snow routine of HBV. The melt of snow starts when mean daily temperature is above a certain Threshold Temperature (TT). The rate of snow melt depends on variable $CFMAX$. Other parameters are, snowfall correction factor $SFCF$, water holding capacity CWH, and the refreezing coefficient CFR. Default values for all

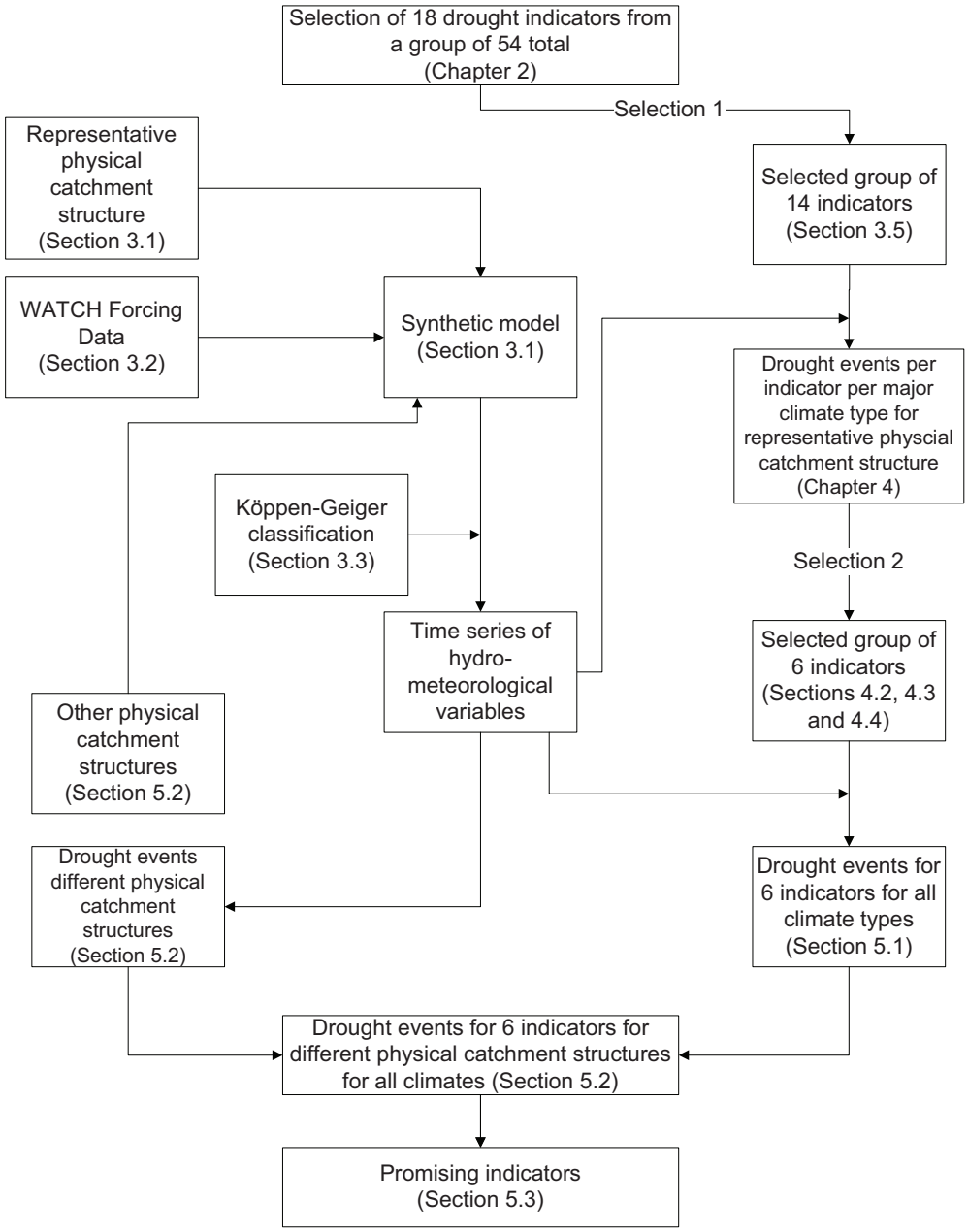

Figure 3.1: Research approach.

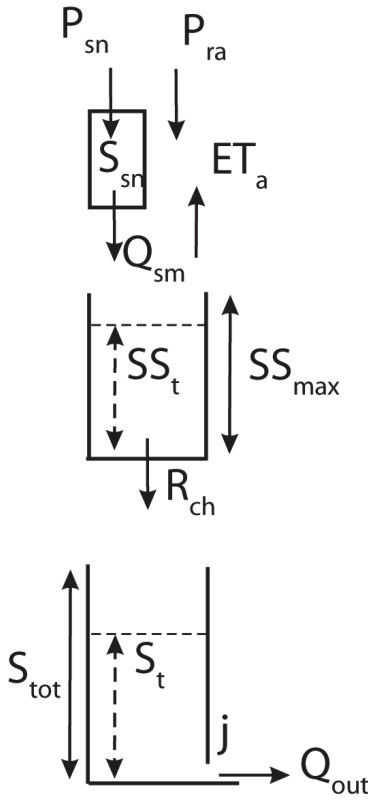

Figure 3.2: The model structure of the NUT_DAY model. The top reservoir is used to simulate the snowpack. The middle reservoir is used for the simulation of soil moisture, were precipitation (P) can enter either directly (P_{ra}) or via snow melt (P_{sn}). The bottom reservoir simulates the groundwater, were recharge (R_{ch}) can enter via the soil moisture and discharge (Q_{out}) can leave the groundwater.

snow parameter can be found in Table 3.1 as well as the range and units for all snow parameter used in NUT_DAY. The default values are the values that were used to run the model for average conditions.

Table 3.1: Snow parameter from NUT_DAY: default values and ranges.

Parameter	Description	Default value	Min	Max	Unit
TT	Threshold temperature	0.0	-1.5	2.5	$°C$
$CFMAX$	Degree-day factor	2.5	1	10	$mm°C^{-1}d{-}1$
$SFCF$	Snowfall correction factor	0.8	0.4	1.2	-
CWH	Water holding capacity	0.1	0.0	0.2	-
CFR	Refreezing coefficient	0.05	0.0	0.1	-

3.1.2 Soil properties

Soils used in the NUT_DAY program are from the Staring series (Wösten *et al.*, 2001), which is used as a standard series in the Netherlands for the description of top,- and subsoils. In the Staring series, soil moisture rentention curves, saturated and unsaturated conductivities are given for a series of 18 top,- and subsoils. The volumetric water contents from the moisture retention curves and the thickness of the topsoil and subsoil are used by NUT_DAY to calculate the total amount of moisture available in the soil. The amount of soil moisture is calculated for field capacity, the point where reduction in the potential evapotranspiration occurs (critical point) due to water stress and the point where actual evapotranspiration is zero and vegetation severly suffers (wilting point), are also calculated with the Staring properties. The values of field capacity, critical point and wilting point are related to the pF

curve values of 2.0, 3.0, and 4.2, respectively. In this research 3 different soil types are used: coarse

Table 3.2: Soil moisture supply capacity for the used soils.

Soil type	Field capacity (mm)	Critical point (mm)	Wilting point (mm)
Coarse sand	36.6	8.2	4.7
Light silty loam	168.9	95.2	43.5
Sandy loam	178.3	83.8	23.5

sand, light silty loam, and sandy loam. The soil moisture supply capacity for these soils can be found in Table 3.2. These are calculated for a topsoil of 30 cm and a subsoil of 20 cm. This results in a rooting depth of 50 cm, which is representative for grass.

3.1.3 Linear reservoir

In NUT_DAY a linear reservoir approach according to De Zeeuw-Hellinga equation (Ritzema, 1994), is included to simulate discharge (Section 3.1). Outflow from the linear reservoir is determined by the j-factor, which is more in detail explained by Van Lanen *et al.* (2010b). The higher the j-factor, the slower water will disappear from the groundwater system. Values for j used in this research are 100, 250, and 1000 days.

3.1.4 Bypass

In situations with high precipitation, bypass flow can occur in the model. In clay the phenomena of bypass flow is very common (Van Stiphout *et al.*, 1987). The bypass is adjusted to the unsaturated conductivity of the specific soil used in NUT_DAY. It was assumed that the infiltration rate of precipitation into the soil cannot be higher than the unsaturated hydraulic conductivity at field capacity (k_{fc}) . When the precipitation is larger than k_{fc} the excess will go through the bypass directly to the linear reservoir of the model. The bypass will only be active when soil moisture is below critical point, otherwise it is assumed that all precipitation infiltrates into the soil, or go directly to the linear reservoir because the soil is at field capacity. A more detailed description of this process can be found in Van Lanen *et al.* (2010b).

3.2 The WATCH Forcing Data

The WATCH Forcing Data (WFD) were used as input data for the synthetic model (Section 3.1). The WFD are a major deliverable of the EC-FP6 WATCH project[3]. A full description of the WFD can be found in Weedon *et al.* (2010). For the synthetic model 3 meteorological variables are needed, namely precipitation (total of rain and snow), temperature, and potential evapotranspiration. In the WFD two different precipitation datasets are available, CRU TS 2.1 (Mitchell & Jones, 2005) and GPCC v4 (Rudolf & Schneider, 2005; Schneider *et al.*, 2008; Fuchs, 2008). Both separated precipitation in rain and snow. The synthetic model uses total precipitation as input. The HBV approach is later applied to separate it in snow and rain (Section 3.1) The GPCC v4 data is preferred over the CRU data because of the higher number of observations used in the GPCC v4 dataset (Weedon *et al.*, 2010). Therefore, GPCC precipitation is used in this research. The resolution of GPCC v4 is 0.5° by 0.5° with a temporal resolution of one month. The CRU TS 2.1 dataset (Mitchell & Jones, 2005) is used in the WFD for the temperature values with the same spatial en temporal resolution as the GPCC. In the WFD the ERA-40 reanalysis dataset (Uppala *et al.*, 2005) has been used to calculate daily values for all variables. The daily values are bias-corrected on a monthly base with the CRU (temperature) and GPCC (precipitation) datasets. Potential evapotranspiration is not provided in the WFD and therefore has to be calculated. The calculation of the reference evapotranspiration is done with the Penman-Monteith equation (Allen *et al.*, 2006). The reference evaporation (ET_0) was calculated with:

$$ET_0 = \frac{0.408 * \Delta(R_n - G) + \gamma \frac{900}{T+273.15} u_2 (e_s - e_a)}{\Delta + \gamma(1 + 0.34 u_2)} \quad (6)$$

[3]www.eu-watch.org

where ET_0 is the reference evapotranspiration ($mm\ d^{-1}$), R_n is net radiation at the surface ($MJm^{-2}\ d^{-1}$), G is the soil heat flux density ($MJ\ m^{-2}\ d^{-1}$), T is the mean daily temperature at 2 m height ($^{\circ}C$), u_2 is the wind speed at 2 m height ($m\ s^{-1}$), e_s is the saturation vapour pressure (kPa), $e_s - e_a$ is the saturation vapour pressure deficit (kPa), e_a is the actual vapour pressure (kPa), Δ is the slope vapour pressure curve ($kPa\ ^{\circ}C^{-1}$), and γ is the psychrometric constant ($kPa\ ^{\circ}C^{-1}$). All variables in the Penman-Monteith equation were either extracted from the WFD or calculated from variables provided through the WFD. The variables needed are the mean daily temperature (T), and maximum and minimum temperature (T_{min} and T_{max}). T_{min} and T_{max} are used to calculated the saturated vapour pressure (e_s) with:

$$e^0(T) = 0.6108exp\left[\frac{17.27T}{T + 237.3}\right] \tag{7}$$

$$e_s = \frac{e^0(T_{max}) + e^0(T_{min})}{2} \tag{8}$$

where $e^0(T_{max})$ and $e^0(T_{min})$ are first calculated using equation 7, before e_s is calculated. e_s can also be calculated using T, which results in a lower estimation of e_s that causes an underestimation of the reference evapotranspiration (Allen *et al.*, 2006).
The actual vapour pressure (e_a) is calculated with q, the specific humidity (kg/kg) with:

$$e_a = \frac{q * P}{\epsilon} \quad \text{from Stull (2000)} \tag{9}$$

where ϵ is the ratio molecular weigth of water vapour/dry air which is equal to 0.62 and P the pressure in kPa. Net Radiation is calculated with short wave and net long wave radiation, both are provided through in the WFD. The soil heat flux density G is assumed to be zero because it is very small compared to net solar radiation R_n (Allen *et al.*, 2006). It was assumed that the potential evapotranspiration equals the reference evapotranspiration (ET_0), which is a fair approach for grass.

3.3 Köppen-Geiger classification

Performance of drought indicators will be investigated for different climate types of the world. The Köppen-Geiger classification system has been chosen for this study, because it is still the most frequently used climate classification (Kottek *et al.*, 2006). The application of this climate classification on the WATCH Forcing Data (WFD) enables the possibility to indentify locations in a particular climate type. The first Köppen classification was made by Köppen (1900) and updated by Geiger (1954; 1961). Based on different vegetation types, Köppen distinguished five different major climate types and compiled a global map. The world is distributed in the equatorial zone (A), the arid zone (B), the warm temperature zone (C), the snow zone (D), and the polar zone (E). The major climate types are subdivided into subtypes based on precipitation regime and air temperature. This results in a classification system of 31 different climate subtypes. The original maps of Köppen and Geiger were based on observations, which led to unequal spatial observation density. Peel *et al.* (2007) used the Global Historical Climatology Network version 2.0 (GHCN) dataset (Peterson & Vose, 1997) to make a revised Köppen-Geiger map of the world. The availability of data in the GHCN is much higher than when Geiger made the update of the Köppen-Geiger map of the world. A resolution of 0.1° by 0.1° was used to get a detailed global map. Since global datasets of precipitation and temperature have become available through interpolation of observations, digital versions of the original Köppen-Geiger maps are made by Kottek *et al.* (2006); Rubel & Kottek (2010). These maps have a 0.5° by 0.5° resolution and are available on a global scale. The difference between the study of Peel *et al.* (2007) and Kottek *et al.* (2006) is the interpolation of data. While, Kottek *et al.* (2006) relied on the interpolation of the CRU TS 2.1 (Mitchell & Jones, 2005) and GPCC (Rudolf & Schneider, 2005; Schneider *et al.*, 2008; Fuchs, 2008) dataset. Peel *et al.* (2007) made their map based on his own interpolation from the GHCN dataset. The Köppen-Geiger climate type can be determined for every location on the globe using one of these or both maps.
In this study a global map of the Köpen-Geiger climate classification has been made with the WFD. This was done to be able to compare location in the study based on climate type. To determine the climate of a certain location on the globe, minimally 30-year time series have to be used (World Meteorological Organization, 2010). From these time series, monthly values for precipitation and temperature have

to be calculated. For the identification of a climate type for a certain location, first the precipitation threshold (P_{th}) in mm has to be calculated with:

$$P_{th} = \begin{cases} 2 * T_{ann} & \text{if} > 66\ \% \text{ of precipitation occurs in winter} \\ 2 * T_{ann} + 28 & \text{if} > 66\ \% \text{ of precipitation occurs in summer} \\ 2 * T_{ann} + 14 & \text{otherwise} \end{cases} \quad (10)$$

where T_{ann} is the mean annual temperature in $°C$. The determination of B climates has to be done first, because they are only based on the value of P_{th}, followed by the determination of the E climates because they only depend on temperature conditions. When first other major climate types are determined, a B or a E climate can be wrongly classified because they match the requirements of other major climates as well.
After the major climate type is determined the subtype has to be found. This subtype will add a second letter to the climate. This letter is based on the precipitation regime, except for E climates where this letter is based on temperature. For the B, C, and D climates a third letter is added based on the temperature regime Eventually the procedure which in total results in 31 climate types. The full list of available subtypes and conditions can be found in Table 3.3. In this study, the Köppen-Geiger map of climate types across of the whole world was determined by using 44 years of WATCH Forcing Data (WFD). The map from Kottek *et al.* (2006) was not suitable since the WFD has used a different precipitation dataset (Weedon *et al.*, 2010). For a proper identification of the climate type and a consistent use of the true series of meteorological data for a selected location a new map had to be made based on WFD. The map (Annex II) was used in this study to select the different locations and its associated climate.

3.4 The threshold method

Time series of meteorological and hydrological variables are retrieved from the synthetic model (Section 3.1). These time series are used to calculate drought indicator performance and applied the threshold approach. The threshold method or truncation level method originates from the theory of runs developed by Yevjevich (1967) and has been widely used since (Smakhtin, 2001). With the threshold method, different drought characteristics can be determined (e.g duration and deficit volume) (Tallaksen *et al.*, 1997; Hisdal *et al.*, 2004; Fleig *et al.*, 2006; Tallaksen *et al.*, 2009). The method is based on a threshold, when streamflow or another hydrometeorological variable is below this threshold it is considered a drought situation (Dracup *et al.*, 1980; Hisdal *et al.*, 2004). The threshold can be a fixed threshold (FT) for the whole simulation periode, or a variable threshold (VT), which varies during the year for every season, month or day (Fleig *et al.*, 2006). The choice for a fixed or variable threshold is dependent on the purpose of the research. The threshold method can also be applied to precipitation, soil moisture content, and groundwater levels, but was originally developed for discharge. To calculate the threshold, first all observed data are sorted from low to high. For drought determination the highest x percent is taken, as a normal or wet situation, everything below x percent will be a drought situation. The percentage that is chosen for x depends on the purpose and location of the study. In arid and semi-arid conditions x can be as high as 50%, while normal values of x are between 70% and 95% (Hisdal *et al.*, 2004).
The threshold can be determined based on data from complete time series, which is done for a FT. When a monthly VT is applied, observations for every month are combined and sorted separately, before the lowest x percent is determined for that month. When the moving average of the monthly VT is taken with linear interpolation, a VT can be determined. This will result in a daily threshold derived from a 30-day moving monthly threshold. The yearly FT, monthly VT, and VT are presented in Figure 3.3. For all types of threshold a drought is present if observed data are below the threshold,. The severity of a drought can be determined by the calculation of the deficit volume. The higher this volume, the more severe a drought will be. The deficit volume at time t ($D(t)$) can be calculated with:

$$D(t) = \begin{cases} \tau(t) - X(t) & \text{for } X(t) < \tau(t) \\ 0 & \text{for } X(T) \geq \tau(t) \end{cases} \quad (11)$$

Table 3.3: Description of Köppen-Geiger classification (from Kottek *et al.* (2006)).

1st	2nd	3rd	Decription	Criteria
A			**Equatorial climates**	$T_{Mmin} \geq 18°C$
	f		Rainforest, fully humid	$P_{min} \geq 60$ mm
	m		Monsoon	$P_{ann} \geq 25(100 - P_{min})$
	s		Savannah with dry summer	$P_{min} < 60$ mm in summer
	w		Savannah with dry winter	$P_{min} < 60$ mm in winter
B			**Arid climates**	$P_{ann} < 10P_{th}$
	S		Steppe climate	$P_{ann} > 5P_{th}$
	W		Desert climate	$P_{ann} \leq 5P_{th}$
		h	Hot	$T_{ann} \geq 18°C$
		k	Cold	$T_{ann} < 18°C$
C			**Warm temperate climates**	$-3°C < T_{Mmin} < 18°C$
	s		Dry summer	$P_{smin} < P_{wmin}, P_{wmax} > 3P_{smin}$, and $P_{smin} < 40$ mm
	w		Dry winter	$P_{wmin} < P_{smin}$ and $P_{smax} > 10P_{wmin}$
	f		Fully humid	Not Cs or Cw
		a	Hot summer	$T_{Mmax} \geq 22°C$
		b	Warm summer	Not a and at least 4 months $T_{mon} \geq 10°C$
		c	Cool summer and cold winter	Not a or b and $T_{Mmin} > -38°C$
D			**Snow climates**	$T_{Mmin} \leq -3°C$
	s		Dry summer	$P_{smin} < P_{wmin}, P_{wmax} > 3P_{smin}$, and $P_{smin} < 40$ mm
	w		Dry winter	$P_{wmin} < P_{smin}$ and $P_{smax} > 10P_{wmin}$
	f		Fully humid	Not Ds or Dw
		a	Hot summer	$T_{Mmax} \geq 22°C$
		b	Warm summer	Not a and at least 4 months $T_{mon} \geq 10°C$
		c	Cool summer and cold winter	Not a or b and $T_{Mmin} > -38°C$
		d	Extremely continental	Not a or b and $T_{Mmin} \leq -38°C$
E			**Polar climates**	$T_{Mmax} \leq 10°C$
	T		Tundra climate	$0°C \leq T_{Mmax} < 10°C$
	F		Frost climate	$T_{Mmax} < 0°C$

P_{min}	Minimum monthly precipitation	P_{ann}	Mean annual precipitation	P_{smin}	Minimum summer precipitation
P_{wmin}	Minimum winter precipitation	P_{smax}	Maximum summer precipitation	P_{wmax}	Maximum winter precipitation
T_{Mmin}	Minimum monthly temperature	T_{Mmax}	Maximum monthly temperature	T_{mon}	Monthly temperature

Winter is October till March on Northern Hemisphere and April till September on the Southern hemisphere

Summer is April till September on Northern Hemisphere and October till March on the Southern hemisphere

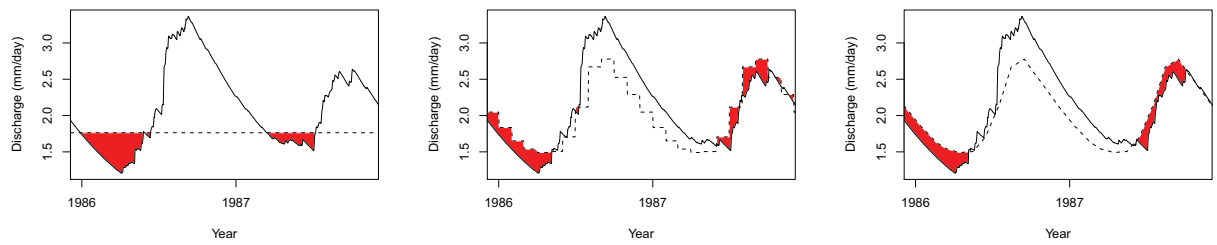

Figure 3.3: One discharge serie (solid line) for a fixed threshold(left), a monthly variable threshold(middle, and a variable threshold (right). The dashed line is the threshold level with in where the red color indicates, drought deficit volume.

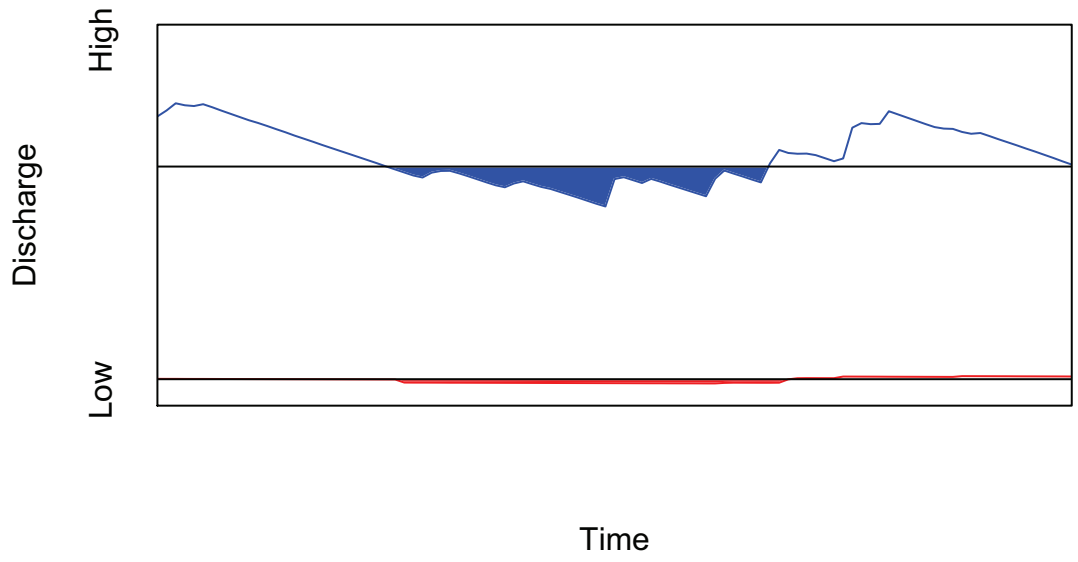

Figure 3.4: Discharge with a fixed threshold for two drought events in different catchments. Durations are identical, deficit volumes are completly different.

where $\tau(t)$ is the threshold, $X(t)$ is the value of variable X, which can be precipitation, soil moisture content or discharge. The deficit volume for a drought event is calculated with:

$$D_j = \sum_{t=S_j}^{L_j} D(t) \tag{12}$$

where j is the drought event, S_j is the value of t at which drought event j begins, L_j is the length of the drought, and D_j the deficit volume of the drought. The deficit volumes of precipitation and discharge have a physical meaning. For precipitation and the discharge, the deficit volume equals the accumulated shortage of water during the drought. To compensate for the water shortage created during the drought event, the same amount of water should be replenished. Another number to indicate the severity of a drought is intensity. The intensity of each drought event (I_j) is calculated with:

$$I_j = \frac{D_j}{L_j}. \tag{13}$$

For precipitation and discharge, the intensity indicates the average flux (in $mm\ d^{-1}$) below the threshold. For the soil moisture content, the intensity is the average soil moisture content below the threshold. Intercomparison of droughts based on deficit volume is very difficult since indicator performance is not the same for different catchements (Van Lanen, 2010, pers. communication). In Figure 3.4 discharge with a fixed threshold is depicted for two different catchments. In both catchments a drought event is present with completely different drought deficit volumes. However, drought durations for both events are equal. Although these durations are equal the drought in the lower catchment (red line) will have a smaller deficit volume than the drought present in the upper catchment (blue line). The threshold of the upper catchment is much higher, which will result in higher deficit volumes. The very low threshold of the lower catchment, will result in very low deficit volumes, although drought may be very severe for this catchments. When both catchments are compared based only on deficit volumes, the drought in the upper catchments would be more sever. If the comparison would be done based on drought duration, these droughts would be of equal severity. Deficit volumes are used in this study as on of the drought characteristic, analysis of this characteristic should be done with some precaution.
To deal with drought ev ents that are interdependent, different pooling methods have been tested by Fleig *et al.* (2006). The Moving-Average procedure is used with a fixed threshold. With this procedure, small

peaks above the threshold are removed by using the running average of the previous n-days (Tallaksen *et al.*, 1997).

3.5 Selected drought indicators

In this section a more detailed description of selected indicators from Chapter 2 is given, including equations to calculate the performance of each indicator and its classification (e.g. duration of droughts, severity of droughts, distinction of drought categories). The indicators were selected based on their strengths and weaknesses (Section 2) in combination with hydrological expert knowledge. Also two new indicators are introduced, which likely will overcome some weak points of other methods. The Moving Average precipitation (Section 3.5.1) uses a moving average to overcome difficulties in zero values of precipitation data. The standardized streamflow index (Section 3.5.3) uses a normalized gamma distribution to have a better estimation of low flows and is based on the same theory as the standardized precipitation index (Section 3.5.1). Fruthermore the SPI (Section 2.1) has been modified for use on a daily time step (Section 3.5.1).

3.5.1 Meteorological drought indicators

The Standardized Precipitation Index

For the calculation of the Standardized Precipitation Index (SPI),(Section 2.1), long-term records of precipitation are needed. Guttman (1999) recommends to use at least 50 years of data for drought periods of 1 year or less, and more for multi-year droughts. However, other studies by Hayes (2006) and Naresh Kumar *et al.* (2009) used shorter periods of 39-, and 30-years, respectively. These long-term records (X) are converted into log-normal values after zero values have been removed, to calculate the statistic U with:

$$U = ln(\overline{X}) - \frac{\sum ln(X)}{N} \tag{14}$$

where N is the number of observations. The statistic U is then used for the calculation of two shape parameters (α and β) of the gamma distribution with :

$$\alpha = \frac{\overline{X}}{\beta} \quad \beta = \frac{1 + \sqrt{1 + \frac{4U}{3}}}{4U} \tag{15}$$

. These shape parameters are then implemented in the basic equation of the gamma distribution:

$$G(x) = \frac{\int_0^x x^{a-1} e^{\frac{-x}{\beta}} dx}{\beta^{\alpha} \Gamma(\alpha)} \tag{16}$$

To account for the zero-values of precipitation in the long-term records a new cumulative probability function is introduced:

$$H(x) = q + (1 - q)\, G(x) \tag{17}$$

where q is the percentage of zero-values. This new probability function is transformed into a standard normal random variable with mean zero and variance of one. Methods for this transformation can be found in Edwards & McKee (1997) and Naresh Kumar *et al.* (2009). The created random variable is the value of the SPI. For this research the SPI for 1-month is used as an indicator, to insure that the SPI performs like a precipitation drought indicator. For longer timescales the SPI will perform more like a soil moisture drought indicators (McKee *et al.*, 1993). In this research, the SPI is supposed to be a precipitation drought indicator.
If on a particular location in the world a particular month of the year is dry almost every year (e.g 90% of the years) the gamma distribution fitted through this point is not representative. Therefore, the estimated α and β parameter are discarded and the SPI is set to zero (normal conditions) by the program used in this study. This results in shorter drought periods, while in reality a few months with precipitation occur which would have interrupted a long drought.
Positive SPI values indicate greater than median precipitation, while negative values of the SPI indicate

Table 3.4: Drought categories for the SPI.

SPI value	Drought category
0 to -0.99	Normal conditions
-1.00 to -1.49	Moderate drought
-1.5 to -1.99	Severe drought
-2.00 or less	Extreme drought

below median precipitation. Because of the normal distribution of the SPI, values lie within one standard deviation at approximately 68% of the time, within two standard deviations 95% of the time and within three standard deviations 98% of the time. Therefore, McKee *et al.* (1993) proposed the drought classification as described in Table 3.4. This original classification will not be used in this research.

Daily SPI

The daily SPI is developed in this study to overcome the difficulties with the standard SPI using only monthly values. SPI values are calculated for every single day based on a moving monthly time frame (i.e. 30-day backwards moving average). The parameters α and β are estimated for each day are based on the previous 30 days with equation 15. With these α and β SPI values can be calculated for each day separately using equations 16 and 17. Since values at the end of the month are equal to the monthly SPI values which are calculated at the last day of the month, the differences between the monthly SPI and daily SPI are large. Therefore, it is justified to use a daily SPI instead of the monthly SPI.

Effective Drought Index

The Effective Drought Index (EDI) is calculated based on Effective Precipitation (EP) data (Section 2.1), considering the loss of precipitation due to evaporation and runoff. Byun & Wilhite (1999) explored different equations for the EP. They suggest:

$$EP_i = \sum_{i}^{n=1} \left[(\sum_{n}^{m=1} P_m)/n \right] \tag{18}$$

where i as the number of days of the time window, n running from 1 till i and P_m denotes the precipitation of m days ago in $mm\ d^{-1}$. This equation is most appropriate, assuming that runoff is highest immediately after rainfall (Lee, 1998; Shim *et al.*, 1998). The next step in the calculation of the EDI is:

$$EDI = \frac{EP_i - \mu}{\sigma} \tag{19}$$

where μ is the mean of effective precipitation, which is subtracted from the EP and divided by σ, the standard deviation of the EP. The value of i is often set at as 365, because the is this most dominant precipitation cycle worldwide (Byun & Wilhite, 1999). Higher or lower values of i indicate precipitation cycles which are longer or shorter in time, respectively.
The classification of the EDI has been done by Smakhtin & Hughes (2007) and is identical to the classification of the SPI (Table 3.4).

Consecutive Dry Days

The number of Consecutive Dry Days (CDD) is the number of dry days between two wet days (Section 2.1). This is calculated with:

$$C(n) = \sum_{n-L}^{n} 1 \tag{20}$$

where $C(n)$ is the number of consecutive dry days and L is the last wet day. At the first day of the time series ($n = 0$), L is supposed to be 0.
The number of consecutive dry days is calculated for every day of the year. The x percentile is calculated for the time series and applied as threshold. If the number of consecutive dry days is above this threshold

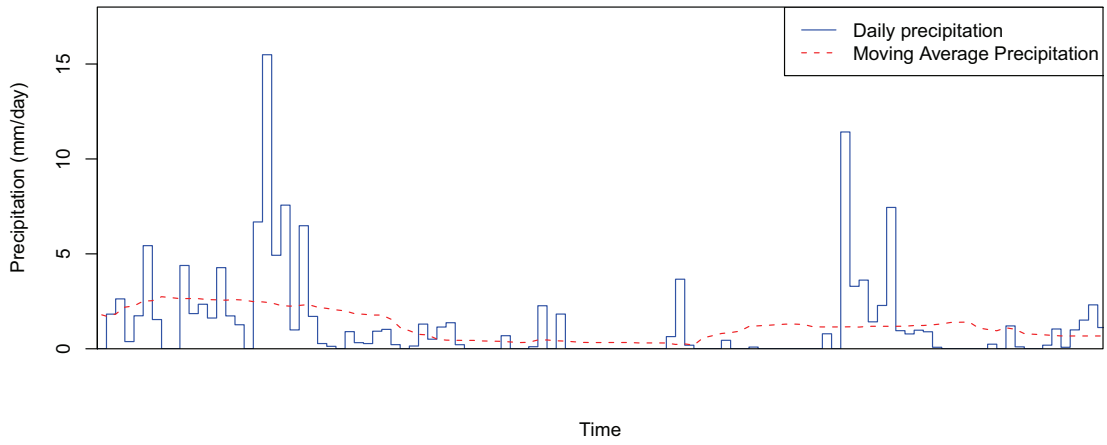

Figure 3.5: Example of daily and 30-day moving average precipitation.

a drought occurs. The higher the number of consecutive dry days, the more severe a drought will be. No classification is known for this method.

Moving Average Precipitation with a Variable Threshold

The Moving Average Precipiation with a Variable Threshold (MAPVT) is newly developed drought indicator in this study. For precipitation, a method is developed to overcome a large number of dry days. By taking the n-days moving average of a precipitation time series, zero values in the time series are largely replaced and cause less problems. When n is 30 days, the centered moving average of the current day will be calculated for -14 to + 15 days. This 30-day averaging leads to an approximation of the monthly precipitation. However, with this method still daily values are used
This Moving Average Precipitation with a Variable Threshold (MAPVT),(Section 3.4) is used as meteorological drought indicator. The MAPVT is calculated in two steps and it is based only on precipitation data. The Moving Average Precipitation (MAP) is calculated with:

$$MAP(t) = \sum_{t-s/2+1}^{t+s/2} P(t) \tag{21}$$

where $P(t)$ is the precipitation in $mm\ d^{-1}$ on a particular day t, and s is the number of days used for the moving average. In this study, s is set at 30 days.
The MAP cannot be calculated for the first $s/2+1$ days, as well as the last $s/2$ days. After the calculation of MAP, a variable threshold is applied to obtain the MAPVT (Section 3.4).

3.5.2 Soil moisture drought indicators

Palmer Drought Severity Index

The calculation of the Palmer Drought Severity Index (PDSI),(Section 2.2) uses a soil water balance with a monthly time step (Alley, 1984; Karl, 1986). The PDSI uses a two-layer soil model with two important assumptions. The first assumption is that the first layer contains 25 mm of soil moisture storage, whereas the soil moisture storage of the second layer can be adjusted to the location based on the soil characteristics. The second assumption is that all water in the first layer is used before the second layer will start to loose water (Alley, 1984; Weber & Nkemdirim, 1998).

Table 3.5: Drought categories for the PDSI.

PDSI value	Drought category
1.49 to -1.49	Near normal
-1.50 to -2.99	Mild to moderate drought
-3.00 to -3.99	Severe drought
-4.00 or less	Extreme drought

The second step is the calculation of four monthly varying climate dependent coefficients:

$$\begin{aligned} \alpha_j &= \overline{ETa_j}/\overline{ET0_j} \quad \beta_j = \overline{R_j}/\overline{PR_j} \\ \gamma_j &= \overline{RO_j}/\overline{PRO_j} \quad \delta_j = \overline{L_j}/\overline{PL_j} \end{aligned} \tag{22}$$

where j is the number of the specific month of the year. ETa, $ET0$, R, PR, RO, PRO, L and PL are the actual evapotranspiration, potential evapotranspiration, recharge, potential recharge, run-off, potential run-off, loss and potential loss, respectively, all in mm per month. Detailed information about the calculation of the coefficients can be found in Alley (1984); Weber & Nkemdirim (1998); Cutore *et al.* (2009). Next, the differences (d) between the actual precipitation and the Climatically Appropriate For Existing Conditions ($CAFEC$), are calculated using:

$$d_i = P_i - (\alpha_j + \beta_j PR + \gamma_j PRO + \delta_j PL) \tag{23}$$

where P_i is precipitation in mm of the month i and $(\alpha_j + \beta_j PR + \gamma_j PRO + \delta_j PL)$ is the $CAFEC$ in mm. The Z-index is calculated with:

$$Z_i = d\frac{17.67K'_i}{\sum_{j=1}^{12}\overline{D_j}K'_j} \tag{24}$$

where D_j is the absolute value of all d_i values for each month i, K'_i is:

$$K'_i = 1.5log_{10}\left(\frac{\frac{\overline{ET0_i}+\overline{R_i}+\overline{RO_i}}{\overline{P_i}+\overline{L_i}} + 2.8}{\overline{D_j}}\right) + 0.5 \tag{25}$$

Finally the PDSI is calculated for each time step i with:

$$X_i = 0.897X_{i-1} + \left(\frac{1}{3}\right)Z_i \tag{26}$$

with X_i is the PDSI value of the current month.
Theoretically the values for the PDSI can vary between +10 and -10 (Dai *et al.*, 2004). However, values normally are between +4 and -4. Where +4 indicates extremely wet and -4 extremely dry conditions (Alley, 1984; Hayes, 1999). The dry part of the of the PDSI classification, can be found in Table 3.5.

Palmer Z-index

The Palmer Z-index (Section 2.2) is an intermediate term of the PDSI (equation 24) and represents the moisture anomaly of the current month. The Z-index reacts quickly to changes in soil moisture values without a time delay as the PDSI (Karl, 1986).

Soil Moisture Deficit Index

The Soil Moisture Deficit Index (SMDI),(Section 2.2), needs a water balance model or observed soil moisture data for the calculation of available soil moisture (Niemeijer, 2008). Long- term records of soil moisture for every week (j) of the year are required for the estimation of the median, minimum and maximum available soil moisture (Narasimhan & Srinivasan, 2005). Using the long-term median (MSW_j), minimum ($minSW_j$), and maximum ($maxSW_j$) available soil moisture ($SW_{i,j}$ in mm), weekly

values (i) for the soil moisture deficit ($SD_{i,j}$) are calculated using the following equations:

$$SD_{i,j} = \frac{SW_{i,j} - MSW_j}{MSW_j - minSW_j} * 100 \quad if\ SW_{i,j} \leq MSW_j$$
$$SD_{i,j} = \frac{SW_{i,j} - MSW_j}{maxSW_j - MSW_j} * 100 \quad if\ SW_{i,j} > MSW_j \tag{27}$$

where $SD_{i,j}$ is the soil water deficit (%) and $SW_{i,j}$ the weekly soil water availability in mm (Narasimhan & Srinivasan, 2005). SD values can vary from -100 to +100%, representing very dry or very wet conditions, respectively. The PDSI is used as a tool for comparison with the SMDI, therefore the SMDI is transformed in the same classification as the PDSI. The results is that the SMDI for any week (i) is given by:

$$SMDI_1 = \frac{SD_1}{50} \qquad \text{Initial value}$$
$$SMDI_i = 0.5 SMDI_{i-1} + \frac{SD_i}{50} \tag{28}$$

Since the values of SD are dimensionless, comparison between different climate regions is possible as well (Narasimhan & Srinivasan, 2005).

Soil moisture content with a Variable Threshold

The Soil moisture content with a Variable Threshold (SVT)(Section 2.2) as a soil moisture drought indicator. To calculate the SVT, a variable threshold (Section 3.4) is applied to the soil moisture content of a particular day (S_i).

Accumulated snow and soil moisture content

The Accumulated Snow and Soil Moisture content (ASSM) is newly developed in this study. The ASSM is calculated with:

$$ASSM_i = AS_i + SM_i \tag{29}$$

where i is the day, AS_i the accumulated snow (in mm) and SM_i the soil moisture content (in mm). Do identify drought the threshold (Section 3.4) is applied in the same manner as done for the Soil moisture content with a Variable Threshold (Section 3.5.2).

3.5.3 Hydrological drought indicators

Groundwater Resource Index

The Groundwater Resource Indec (GRI) is based on four components of the water balance, namely precipiation, evapotranspiration, changes in soil moisture, and groundwater storage (Section 2.3). For the calculation of soil moisture storage and groundwater storage, a water balance model is needed. From the model, only the groundwater retention is used as variable in the calculation of the GRI. The GRI is defined as:

$$GRI_{i,j} = \frac{D_{i,j} - \mu_{D,j}}{\sigma_{D,y}} \tag{30}$$

where $GRI_{d,y}$ is value of the GRI at day i in year j and D is the groundwater retention of the same day. $\mu_{D,j}$ and $\sigma_{D,j}$ respectively are the mean and standard deviation of D for day d. For the calculation of $\mu_{D,j}$ and $\sigma_{D,j}$, long term records of 30 year are recommended by Mendicino *et al.* (2008).
Since there has been no classification for the GRI, the classification of the SPI is used. The same classification can be applied to both methods, because of the normal distribution of both the SPI and GRI.

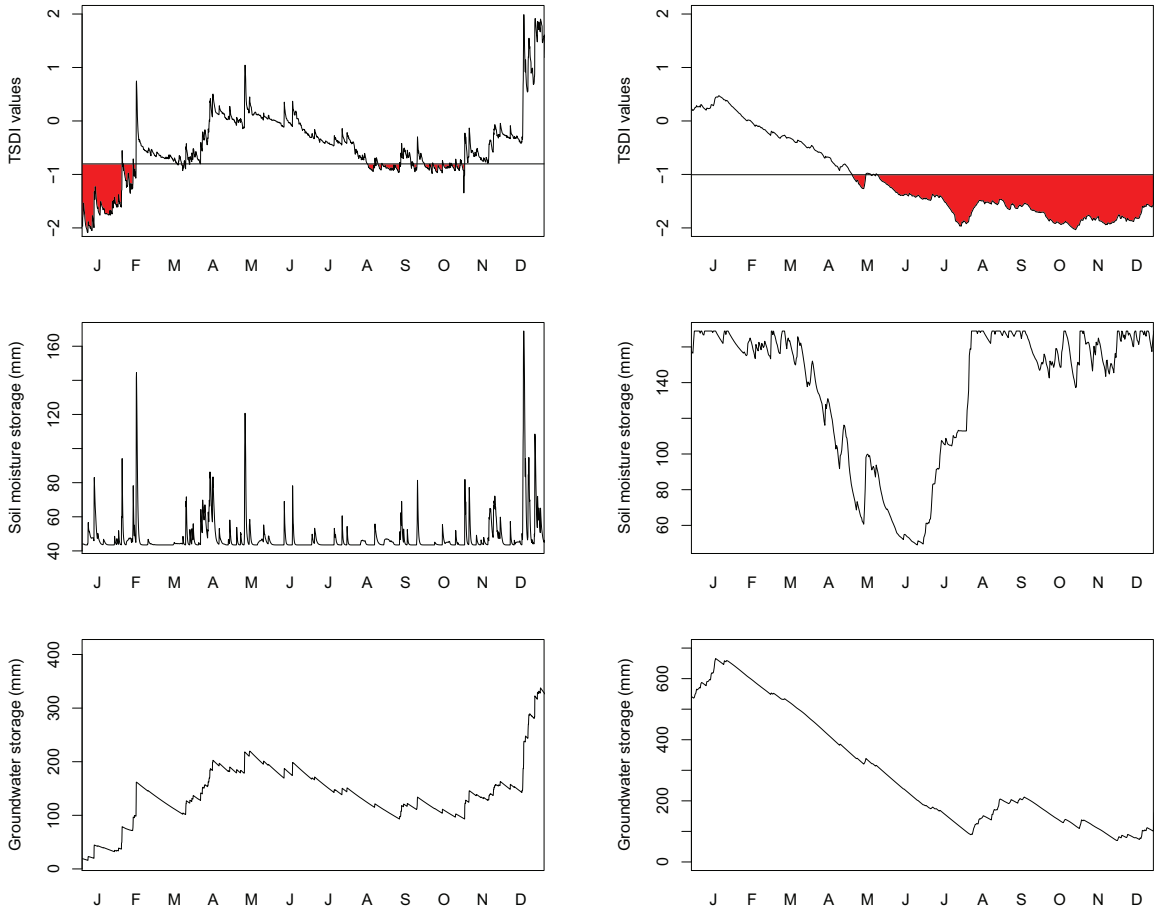

Figure 3.6: Performance of the Total Storage Deficit Index (TSDI) for a selected year (1995). Left, fluctuating TSDI values for an location with low recharge. Right, more constant TSDI values for a location with high recharge. The horizontal line is a representation of the threshold, the deficit volumes are indicated in red. Both storage components of which the TSDI is composed are given in the lower figures. Left, the soil moisture and storage values for the low recharge situation, Right, the soil moisture and storage values for the high recharge situation.

Total Storage Deficit Index

The calculation of the Total Storage Deficit Index (TSDI),(Section 2.3) is based on the calculation of the SMDI (Yirdaw *et al.*, 2008). The mean, maximum and minimum for every day (i) of the year (j) and the TSDI are calculated for a daily time step.
First, the Total Storage Deficit ($TSD_{i,j}$) is calculated with:

$$TSD_{i,j} = \frac{TSA_{i,j} - MTSA_j}{MaxTSA_j - MinTSA_j} * 100 \tag{31}$$

where TSA is the total storage (soil moisture and groundwater) at day i of year j. $MTSA_j$, $MaxTSA_j$, and $MinTSA_j$ are the mean, maximum, and minimum of the TSA for that day of the year, respectively. The $TSDI$ is calculated by standardizing the TSD values with:

$$TSDI_i = \frac{TSD_i - \mu}{\sigma} \tag{32}$$

where μ is the average value of TSD and σ is the standard deviation from the mean.
The performance of the TSDI can be like a soil moisture or hydrological drought indicator. This is the result of the combination of both the storage in the unsaturated zone and groundwater, in the calculation of the TSDI. In regions with high precipitation and recharge, the TSDI performs more like a hydrological drought indicator. In these climates the amount of water in the unsaturated zone is small compared to the amount of water in the saturated zone due. In regions with a low precipitation, the performance of the TSDI is more like a soil moisture drought indicator, because soil moisture is more important in these climates (Yirdaw *et al.*, 2008). In Figure 3.6 this difference in performance is shown.

Discharge with a Variable Threshold

The Discharge with a Variable Threshold (QVT),(Section 2.3) is calculated in the same manner as the Soil Moisture content with a Variable Threshold (Section 3.5.2).

Standardized Streamflow Index

The Standardized Streamflow Index (SSI) is based on the same concept as the SPI. The SSI has been newly developed in this study and uses a normalized gamma distribution for the daily discharge.
The SSI is classified as a hydrological drought indicator. The only variable taken into account, is the discharge.
The indicator is developed to have better performance at locations where streamflow is zero for part of the year. When applying the threshold method, all the zero flows can cause difficulties (Simmers, 2003). With the use of the normalized gamma distribution these problems are solved.

3.5.4 Combined drought indicator

Aggregate Drought Index

The Aggregate Drought Index (ADI) is composed of six different variables (Section 2.4). The calculation of the ADI is complicated because of the six different variables. First, a matrix,

$$\mathbf{O}(example) = \begin{bmatrix} 1.34 & 0.54 & 61 & 1.15 & 216 & 0.98 \\ \vdots & \vdots & \vdots & \vdots & \vdots & \vdots \\ 2.32 & 3.56 & 132 & 1.60 & 502 & 0.23 \end{bmatrix} \tag{33}$$

is composed with n by p dimensions, were n is the number of years of data and p the number of variables. For all the data in $\mathbf{O}$, the means are subtracted and every element is divided by the standard deviation, which results in matrix $\mathbf{X}$. Correlations for each variable are calculated from matrix $\mathbf{X}$ to

obtain correlation matrix $\mathbf{R}$:

$$\mathbf{R}(example) = \begin{bmatrix} 1 & -0.68 & 0.4 & 0.32 & 0.38 & -0.27 \\ \vdots & \vdots & \vdots & \vdots & \vdots & \vdots \\ -0.27 & 0.38 & -0.54 & 0.96 & 0.74 & 1 \end{bmatrix} \tag{34}$$

From $\mathbf{R}$ the eigenvector (e_1) is calculated, which is associated with the first eigenvalue. $\mathbf{X}$ and e_1 are multiplied into vector $\mathbf{X}e_1$ for which the standard deviation is calculated. The ADI is then calculated with:

$$ADI = \frac{\mathbf{X}e_1}{\mu} \tag{35}$$

where $\mathbf{X}e_1$ divided by μ, equals the standard deviation.

4 Drought characterization

Drought events identified with the selected indicators are investigated in this chapter for all major climate types (Figure 3.1). The indicators are divided into meteorological, soil moisture, hydrological, and combined drought indicators to obtain a better overview of the individual performance compared to other indicators of the same category. The performance of the indicators in the same category is illustrated for two contrasting climatic regions. The performance of all indicators is provided in Annexes IV, V, VI and VII. Time series of meteorological data are extracted from the WATCH Forcing Data (Section 3.2), while time series of soil moisture and discharge are simulated using NUT_DAY (Section 3.1), which is driven by WATCH Forcing Data. For better understanding, part of time series for every indicator is also included in Annexes IV, V, VI and VII. The simulations with NUT_DAY are done for a representative physical catchment structure which implies a soil with a light silty loam texture (Table 3.2) and a linear reservoir with a j-factor of 250 days (Section 3.1). In this chapter only the differences of indicator performance for the major climates are presented.

4.1 Intercomparison procedure of drought indicators

Each category of indicators is evaluated based on the performance on five locations; one location from each major climate type (Table 4.1). Two are investigated in more detail for each catagory of drought indicators. For the characterization of droughts, methods are needed to discriminate between drought

Table 4.1: Description of locations from major climate types used in intercomparison of drought indicators.

Location	Climate type	Coordinates	Average annual precipitation (mm)	Average annual temperature (°C)	Section
Brasil	Am	N 2°15' W 52°15'	2008	26.6	4.2
New Guinea	Af	S 2°45' E 137°45'	3039	26.7	4.3
Australia	BWh	S 25°45' E 131°15'	292	20.9	4.4
Germany	Cfb	N 51°15' E 7°45'	1186	8.4	4.2 & 4.4
Russia	Dfc	N 63°15' E 67°45'	593	-1.2	4.3
Canada	ET	N 69°45' E -73°45'	313	-14.3	-

and non-drought situations. In addition to applying the threshold method to precipitation (MAPVT), soil moisture (SVT), and discharge(QVT), the threshold method (Section 3.4), is also used for the detection of drought events in all other indicators (Section 3.5). For every indicator either a fixed or variable threshold of 80% (Section 3.4), is used to exclude minor droughts and to focus on major droughts only. The 80% threshold is used for all indicators to ensure that for each indicator a drought occurs in 20% of the time series, which makes comparison between indicators easier since the total drought duration is equal for every indicator. On most indicators a fixed threshold was applied, since they are already compensated for the monthly variations of the climate. Exceptions are the Effective Drought Index (EDI), Moving Average Precipitation with a Variable Threshold (MAPVT), Soil moisture content with a Variable Threshold (SVT), and Discharge with a Variable Threshold (QVT), to which a variable threshold was applied.
Expert knowledge is used for the selection of the most promising drought indicators per category. For each category different criteria apply:

- The drought duration is expected to get longer from meteorological, soil moisture to hydrological drought at a specific location (Peters *et al.*, 2003). Indicators should reflect this. The combined drought indicators should have durations, which are intermediate, because they are composed of all three types of indicators.

- Deficit volumes should increase from meteorological, soil moisture to hydrological drought. Droughts that last longer are likely to result in larger deficit volumes (Peters *et al.*, 2003).

Drought indicators which do not perform according to the above-mentioned criteria are excluded for further research. Drought indicators that perform according to the two expectations are evaluated based on a second set of criteria, namely:

- The temporal resolution of the indicator; a daily scale is preferred over a monthly or yearly.
- Physical meaning of the indicator; if an indicator has a physical meaning it is preferred over dimensionless indicators.
- Calculation time of the indicator; small calculation time are preferred.
- Climate independent; is the performance of the indicator consistent throughout the different climate types.

The intercorrelation between all drought indicators is calculated for every location and included in Annex III. The intercorrelation is expected to be an important tool to assess the agreement between indicators.
After the above-mentioned set of criteria has been applied to the indicators and the intercorrelations are interpreted, a final selection of indicators (Figure 3.1: selection 2) is made for further research (Chapter 5).

4.2 Meteorological drought indicators

The performance of the five different meteorological indicators is investigated in this section. The daily Standardized Precipitation Index (SPI), Effective Drought Index (EDI), Consecutive Dry Days (CDD), Moving Average Precipitation with a Variable Threshold (MAPVT), and the Palmer Drought Severity Index (PDSI) were selected (Section 3.5). The PDSI is also included into this selection, because originally it is classified as a meteorological drought indicator (Section 2.2). To illustrate the outcome for the selected meteorological drought indicators, two locations from different major climate types are used (Table 4.1). The major climate types A and C were chosen from the five climate types as representative locations, the results of all climate types are described in Annex IV. The A-climate has a precipitation regime with a very high seasonality, while the C-climate has a more constant precipitation regime. In both cases, snow and rain are combined into precipitation since none of the meteorological indicators makes a deviation between snow and rainfall (Section 2.1). On the first location (Brasil) more than half of the yearly precipitation (2008 mm) occurs in the period from January till April. On the second location (Germany) precipitation is equally spread throughout the year and the total is 1186 mm per year. More details of both precipitation regimes can be found in Figure 4.1. All five selected meteorological drought

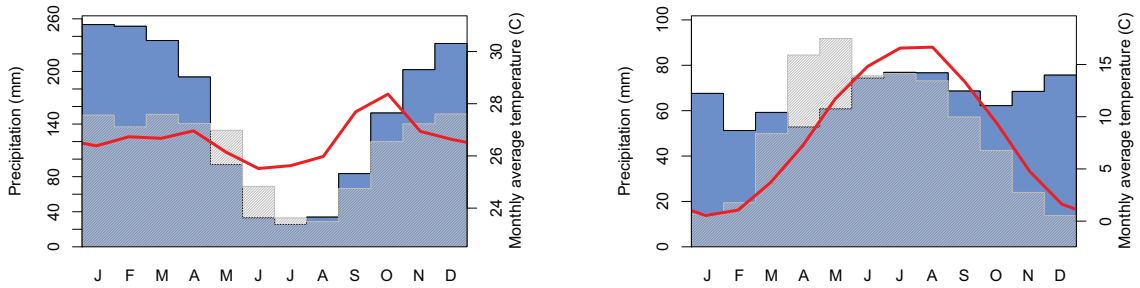

Figure 4.1: Average climate data for the two selected locations; one in Brazil (A-climate, left) and one in Germany (C-climate, right). The red line shows the monthly average temperature. In blue the precipitation is given and in grey the actual evapotranspiration is presented.

indicators were used to select droughts in the period from 1958 to 2002 from the daily time series. The indicators are compared based on number of droughts, average durations and average deficit volumes to get insight in the performance of each indicator. The simulation of the PDSI was done with a soil moisture content of maximum 169 mm (Section 3.5.2). The drought characteristics of each indicator

Table 4.2: Performance of selected meteorological drought indicators for two selected major climate types.

	Brazil			Germany		
Indicator	Number	Average duration (d)	Average deficit	Number	Average duration (d)	Average deficit
SPI	207	15.52	10.37(d)	236	13.61	9.434(d)
EDI	93	33.42	10.12(d)	159	19.82	10.36(d)
CDD	662	21.07	35.64(d^2)	892	14.79	23.93(d^2)
MAPVT	189	16.35	13.46(mm)	226	14.09	8.661(mm)
PDSI	11	287.8	2409(d)	17	186.2	1571(d)

for the selected locations can be found in Table 4.2. The table shows a difference between the drought events in Brazil and Germany. The number of droughts (for every indicator) in Germany is higher than in Brazil, which consequently results in a shorter average duration in Germany. The deficit volumes for each indicator are smaller in the more temperate climate of Germany than in the monsoon climate of Brazil, because of the higher rainfall intensities in Brazil (Figure 3.4). In general, it can be concluded that the droughts in Brazil are smaller in number, but are more severe, when they occur.
The difference between the indicators is very large. There are indicators with a very low number of droughts like the PDSI and indicators with a very high number of droughts like the CDD. The lower number of droughts also results in longer durations and higher deficit volumes for the PDSI than for the other indicators. The SPI, EDI, and MAPVT are all in the intermediate range with an average of $2 - 4$ droughts per year.
From these 5 indicators, a selection was made based on expert knowledge (Section 4.1). Typical to a meteorological drought is the rather short duration (Wilhite, 2000). Due to the incorporation of soil moisture storage in the PDSI, the number of droughts seems too low for a good meteorological indicator. Table III.1(Annex III) also suggest that the PDSI performs more like a hydrological drought indicator. Correlations for this location between the PDSI and hydrological drought indicators are on average 0.8, while the average correlation for meteorological drought indicators is 0.3 (maximum 0.54). On the other hand, the number of droughts in the CDD is too high. A location is already in a drought after two dry days according to the CDD (e.g. Figure IV.1), which does not support the definition of a drought (Chapter 1). In the climate of Germany, while this will not affect the hydrological system in a way that it is called a drought. However, the CDD is more useful in very dry climates, like the B-climates (Table IV). In these locations it is not exceptional to have a long period (a couple of month up to multiple years) without precipitation, and the number of dry days will become much higher than in other climate types. In Germany and Brazil, the 80% threshold value of the CDD is 2 days, while in Australia (B-climate) the computed threshold is placed at 38 rainless days. In these regions with very low precipitation rates, other indicators fail because they are a very large part of the time equal to zero due to the absence of precipiation. Therefore, the CDD is a good method to deal with these (extremely) dry situations (Figure 4.2). However, on a global scale the CDD is not very useful because of the large number of droughts in temperate and wet climates. Correlations for the CDD are mostly negative (Annex III), which is caused by the value of the CDD getting higher, with the continuation of a drought situation.
In summary, the CDD and the PDSI are likely not to be good indicators for meteorological droughts on a global scale. Therefore, the SPI, EDI, and MAPVT were selected for further use (Chapter 5), because their properties agree with the expected properties of a meteorological drought indicator.

4.3 Soil moisture drought indicators

For the intercomparison of the soil moisture drought indicators six indicators were selected (Section 3.5). The Total Storage Deficit Index (TSDI), Soil Moisture Deficit Index (SMDI), Soil moisture with a Variable Threshold (SVT), Accumulated Snow and Moisture Content (ASSM), Palmer Drought Severity Index (PDSI), and Palmer Z-Index (Z-Index) are used as indicators for soil moisture droughts. Intercomparison of different soil moisture drought indicators is done with a location in Papua New Guinea, and a location in Russia (Table 4.1). The first location is at the equator with high precipitation rates

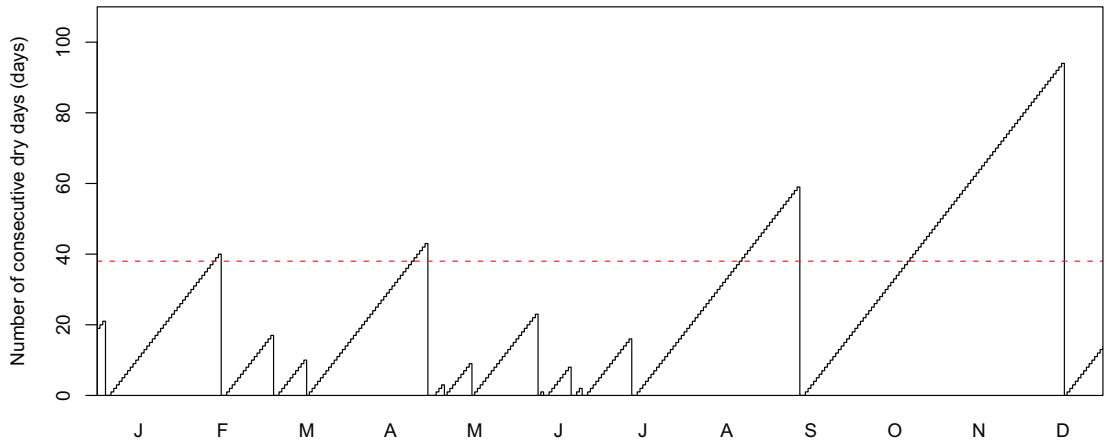

Figure 4.2: The number of Consecutive Dry Days (CDD) for a B-climate in Australie (Table 4.1), for a representative year (1958). The red dotted line gives the threshold.

and soil moisture reaches field capacity after almost every rainfall event. Although evapotranspiration rates are also very high, there is a large precipitation excess which will cause very moist soils. The second location is in a snow-affected climate where soil moisture is not replenished for a large part of the year due to snow accumulation on the surface. A slow depletion of the soil moisture content during the snow period causes low soil moisture content, which is replenished during snow melt in spring or summer. A snow-affected climate is chosen because a large part of the world (48% and 61% if Antarctica is included) is influenced by snow accumulation. Snow accumulation in Russia can be up to 257 mm per year (snow-water equivalent). Long-term monthly averages of precipitation and temperature can be found in Figure 4.3. Simulations for both locations were carried out with NUT_DAY (Section 3.1).

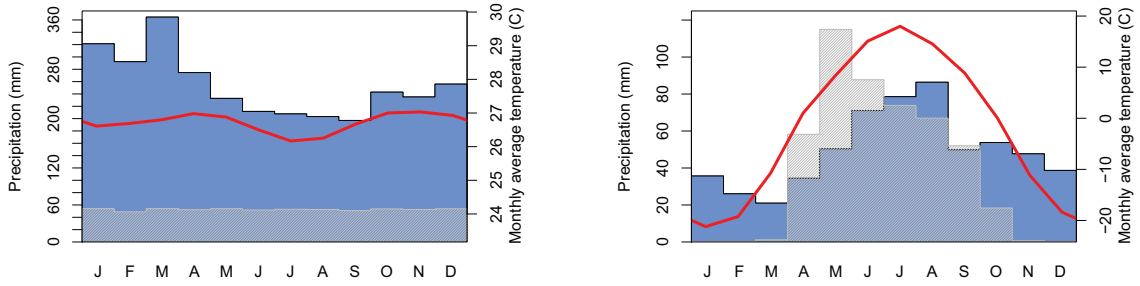

Figure 4.3: Average climate data for the two selected locations; one in Papua New Guinea (A-climate, left) and one in Russia (D-climate, right). The red line shows the monthly average temperature. In blue the precipitation is given, and in grey the actual evapotranspiration is presented.

The simulation of the Z-index and PDSI were done with a soil moisture content of maximum 169 mm (Section 3.5.2). The performance of all indicators for both locations is shown in Table 4.3. The results for all major climate types are given in Annex V. The number of soil moisture drought events has a large variation in Papua New Guinea for the different indicators, while the variation in Russia is much lower. Due to the snow accumulation and snow melt peak, soil moisture content has a more stable yearly cycle in Russia than Papua New Guinea. The average duration of drought events in Russia is longer, which is caused by droughts that already occur before the start of winter. When a drought occurs in this time of year, it does not stop before the snow melt peak, because there is no replenishment of soil water in the winter when snow is accumulated on the surface. This will result in a drought which will last all winter long, without the system getting the change to recover (Van Loon *et al.*, 2010).
The difference between indicators is very large for Papua New Guinea. Three indicators (SMDI, SVT

Table 4.3: Performance of selected soil moisture drought indicators for two selected major climate types.

	Papua New Guinea			Russia		
Indicator	Number	Average Duration (d)	Average Deficit	Number	Average Duration (d)	Average Deficit
TSDI	79	40.66	24.12 (d)	109	29.46	11.04 (d)
SMDI	555	5.789	3.256 (d)	151	21.28	11.52 (d)
SVT	766	4.172	29.04 ($mm\ d$)	191	15.88	85.94 ($mm\ d$)
ASSM	766	4.172	29.04 ($mm\ d$)	255	13.31	146.4 ($mm\ d$)
PDSI	9	351.9	387.8 (d)	13	245.8	170.1 (d)
Z-Index	70	44.77	17.74 (d)	66	47.51	9.935 (d)

and ASSM) have a very low average duration (4–6 days), while for Russia the durations are much longer for these indicators (13–21 days). The TSDI has a slower response, this is caused by storage components which are included in this indicator (Section 3.5.3). The TSDI includes snow accumulation and groundwater storage. If a drought occurs according to the TSDI at the beginning of winter, the system can recover with snow accumulation and without replenishment of the soil moisture content due to increase of storage in other components. The Z-Index uses monthly average soil moisture which results in less droughts, with a longer duration. Due to the monthly time step and a long memory, the PDSI has a low number of drought events.

Based on the predefined criteria (Section 4.1) expert knowledge only the TSDI and SVT will be used for the analysis of drought on a global scale (Chapter 5). The TSDI is selected because it captures all storage (Section 2.3) in the system and does not show a very high number of droughts. The SVT is chosen because of the physical nature of the indicator. Although the number of droughts identified the SVT is very high in Papua New Guinea, the number of droughts in Russia is much lower, which is to be expected from a soil moisture drought indicator (Section 4.1). The SMDI is not selected because: (i) the similar calculation procedure as the TSDI and SVT, (ii) the use of soil moisture content, like the SVT. Therefore, the SMDI will not add any unique aspects which are already not captured by either the TSDI or SVT. The ASSM is not selected because of it captures the same processes as the SVT and the longer calculation time. The Z-index and PDSI are excluded because of the monthly time scale and the way soil moisture is simulated (Section 3.5.2) which is different from all other methods. Specific soil properties (Table 3.2) cannot be represented in a sufficient manner by the Palmer-indicators. Therefore, the intercomparison of the Palmer-indicators (PSDI and Z-Index) and other drought indicators is difficult.

4.4 Hydrological drought indicators

The performance of the four selected hydrological drought indicators (Section 3.5.3), is illustrated with the results from two different climate types. The selected indicators are the Total Storage Deficit Index (TSDI), the Groundwater Resource Index (GRI), the Discharge with a Variable Threshold (QVT), and the Standardized Streamflow Index (SSI). They are used to detect drought in discharge (QVT and SSI) and groundwater storage (GRI and TSDI). The number of drought in discharge and groundwater storage are strongly related because of the model strucutre of NUT_DAY (Section 3.1). For the comparison of hydrological drought indicators, the B and C climate are selected (Table 4.1). The performance of each hydrological drought indicator for all climate types is described in Section VI. The low or intermediate streamflow rates in B climates make it very hard for hydrological drought indicators to perform well in there. On the other hand, C climates have a very constant rate of streamflow which makes them very suited for the application of hydrological drought indicators. One challenge for all hydrological drought indicators using streamflow is to cope with no streamflow for part of the year. This readily leads to a very poor performance. Therefore, a location in Australia (little streamflow) was chosen rather than a location in the Sahara (no streamflow). Selection of a Sahara location would have made comparison with other climates very difficult.

The B climate has a low average yearly precipitation (Table 4.1) and hence the precipitation excess is as low as 100 mm per year. The C climate has a much higher average yearly precipitation, which results for the selected location in an excess of 875 mm. Precipitation rates and precipitation excess for both

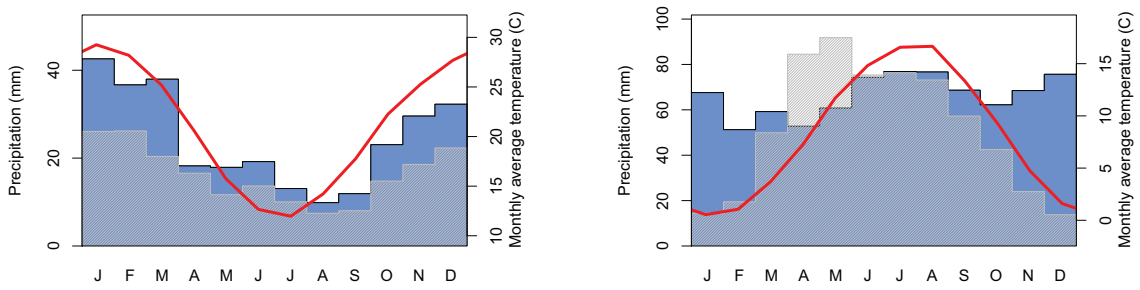

Figure 4.4: Average climate data for the two selected locations: one in Australia (B-climate, left) and one in Germany (C-climate, right). The red line shows the monthly average temperature. In blue the precipitation is given and in grey the actual evapotranspiration is presented.

Table 4.4: Performance of selected hydrological drought indicators for two selected major climate types.

		Australia			Germany	
Indicator	Number	Average Duration (d)	Average Deficit	Number	Average Duration (d)	Average Deficit
TSDI	59	54.46	28.66 (d)	39	82.38	39.47 (d)
GRI	17	189.0	102.1 (d)	20	160.7	74.55 (d)
QVT	19	170.5	8.03 (mm)	23	140.0	14.75 (mm)
SSI	15	214.2	162.8 (d)	11	292.1	144.5 (d)

locations are given in Figure 4.4. The detection of droughts was done with 4 different indicators. The results are shown in Table 4.4. The hydrological drought indicators are expected to have fewer droughts with a longer duration than the meteorological and soil moisture drought indicators (Section 4.1). In the B-climate, the TSDI has the highest number of droughts (n=59), because the TSDI operates in two different ways. The TSDI focuses either on soil moisture or groundwater storage (Section 3.5.3). However, in both situations, the TSDI combines soil water and groundwater storage, but the focus is primarily on soil moisture or groundwater. The GRI focuses only on groundwater (Section 3.5.3). Because of this slow responding component of the hydrological cycle the GRI has a very low number of droughts with a high average duration (Table 4.4). The TSDI is chosen rather than the GRI as hydrological drought indicator for further research (Chapter 5), because of the linear reservoir in NUT_DAY (Section 3.1). The linear reservoir causes the storage and discharge to be linearly related. Therefore, GRI performance is not be significantly different from the QVT. Correlations which are higher than 0.95 (except Russian location) confirm this (Annex III). The QVT is also chosen because of its wide application in drought research (e.g. Van Loon *et al.* (2010)).

4.5 Combined drought indicators

Table 4.5: Performance of the selected combined drought indicator for two selected major climate types.

		Australia			Germany	
Indicator	Number	Average Duration (d)	Average Deficit	Number	Average Duration (d)	Average Deficit
ADI	1137	2.826	1.896 (d)	1380	2.328	0.612 (d)

Only one indicators was selected from this category, namely the Aggregate Drought Index (ADI) (Section 3.5). The ADI is not related to any other type of drought indicators, however, the theoretically

it resembles hydrological drought indicators most. Therefore, as for the hydrological indicators (Section 3.5.3) the B and C climate are used to illustrate the results of the ADI. The details of both locations are described in Figure 4.4. The climatic results for the all climate types are given in Section VII. The results for climate types B and C are shown in Table 4.5. The ADI has the highest number of droughts, compared to all previous drought indicators. Even the meteorological drought indicators have a lower number of droughts (Table 4.5). Meteorological drought indicators are expected to have a higher number than a combined indicator, which is assumed to have intermediate number of droughts (Section 4.1). This number is too high for wider analysis on a global scale (Chapter 5). The ADI shows no correlation with any of the previously selection indicators (Annex III). Therefore, the ADI is not selected for further research.

5 Impact of hydroclimate and physical catchment structure

In this chapter, the effect of the physical catchment structure and the full range of hydroclimate conditions on the performance of drought indicators are further analyzed (Figure 3.1). This is done for the final selection of drought indicators (Sections 4.2, 4.3 and 4.4).
First, the effect of using all 31 climatic regions is determined in Section 5.1. A rather large set of locations in all 31 climatic regions is further investigated. Summary statistics for each indicator are presented to give a comprehensive overview of the general performance of an indicator in different climates. In Section 5.2 the effect of the physical catchment structure is further investigated by changing the soil type and groundwater response time (j-factor). Again, summary statistics are given to show performance of the indicators as a response to different physical catchment structures. In this chapter the finally selected 6 indicators are used for this more detailed analysis, namely: the Standardized Precipitation Index (SPI), the Effective Drought Index (EDI), the Moving Average Precipitation with a Variable Threshold (MAPVT), the Total Storage Deficit Index (TSDI), the Soil Moisture with a Variable Threshold (SVT) and the Discharge with a Variable Threshold (QVT). The performance is evaluated by using the number of droughts and the deficit volumes as drought characteristics. Drought duration is not explained because of the high negative correlation between the number of droughts and the drought duration (Table 4.2 to 4.5).

5.1 The impact of the hydroclimatic conditions on the performance of drought indicators

Changing the hydroclimatic conditions could have a large impact on droughts characteristics. The differences between hydroclimates can be relevant for the performance of the different selected indicators. The variation within a particular climatic region according to Köppen-Geiger (Section 3.3) can also have its impact on the performance. A map (Annex II) of all climates according to Köppen-Geiger based on the WATCH Forcing Data (WFD) has been made (Section 3.3). For each climatic region, 2% of the cells was selected with a minimum of 20 cells and a maximum of 50 cells. This to ensure that each climatic region has a representative number of locations for further analysis. The locations are randomly selected across the world to ensure a good estimation of the sensitivity to changes in the climate. A map with all selected locations (total 961 locations) can be found in Annex VIII. In this section, only a selection

Table 5.1: Mean number of droughts for some selected climate types and six drought indicators (1958-2002).

Climate type	SPI	EDI	TSDI	MAPVT	SVT	QVT
Af	256	152	71	242	421	49
Aw	249	144	92	217	259	30
BWk	179	91	224	173	131	2
BWh	64	43	202	101	87	3
BSh	224	118	147	198	228	8
Cfa	305	185	108	245	293	24
Csa	265	136	80	214	181	29
Cwc	268	156	102	253	293	17
Dfd	279	184	74	249	89	10
Dsa	278	156	81	224	162	20
Dwa	298	163	139	252	231	12
EF	297	141	4	221	5	1
ET	276	145	53	226	87	21

of the results is described. Tables with all results can be found in Annex IX. In Table 5.1 the number of droughts for a selected number of representative climate types has been given to get a quick overview of the performance for each indicator. For droughts in the precipitation, drought indicators (i.e. SPI, EDI, MAPVT) have a very similar pattern in terms of number of droughts throughout the different climates.

Table 5.2: Mean deficit volumes of droughts for six selected drought indicators and a selection of some climate types (1958-2002).

Climate type	SPI (d)	EDI (d)	TSDI (d)	MAPVT (mm)	SVT ($mm\ d$)	QVT (mm)
Af	8.06	8.32	22.1.9	14.2	104	31.1
Aw	7.39	4.94	14.8	6.57	91.4	16.4
BWk	7.05	7.11	3.57	0.55	9.81	$1.47 * 10^{-6}$
BWh	0.0549	9.46	2.5	0.0429	2.93	$3.6 * 10^{-5}$
BSh	7.72	5.65	3.74	3.32	36.5	2.21
Cfa	6.27	5.81	11.7	6.55	119	15.4
Csa	8.25	5.74	15.9	3.91	123	12.5
Cwc	7.38	4.36	10.1	3.22	74.5	11.1
Dfd	6.85	4.85	14.0	1.71	304	3.42
Dsa	7.61	6.13	17.0	2.68	164	9.67
Dwa	6.58	3.61	5.66	2.79	68.1	8.16
EF	6.42	8.04	229	1.86	893	0.0951
ET	6.73	6.66	29.0	1.49	216	6.73

The very dry BWh and BWk climates are the only exception. The response of the Moving Avarage Precipitation with a Variable Threshold (MAPVT) and the Standardized Precipitation Index (SPI) is very much alike, while the The Effective Drought Index (EDI) has a slower response to precipitation events than the SPI and MAPVT (Annex IV). This also affects the number of droughts which is lower for the EDI compared to the SPI and MAPVT (Table IX). The memory in the EDI of 365 days is the reason for this, (Section 3.5.1). This results in a slower response of this indicator to new precipitation events leading to longer droughts. The SPI and the MAPVT both have a memory of 30 days in this research (Section 3.5.1 and 3.5.1), which makes that both indicators by nature have a faster response to changes in the precipitation (shorter droughts).
Of special interest are the extreme climates, like the B and E climates, where most challenges are expected due to low precipitation and streamflow. The BWh climate has a significantly lower number of droughts for all precipitation drought indicators, however the SPI shows the largest decrease. This is partly caused by the fact that the SPI has troubles with fitting a gamma distribution through the low number of months with precipitation (Section 3.5.1). The EDI and the MAPVT do not suffer from this problem and will have a more reliable performance in these months.
The number of streamflow droughts (QVT) in the EF climates is extremely low (n=1). This indicates no or incidental streamflow, which is caused by the large simulated snow accumulation (up to 40 m water equivalent). This snow accumulation is not compensated by snow melt, because temperatures in the EF climates do normally not rise above 0°C. Under these extreme situations drought indicators that focus on discharge, like the Discharge with a Variable Threshold (QVT), are not suited to detect droughts. Precipitation and soil moisture drought indicators have less problems with drought detection. Soil moisture is once in a while replenished by very short periods of snow melt, while precipitation, of course, occurs in this climate type.
The performance of the Total Storage Deficit Index (TSDI) is very much dependent on the hydroclimatic region (Table 5.1). In the A and C climates the performance of the TSDI is like a hydrological drought indicator (high recharge rates), while in the other climates the performance is like a soil moisture drought indicator (Section 3.5.3). The number of discharge droughts (QVT) in the B climate is lower than in the other climate types (Table 5.1). It was concluded that a lack of discharge may cause this, the very small deficit volumes typical for the B climates (Table 5.2) support this conclusion. In this situation these low deficit volumes indicate that discharge values are very low or discharge is absent for a long time. To obtain such low deficit volumes, the threshold should be equally low, otherwise the difference between discharge and the threshold would still be large (Figure 3.4). The same is true for the EF climate where the deficit volume is slightly higher due to some occasional snow melt and associated higher flows. However, discharge values and thresholds are still very low, which results in very low deficit volumes. The deficit volumes of the MAPVT show that in the A and C climates the deficit in the precipitation is larger than in other climates, which is caused by higher rainfall rates for these climate types (higher

Table 5.3: Mean number of droughts for two selected drought indicators for some selected climate types, and an average soil (Section 3.1), and different values of the j-factor (1958-2002).

	TSDI			QVT		
Climate type	j=100	j=250	j=1000	j=100	j=250	j=1000
Af	110	71	36	70	49	27
Aw	137	92	50	41	30	18
BWk	258	224	192	2	2	2
BWh	230	202	168	3	3	2
BSh	192	147	93	13	8	6
Cfa	164	108	65	30	24	13
Csa	113	80	38	41	29	19
Cwc	154	102	47	24	17	8
Dfd	90	74	62	20	10	6
Dsa	119	81	45	29	20	12
Dwa	201	139	53	17	12	7
EF	4	4	4	2	1	1
ET	65	53	39	33	21	13

threshold). The deficit volumes in the dryer climates (BW and E) show low values for all indicators (e.g. MAPVT, SVT and QVT). The deficit volumes identified by the SVT are the highest in the climates which are affected by snow (D and E). This is due to the large simulated deficit volume which can develop under the snow cover (Van Lanen *et al.*, 2010b), before the deficit is replenished by snow melt water (Section 4.3).

5.2 The impact of the physical catchment structure on the performance of drought indicators

For the simulation with the synthetic model (Section 3.1), the groundwater system, so far, has been represented by a linear reservoir with a j-factor of 250 days to study the performance of different types of drought indicators. In this section, the effect of different physical catchment structures is studied (Figure 3.1). The effect of different j-factors is studied, by looking at a fast responding catchment with a j-factor of 100 days and a slowly responding catchment with a j-factor of 1000 days. Next, the soil type is changed from a light silty loam soil to: (i) a coarse sand soil and (ii) a sandy loam. These changes in physical catchment structure only affect the soil moisture and or hydrological drought indicators, since meteorological drought indicators are by nature not affected by the physical catchment structure.

5.2.1 Response groundwater system: j-factors

In this section the effect of changes in the groundwater system through the j-factor are represented. The j-factor has been changed from 100 days to 1000 days to study the effect on the performance of hydrological drought indicators. Initial conditions and forcing (precipitation and evapotranspiration) were the same for all j-factors. In Table 5.3, the mean number of droughts for different j-factors is given for a selection of climate types. The outcome for all climates is given in Annex X. The results of different j-factors are described for the Total Storage Deficit Index (TSDI) and Discharge with a Variable Threshold (QVT), because these are the only two selected hydrological indicators. The other selected indicators do not use discharge nor groundwater storage and hence are affected by the changes in the j-factor. The physical meaning of the increase of the j-factor is that a slower responding catchment is simulated (Section 3.1). In Figure 5.1 different values of j are used to show the effect on the simulation of groundwater discharge for an average year in a C climate. For the three simulation runs all model parameters were kept constant apart from the j-factor. The decrease in the number of droughts is expected for a slow responding catchment, since response times become longer (Van Lanen *et al.*, 2004). With an increase of the j-factor the Total Storage Deficit Index (TSDI) reflects more groundwater storage than soil moisture storage (Section 3.5.3). More water is stored in the groundwater for a high j-factor,

Table 5.4: Mean deficit volumes of droughts for two selected drought indicators, some selected climate types, an average soil (Section 3.1) and different values of the j-factor (1958-2002).

	TSDI (d)			QVT (mm)		
Climate type	j=100	j=250	j=1000	j=100	j=250	j=1000
Af	13.9	22.1	51.3	25.3	31.1	27.3
Aw	8.1	14.8	26.5	13.7	16.4	17.8
BWk	3.23	3.57	3.35	$4.99 * 10^{-15}$	$1.47 * 10^{-6}$	0.00123
BWh	2.93	2.5	2.3	$1.54 * 10^{-10}$	$3.6 * 10^{-5}$	0.0135
BSh	2.82	3.74	10.7	0.281	2.21	7.24
Cfa	6.91	11.7	19.6	12.2	15.4	13.3
Csa	10.8	15.9	31.5	11	12.5	10.2
Cwc	8.51	10.1	24.2	11.2	11.1	14.2
Dfd	14.3	14	20.9	1.29	3.42	5.48
Dsa	10.6	17	31.6	7.02	9.67	9.51
Dwa	4.48	5.66	22.5	1.24	8.16	17.4
EF	238	229	218	0.0925	0.0951	0.167
ET	22.8	29	33.4	5.33	6.73	6.71

this makes fluctuations in the soil moisture storage less important for the TSDI. This decreases the number of droughts (Table 5.3) and results in higher deficit volumes (Table 5.4).

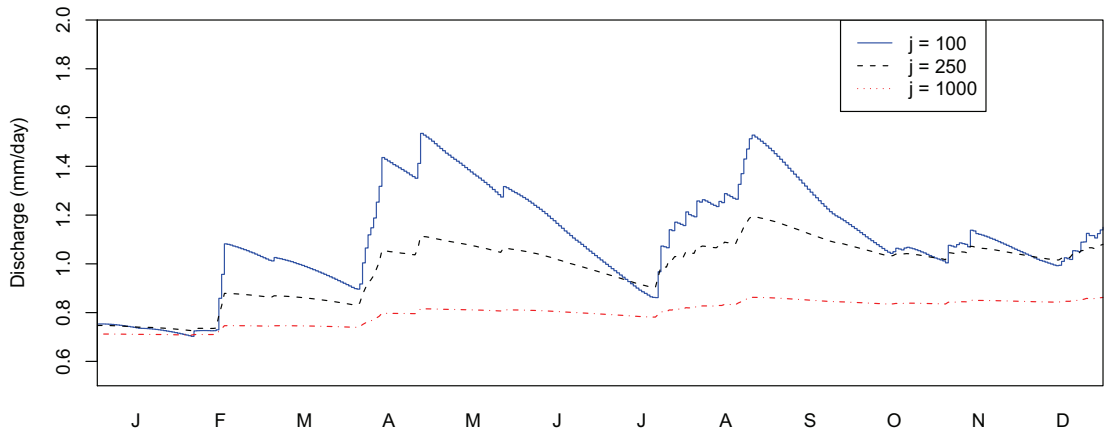

Figure 5.1: Groundwater discharge for j-factors of 100, 250 and 1000 days. Initial conditions and forcing (precipitation and evapotranspiration) are the same for all simlutions. Recharge to the groundwater is the same for al simulation, only the j-factors differ. The simulation is done for a C climate.

5.2.2 Soil types

The effect of a change in soil type on the performance of selected drought indicators was studied for all three soil types (Table 3.2). This implies that the soil texture of the average soil (light silty loam) has been changed. A j-factor of 250 days was used. The results for all climate types can be found in Annex XI. The outcome for a selection of climate types is in Table 5.5. Coarse sand has the lowest soil storage capacity[4] of the three selected soils used for the intercomparison (Table 3.2). The light silty loam has an average capacity to store water, and the sandy loam has the highest soil water storage capacity. Based on expert knowledge, it is expected that the available soil moisture in a coarse sandy soil is most vulnerable for long

[4]Soil moisture storage capacity is defined in this study as the amount of soil water available between field capacity and wilting point (Section 3.1)

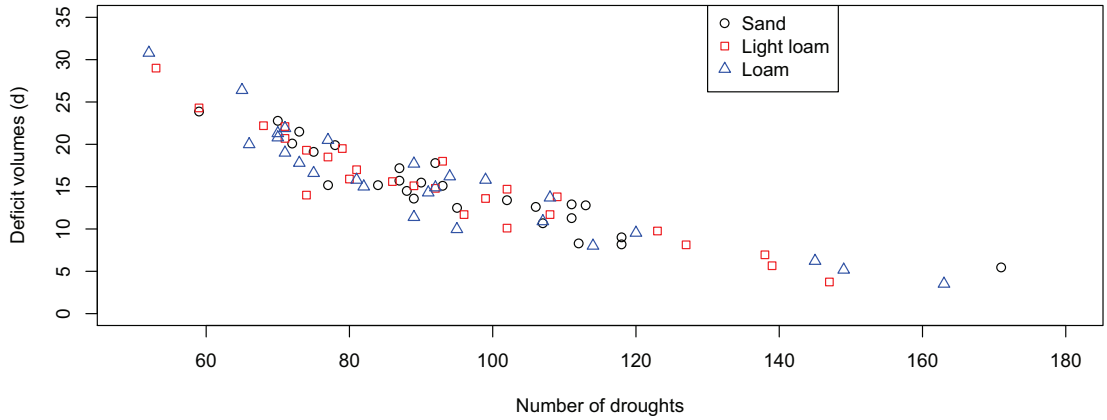

Figure 5.2: The mean number of droughts versus the mean deficit volumes of droughts, identified by the TSDI. For all climate types, the mean number of droughts and mean deficit volumes have been plotted (Section XI). Only the B-climates and EF climate have been excluded from this plot, values for these climates can be found in Section XI.

periods with low precipitation. Due to this low capacity to store water of the sandy soil, the recharge to the groundwater system is higher than for the other two soils in wet periods. Another important process is the reduction of potential evapotranspiration due to shortage of water in the unsaturated zone (Van Lanen *et al.*, 2010b). In sandy soil this reduction will be larger due to the lower soil moisture storage capacity. The soil reachs critical point faster and reduction of the potential evapotranspiration takes place. In the two loamy soils this reduction in potential evapotranspiration occurs after a longer periode of time since the soil water storage capacity in these soils is higher (Table 3.2). Therefore, droughts in soil moisture are more likely to occur in sandy soils than in the two loamy soils, for a fixed threshold. On average the number of droughts identified by SVT decreases, with an increase in the soil water storage capacity as expected (Table 5.5). The Total Storage Deficit Index (TSDI) and Discharge with variable threshold (QVT) show a less profound behavior to the changes in soil type than the SVT. For some climate types, there is no significant difference between the different soil types in the performance of the TSDI. Some climates show a decrease in number of droughts with an increase of storage capacity of the soil moisture, while other climates show an increase. The QVT shows a decrease in the number of droughts which is best shown in the changes from coarse sand to light silty loam. The number of droughts decreases for all indicators. There is not always a difference between the light silty loam and the sandy loam, where the number of droughts shows a small decrease or will stay constant. The changes in deficit volumes show the same pattern. When the number of droughts decreases, durations are longer and deficit volumes increase (Figure 5.2). This is caused by the longer period of time the deficit volume gets to develop. In the B and E climates the mean number of soil moisture droughts in the SVT can increase with a rise in soil moisture storage capacity. Recharge in a B-climate is low which is by the bypass introduced in NUT_DAY (Section 3.1), which is due to very high in case of coarse sand and lower for the loamy soils. The hydrofoob behavior of coarse sand results in a high amount of precipitation, what bypasses the soils and flows directly to the groundwater system. The precipitation, which infiltrates into the unsaturated zone, evaporates the same day, so the drought continues. The bypass is lower in the loamy soils and more precipitation infiltrates into the unsaturated zone. In loamy soils the bypass represents water, which flows through the macropores directly to the groundwater. The deficit volumes identified by SVT show that in the BW-climate the drought lasts for the entire simulated period. A combination of the bypass and high evaporation rates causes, that the soil moisture content will never be above wilting point. This effect for the coarse soils is also visible in the number of droughts and deficit volumes identified by the QVT, which is higher than the number of droughts for the other soil types. This is caused by the bypass which will transport the water directly to the groundwater, so groundwater discharge occurs.

Table 5.5: Mean number of droughts for three selected drought indicators, some selected climate types, j-factor is 250 days and different soil types, Coarse Sand (CS), Light Silty Loam (LSL), Sandy Loam (SL)(1958-2002).

	TSDI			SVT			QVT		
Climate type	CS	LSL	SL	CS	LSL	SL	CS	LSL	SL
Af	70	71	71	678	421	413	58	49	48
Aw	88	92	92	439	259	233	43	30	28
BWk	372	224	218	NA	131	125	7	2	2
BWh	242	202	194	NA	87	84	6	3	3
BSh	112	147	163	210	228	219	19	8	8
Cfa	106	108	107	487	293	256	47	24	22
Csa	84	80	75	278	181	154	46	29	29
Cwc	95	102	95	400	293	263	33	17	14
Dfd	90	74	73	207	89	81	32	10	10
Dsa	87	81	82	250	162	151	44	20	16
Dwa	118	139	149	414	231	210	26	12	9
EF	4	4	4	7	5	10	2	1	1
ET	59	53	52	97	87	81	32	21	19

Table 5.6: Mean deficit volumes of droughts for three selected droughts indicators, a selection of climate types, and different soil types, Coarse Sand (CS), Light Silty Loam (LSL), Sandy Loam (SL)(1958-2002).

	TSDI (d)			SVT ($mm\ d$)			QVT (mm)		
Climate type	CS	LSL	SL	CS	LSL	SL	CS	LSL	SL
Af	22.8	22.1	21.9	23.7	104	128	26	31.1	31.9
Aw	14.5	14.8	14.9	13.3	91.4	120	11.9	16.4	16
BWk	1.01	3.57	4.09	NA	9.81	14.9	0.0492	$1.47 * 10^{-6}$	$7.2 * 10^{-9}$
BWh	0.759	2.5	2.84	NA	2.93	4.26	0.0772	$3.6 * 10^{-5}$	$9.72 * 10^{-7}$
BSh	8.32	3.74	3.52	0.193	36.5	44.6	7.01	2.21	0.957
Cfa	12.6	11.7	10.9	11.9	119	161	10.1	15.4	15.7
Csa	15.2	15.9	16.6	29.5	123	168	8.54	12.5	13.5
Cwc	12.5	10.1	9.97	15.5	74.5	84.7	9.29	11.1	9.34
Dfd	15.5	14	17.8	42.1	304	416	3	3.42	3.33
Dsa	15.7	17	15	33.8	164	208	6.47	9.67	9.92
Dwa	9.01	5.66	5.18	1.2	68.1	97.5	7.14	8.16	5.52
EF	205	229	239	149	893	377	0.0881	0.0951	0.164
ET	23.9	29	30.8	114	216	262	4.91	6.73	7.21

5.3 Evaluation of the final set of selected drought indicators

An important criterion for the suitability of a drought indicator, used for drought analysis on a global scale, is its applicability for all climate types and physical catchment structures. The performance of the final selected six indicators has been tested for different climates and physical catchment structures (Sections 5.1 and 5.2). Based on these results some indicators Seem to be more applicable on a global scale than others. In this section an evaluation of each of the six selected indicators is given. A summary table is included in which each of the indicators is ranked according to the criteria of the evalution (Table 5.7).
Indicators are evaluated on:

- Performance independent of hydroclimatic region
- Performance independent of physical catchment structure
- Performance under extreme situations, like deserts and polar climates (B- and E-climates)
- Physical meaning of indicator
- Complexity of calculation procedure

Table 5.7: Comparison of the final selection of drought indicators. Comparison is done based on the evaluation criteria (Section 5.3).Scores are indicate as: −− (very bad), - (bad), +/- (intermediate), + (good), ++ (very good).

Indicator	Climate	Catchment	Extreme conditions	Physical meaning	Calculation
SPI	−	NR	+/−	−	−−
EDI	+	NR	+	−	−
MAPVT	+/−	NR	+/−	++	+
TSDI	−	−	−−	−	−
SVT	−	−	−−	+/−	++
QVT	+/−	+	−−	++	++

5.3.1 Standardized Precipitation Index

The Standardized Precipitation Index (SPI) is a meteorological drought indicator, which is often used on a global scale (Section 2.1). The SPI uses a monthly (or higher) time resolution (Section 2.1). However, a daily time resolution was required for this research, which was developed (i.e. a daily 30-day backwards moving average (Section 3.5.1)). A normalized gamma distribution was assumed for the calculation of the SPI values (Section 3.5.1). This normalized gamma distribution causes problems in climates with low precipitation, or climates with a very distinct dry period of several months per year. Under these conditions the procedure is unable to give a good estimate of the two shape parameters (α and β) of the gamma distribution (Section 3.5.1). This is reflected in the mean deficit volume identified by the SPI for the BWh-climate, which is very low due to these months without precipitation (Table 5.2). The SPI is a meteorological drought indicator that is independent on the physical catchment structure and hence does not have to be taken into account for the performance of the SPI. Because of the above-mentioned limitations and the complicated calculation procedure, it is not advised to use the SPI on a global scale, although this is not supported by World Meteorological Organization (2010)

5.3.2 Effective Drought Index

The Effective Drought Index (EDI) is not as widely used as the Standardized Precipitation Index (Section 2.1). The EDI is a meteorological drought indicator, which uses normalized distribution with a memory of 365 days (Section 3.5.1). The calculation procedure of the EDI is rather straightforward. Because of the long memory, the indicator faces less problems with the drought analysis for months without precipitation (Section 5.1). The mean deficit volumes identified by the EDI show no difficulties

for the BWh-climate or other extreme climates (Table 5.2). Therefore, the EDI is found to be a better meteorological drought indicator than the SPI. However, the long memory could be a disadvantage for a meteorological drought indicator, since shorter periods with low precipitation have a smaller effect on the EDI values. Like the SPI, the EDI is independent on the physical catchment structure.

5.3.3 Moving Average Precipitation with a Variable Threshold

The last of the finally selected meteorological drought indicators was the Moving Average Precipitation with a Variable Threshold (MAPVT). This indicator takes a 30 days centered moving average to calculate the moving average of the precipitation (Section 3.5.1). This ensures that the MAPVT has no difficulties with a noumber of rainless days. However, months without precipitation still pose difficulties as the aggregation period is not more than 30 days. If a particular month is without rain for more than 20% of the years, the selected 80% threshold for this month will become zero. The MAPVT, however, is not very sensitive to these zeros since no fitting of a gamma distribution has to be done. An advantage of this drought indicator, is that the values of the MAPVT can easily be calculated without fitting or normalization. However, the threshold for the MAPVT should be calculated using long time series of precipitation. The mean deficit volumes of the MAPVT are strongly affected by the hydroclimate (Table 5.2). The physical meaning of the deficit volume of the MAPVT seems to be an advantage compared to the SPI and EDI, since it can be easily calculated how much additional precipitation is required to recover from a particular drought event. Therefore, the MAPVT seems to be the best meteorological drought indicator for drought analysis on a global scale.

5.3.4 Total Storage Deficit Index

The Total Storage Deficit Index (TSDI) uses both the storage in the unsaturated zone and the groundwater for drought analysis (Section 2.3). The performance of the TSDI can be studied for changes both in hydroclimate and physical catchment structure. The TSDI is a normalized combined drought indicator, which can be used for either the detection of soil moisture droughts or the detection of hydrological droughts (Section 3.5.3). The climate condition can determine the performance of the TSDI as either a soil moisture or a hydrological drought indicator. If the precipitation and groundwater storage are high, the performance of the TSDI is more like a hydrological drought indicator. On the contrary, when precipitation and groundwater storage are low, its performance will be like a soil moisture drought indicator (Section 3.5.3). The performance of the TSDI is very dependent on both the hydroclimate (Table 5.1) and physical catchment structure (Table 5.3 and 5.5). This is a disadvantages when the TSDI is used on a global scale, because too much factors influence the performance of the TSDI and evaluation of the performance is difficult. The calculation procedure of the TSDI is complicated, since soil moisture and groundwater storage are required and all values need to be normalized. It is not advised to use the TSDI for drought analysis on a global scale although the use of one indicator to capture all droughts present in the unsaturated and saturated zone is a good concept.

5.3.5 Soil moisture content with a Variable Threshold

The Soil moisture content with a Variable Threshold (SVT) has been proposed in this study to detect soil moisture droughts. Drought detection with the SVT is done with a variable threshold (Section 3.5.2). The performance of the SVT is very sensitive to the climate type (Table 5.1) and soil type (Table 5.5). This strong dependence on the soil type may cause problems. If other models are used the SVT is very sensitive to a classification of the soil type. On a global scale, the SVT has been used in several studies (Section 2.2). However, based on the results from this research, it is not advised to use the SVT for drought analysis on a global scale.

5.3.6 Discharge with a Variable Threshold

For the detection of streamflow droughts, the Discharge with a Variable Threshold (QVT) has been proposed in this study. A variable threshold is calculated with the use of discharge values (Section 3.5.3). The mean number of droughts for the QVT is low for every climate type compared to other indicators (Table 5.1). Without standardization the mean deficit volumes of the QVT have a large variation between hydroclimates (Table 5.2). The deficit volumes indentified by the QVT do have the same

physical meaning as those indentified by the MAPVT. Months without discharge for more than 20% of the years cause difficulties for the application of the QVT, since the 80% threshold will become zero. However, months without discharge are less common than for precipitation, so this problem will occur less often. The QVT seems to be the most promising indicator from all the non-meteorological drought indicators, because it is capable of dealing with dry climates and its physical meaning of the deficit volume.

6 Discussion

In this study the most important assumptions and their uncertainties are discussed in the context of the assessment of the performance of the drought indicators across the world.

6.1 Synthetic model

The synthetic model NUT_DAY uses some simplifications for the simulation of rainfall-runoff process (Section 3.1). These simplifications allowed to perform lots of calculations that were required for this study. However, due to these simplifications some physical processes are not captured well by NUT_DAY, which might affect the simulated of runoff. The most important simplifications of the NUT_DAY are mentioned below.

6.1.1 Soil moisture simulation

The first simplification is the use of a single soil box for the simulation of the soil moisture storage although a two-layer soil profile is used to define the soil moisture supply capacity(Section 3.1). No vertical distribution of for the soil moisture profile is made, which results in no difference between the volumetric water content at the top and the bottom of the soil (Van Lanen *et al.*, 2010b). The subsoil and topsoil defined in NUT_DAY are combined into one soil box (lumped, vertical model), which does not address soil moisture content gradients and a possible limiting maximum infiltration rate at the surface (Van Lanen *et al.*, 2010b). This may effect the simulated soil water balance, especially the root water uptake (i.e. actual evapotranspiration) and the bypass. After a long period without precipitation, the topsoil would be very dry due to evapotranspiration in reality (Van Lanen *et al.*, 2004), whereas NUT_DAY does not take this into account and the grass crop may still transpire at a potential rate if the total soil moisture storage is sufficient.

6.1.2 Linear reservoir

In NUT_DAY, a single reservoir is used for the simulation of discharge, of which the outflow rate is determined by the De Zeeuw-Hellinga approach (Ritzema, 1994). Compared to some other models, which use multiple reservoirs, the current version of NUT_DAY is unable to simulate a slow flow and a quick flow component at the same time. NUT_DAY is designed to simulate groundwater discharge only. Fast components like surface runoff and shallow saturated subsurface flow (interflow) are not captured by the model. However, some adjustments (Section 3.1.3) have been made to make the current version of NUT_DAY more suited for the simulation of the fast groundwater fluctuations caused by precipitation events with a high intensity (e.g. bypass, recharge even if the soil is dryer than field capacity).

6.1.3 Bypass

Bypass in NUT_DAY is activated when a heavy precipitation event occurs and the soil is very dry (Section 3.1). It is assumed that the precipitation infiltration cannot exceed a maximum rate. In this study, this maximum rate is set at the hydraulic conductivity at field capacity. If the daily precipitation exceeds the maximum infiltration rate, bypass is assumed to occur. A second assumption is that bypass is only active when the soil moisture storage is below a critical point (Table 3.2). In these situations, it is assumed that cracks and macro-pores in the soil transport part of the water directly to the groundwater (Section 3.1.4). When the soil is wetter than critical point, all precipitation is assumed to infiltrate into the unsaturated soil. With this bypass approach the response of the groundwater system to heavy precipitation is simulated better with NUT_DAY, but it does not imply that NUT_DAY simulates fast runoff components (Van Lanen *et al.*, 2010b).

6.2 Soil types

The soils used in this research were retrieved from the Staring Series (Wösten *et al.*, 2001). The selection of the soils (Table 3.2) was done from a total of 22 standard soils. These soils were used to identify a few representative soil types which likely can be found acros the world. In this study, three different soil textures have been used; a soil with a low, medium and high soil moisture storage capacity. The

selection of these soil textures was based on the total amount of water available between wilting point en field capacity. Peat soils are excluded from the selection because of their specific characteristics (very high soil moisture storage capacity, dynamic behavior).
The selected rooting depth of 50 cm in this study reflects the rooting depth of grass. However, in some regions across the world this rooting depth will never be reached due to shallow bedrock or permafrost. In regions, where other vegetation than grass is dominant, rooting depths can be even over 200 cm in case no penetration resistant layer occurs (e.g. Schenka & Jackson (2005)). A thicker soil has large effects on the soil moisture capacity and the actual evapotranspiration rates, especially in dryer climates. If rooting depths is larger, the capacity to store water in the unsaturated zone and the actual evapotranspiration increase and the other way around. However, there is a limitation to this process. If rooting depth becomes very large, evapotranspiration will never be reduced because there is enough water stored in the unsaturated zone to overcome very dry periods (Van Lanen *et al.*, 2004). The smaller the storage capacity, the more droughts occur (Section 5.2.2). So, the selected rooting depth may have a profound effect on the magnitude of the drought characteristics and drought indicator performance.

6.3 Köppen-Geiger classification

The Köppen-Geiger classification is a well-known, but a rather old climate classification (Köppen, 1900). Adjustments to the Köppen-Geiger classification have been made by Geiger (1954). The Köppen-Geiger classification is a discrete classification based only on precipitation and temperature. However, other classifications (e.g. Holdridge life zones, Holdridge (1947); Thornthwaite climate classification, Thornthwaite (1948)) are available, and may be better suited to give a climate classification on a global scale.

6.4 Drought concept

Droughts are caused by situations with less than normal water availability. They are present in every hydroclimatic region and appear in different components of the hydrological cycle (Wilhite, 2000). This means that locations, where water is (almost) never available, have an extremely low normal water availability and the threshold will be very low or even zero. These cases should not be called a drought anymore, but it refers to aridity (permanently dry). This also affects the way droughts have to be studied. If NUT_DAY is used for the simulation of soil moisture and groundwater discharge, soil moisture and hydrological drought indicators should not be used, for the very dry climates, like the BW-climates. In these regions very deep groundwater storage is possible (Stahl & Hisdal, 2004). However, due to model structure of NUT_DAY this deep groundwater storage cannot be simulated (model does not distinguish shallow and deep groundwater storage) (Van Lanen *et al.*, 2010b). As long as there is precipitation for most of the years, meteorological drought indicators can still be applied (especially the Effective Drought Index (EDI) and Consecutive Dry Days (CDD)). The CDD is very suited for drought definition in dry climates since it particularly addresses very long dry periods (Section 4.2). However, in wetter climates the CDD is not so useful for the detection of droughts (Section 4.2).
In the EF-climate all precipitation is accumulated as snow and will melt only when temperatures are above 0°C, which is very rare. Soil moisture is also heavily affected by the frozen soils in these climates. These locations (mostly situated on the poles and Greenland) give rise to difficulties for all indicators, except for those which focus only on precipitation. So, streamflow and soil moisture drought indicators face difficulties in the EF-climate, where streamflow is (almost) absent due to average monthly temperatures which are always below 0°C. The BW-climate and EF-climate were included in this research because drought can still be detected with the use of (some) precipitation drought indicators.

7 Conclusions and recommendations

7.1 Conclusions

This study on the performance of drought indicators on the large scale led to the following conclusions:

- For drought analysis on a global scale, both the Moving Average Precipitation with a Variable Threshold (MAPVT) and the Discharge with a Variable Threshold (QVT) are found to be promising drought indicators. The combined use of the MAPVT and QVT allows detection of both meteorological and hydrological droughts and enables intercomparison (Sections 3.5.1 and 3.5.3). The MAPVT and QVT have the advantage, that they are also applicable for drought analysis on a more detailed scale than the global scale. When the threshold can be calculated using data from previous years, real-time drought monitoring on a daily basis can be done with the QVT and MAPVT, without the use of a difficult calculation procedure(Sections 3.5.1 and 3.5.3). Since precipitation and discharge data are widely available this is very useful. Although the QVT has difficulties in very dry, B-climates, it is still selected since all hydrological drought indicators show weak performance in these B-climates (Section 5.1). The MAPVT and QVT are easy to implement and have deficit volumes which have a physical meaning that can be interpreted without difficulties.

- The Standardized Precipitation Index (SPI) faces problems with fitting the gamma-distribution for locations with regularly dry months (Section 3.5.1). There, the estimated α and β parameters of the gamma distribution, are less reliable than a threshold directly derived from the precipitation as done in the MAPVT (Section 5.3).

- In very dry climates (e.g. BW-climates), the long memory of the Effective Drought Index (EDI) is a major advantage for the performance, because the EDI can easily deal with multiple months without precipitation (Section 3.5.1). In these dry periods the EDI considers previous rainfall (up to 365 days back). Therefore, the EDI does not have difficulties at these sites as the SPI and the MAPVT have (Section 5.3).

- The EDI and the MAPVT have a very similar performance (Section 5.3). However, due to the very long memory of the EDI, the MAPVT is preferred for most climate types rather than the EDI. The long memory of the EDI causes a very slow response to new precipitation events, which is not to be expected for meteorological drought indicators (Section 3.5.1). However, the EDI is found to be a better precipitation drought indicator than the SPI since no fitting problems occur (Section 3.5.1).

- The performances of the Soil moisture with a Variable Threshold (SVT) and Total Storage Deficit Index (TSDI) and their associated drought characteristics are very dependent on the selected soil type (Section 5.2.2). For intercomparison studies on a global scale, SVT and TSDI are only meaningful if an adequate soil map with reliable soil textures and associated hydraulic properties would become available. Although it is recognized that this dependency is one of the strong properties of the TSDI and SVT, it is found to be a negative property for an intercomparison of drought characteristics on a global scale as long as no adequate soil information becomes available.

- The climate type has a very large effect on the magnitude of all drought characteristics predicted with different drought indicators (Section 5.1).

- Groundwater systems have a larger effect on the magnitude of drought characteristics as predicted with hydrological or combined drought indicators than soil types for, independent of the hydroclimatic region.

7.2 Recommendations

The study leads to the following recommendations:

- Identification of a standardized deficit volume for MAPVT and QVT, would improve intercomparison of drought characteristics across the globe. So far, drought characteristics for different hydroclimatic regions can only be reasonably compared based on durations and number of events,

which are highly negatively correlated. Without standardization of the deficit volume, comparison of drought severity (i.e. deficit volumes and intensity) can only be done in a qualitative manner. The identification of a standardized deficit volume offers an additional quantitative measure for intercomparison of droughts in different hydroclimates and regions with different physical catchment structures.

- Examination of the drought characteristics predicted with the six, finally selected drought indicators (SPI, EDI, TSDI, MAPVT, SVT and QVT) with observed data from river basins. It needs to be investigated if the use of observed data instead of simulated data with a hydrological model could lead to a different performance of the drought indicators. Especially, soil moisture drought indicators could show different performance for observed soil moisture data.

- Running the MAPVT and the QVT for all cells (about 70 000) instead of the 961 cells in this study (Section 5.1) gives a more comprehensive insight in the performance of both indicators on a global scale. This can be done for a light silty loam soil and a linear reservoir with a j-factor of 250 days. This to get an impression of the distribution of drought characteristics within a climate region.

- Use of other climate classifications than the Kppen-Geiger climate classification. Continuous classifications like the classifications of Holdridge (1947) and Thornthwaite (1948) could give a better picture of the spatial distribution of drought indicator performance across the world. The problem by applying the Kppen-Geiger climate classification is introduced by the discrete distribution. Continuous classifications can cope with inhomogeneity within climate types.

- Application of another threshold. The 80% threshold was selected for this study. This threshold implies that 20% of the time a particular location will be in drought. The effect of the choice of another threshold on the performance of drought indicators needs to be investigated. For instance, if a 70% threshold would have been chosen, some small flow peaks that caused the end of drought event applying a 80% threshold would not be effective anymore.

- Investigation of the effect of the rooting depth on the performance of drought indicators. In this study a rooting depth used of 50 cm was used, which reflects the rooting depth of grass (Van Lanen *et al.*, 2010b). Cropland or other vegetation types usually have another rooting depth. Layers with a high penetration resistance (e.g. shallow bedrock) also affect rooting depth.

- Use of other climate datasets (e.g. NCEP/NCAR, (Kalnay *et al.*, 1996)) to explore the effect of other meteorological input data. This could in the first place lead to a different classification of the climate. Secondly, drought indicator performance could also be affected.

- Use another method to identify drought events and its associated characteristics. In this study the threshold method was used, which is has a duration nature. The 80% threshold was used in this study, which means that the flux or state is equaled or exceeded to 80% of the time. For example, Peters *et al.* (2003) propose a volume-based criterion.

- Use of a Global Hydrological Model (GHM) or a Land Surface Model (LSM) instead of the synthetic model in this study. GHMs and LSMs use a more or less simplified representation of the actual soil and groundwater system for each cell.

- Further examination of, in particular the dependence between MAPVT and QVT (Annex III), and how droughts in precipitation are related to discharge droughts. The MAPVT and the QVT could be used for this purpose since both indicators have the same physical dimensions and calculation procedure (Sections 3.5.1 and 3.5.3). Understanding the mechanism of drought propagation will substantially increase the relevance of drought forecasting, since hydrological droughts can then be predicted from droughts in precipitation.

- Investigation of the performance of MAPVT, using another moving average. In this study, the 30 day centered moving average was used (Section 3.5.1). However, for real-time monitoring this approach would not work, since no future data are available. Hence, the moving average of the previous 30 days is proposed.

- Compare the drought characteristics of both the original classification of the SPI (Table 3.4) and of the drought selected with the threshold method (Section 3.4). Severe and extreme droughts determined with the SPI can be compared with the droughts identified with the threshold method. This comparison will demonstrate if the discrete approach of the SPI is suited for drought detection.
- Use of continuous climate classification systems for impact studies. These systems offer the opportunity to determine mathematical relations between drought characteristics (e.g. average drought deficit volume) and climate variables (e.g. precipitation). With these relations, for example, the effect of climate change (e.g. higher precipitation) could be explored.

References

Agboma, C.O., Yirdaw, S.Z., & Snelgrove, K.R. 2009. Intercomparison of the Total Storage Deficit Index (TSDI) over two Canadian Prairie catchments. *Journal of Hydrology*, **374**, 351 – 359.

Allen, R.G., Pereira, L.S., Raes, D., & Smith, M. 2006. *FAO Irrigation and Drainage Paper No. 56 - Crop Evapotranspiration*. Food and Agriculture Organization.

Alley, W.M. 1984. The Palmer Drought Severity Index: Limitations and Assumptions. *Journal of Climate and Applied Meteorology*, **23**, 1100 – 1109.

Byun, H.R., & Wilhite, D.A. 1999. Objective quantification of drought severity and duration. *Bulletin of the American Meteorological Society*, **12**, 2747 – 2756.

Cutore, P., Di Mauro, G., & Cancelliere, A. 2009. Forecasting Palmer Index using neural networks and climatic indexes. *Journal of Hydrologic Engineering*, **14**, 588 – 595.

Dai, A., Trenberth, K.E., & Qian, T. 2004. A global dataset of Palmer Drought Severity Index for 1870 - 2002: Relationship with soil moisture and effects of surface warming. *Journal of Hydrometeorology*, **5**, 1117 – 1130.

Deni, S.M., & Jemain, A.A. 2009. Mixed log series geometric distribution for sequences of dry days. *Atmospheric Research*, **92**, 236 – 243.

Dracup, J.A., Lee, K.S., & Paulson Jr, E.G. 1980. On the definition of droughts. *Water Resources Research*, **16**(2), 297 – 302.

Edwards, D.C., & McKee, T.B. 1997. Characteristics of 20th century drought in the United States at multiple time scales. *Climatology Report*, **97-2**, Department of Atmospheric Science, Colorado state University, Fort Collins.

Fleig, A.K., Tallaksen, L.M., Hisdal, H., & Demuth, S. 2006. A global evaluation of streamflow drought characteristics. *Hydrology and Earth System Sciences*, **10**, 535 – 552.

Foley, J.C. 1957. *Droughts in Australia : review of records from earliest years of settlement*. Australian Bureau of Meteorology.

Fuchs, T. 2008. *GPCC Annual Report for year 2008*. Annual report. available at: reports and publications section of the GPCC homepage - gpcc.dwd.de.

Garen, D.C. 1992. Revised Surface-Water Supply Index for western United States. *Journal of Water Resources Planning and Management*, **119**, 437 – 454.

Geiger, R. 1954. Landolt-Börnstein. *Chap. Klassifikation der Klimate nach W. Kppen, pages 603 – 607 of: Zahlenwerte und Funktionen aus Physik, Chemie, Astronomie, Geophysik un Technik*. alte Serie, vol. 3. Springer, Berlin.

Geiger, R. 1961. *Überarbeitete Neuausgabe von Geiger, R.: Köppen-Geiger / Klima der Erde*. Wandkarte 1:16 Mill. Klett-Perthes, Gotha.

Gibbs, W.J., & Maher, J.V. 1967. *Rainfall deciles as drought indicators*. Australian Bureau of Meteorology.

Guttman, N.B. 1999. Accepting the Standardized Precipitation Index: A calculation algorithm. *Journal of the American Water Resource Association*, **35**, 311 – 322.

Hayes, M.J. 1999. *Drought Indices*. http://www.geology.um.maine.edu/ges121/lectures/22-drought/indices1.pdf, viewed on 30-11-2009. National Drought Mitigation Center.

Hayes, M.J. 2006. *What is Drought?: Drought indices*. http://drought.unl.edu/whatis/indices.htm, viewed on 01-12-2009. National Drought Mitigation Center.

Hayes, M.J. (ed). 2007. *Drought Indices.* Intermountain West Climate Summary. Western Water Assessment.

Heim, R.R. 2002. A review of Twentieth-Century drought indices used in the United States. *Bulletin of the American Meteorological Society*, **83**, 1149 – 1165.

Hisdal, H., Tallaksen, L.M., Peters, E., Stahl, K., & Zaidman, M. 2001. *Drought event definition, Technical Report No. 6.* Tech. rept. Final report to the Europian Union - ARIDE project.

Hisdal, H., Tallaksen, L.M., Clausen, B., Peters, E., & Gustard, A. 2004. Hydrological Drought Characteristics. *Pages 139 – 198 of:* Tallaksen, L.M, & Lanen, H.A.J. (eds), *Hydrological Drought: Processes and estimation methods for streamflow and groundwater.* Development in Water Science, no. 48. Elsevier.

Holdridge, L.R. 1947. Determination of World Plant Formations From Simple Climatic Data. *Science*, **105**, 367 – 368.

Institute of Hydrology. 1980. *Low flow studies.* Tech. rept. Institute of Hydrology, Wallingford, UK.

Kalnay, E., Kanamitsu, M., Kistler, R., Collins, W., Deaven, D., Gandin, L., Iredell, M., Saha, S., White, G., Woollen, J., Zhu, Y., Leetmaa, A., & Reynolds, R. 1996. The NCEP/NCAR 40-Year Reanalysis Project. *Bulletin of the American Meteorological Society*, **77**, 437 – 471.

Karl, T.R. 1986. The Sensitivity of the Palmer Drought Severity Index and Palmer's Z-Index to their Calibration Coefficients Including Potential Evapotranspiration. *Journal of Climate and Applied Meteorology*, **25**, 77 – 86.

Keyantash, J., & Dracup, J.A. 2002. The quantification of drought: An evaluation of drought indices. *Bulletin of the American Meteorological Society*, **83**, 1167 – 1180.

Keyantash, J.A., & Dracup, J.A. 2004. An aggregate drought index: Assessing drought severity based on fluctuations in the hydrologic cycle and surface water storage. *Water Resources Research*, **40**, W09304.

Kim, D.W., Byun, H.R., & Choi, K.S. 2009. Evaluation, modification and application of the Effective Drought Index to 200-year drought climatology of Seoul, Korea. *Journal of Hydrology*, **378**, 1 – 12.

Kinninmonth, W.R., Voice, M.E., Beard, G.S., de Hoedt, G.C., & Mullen, C.E. 2000. Australian climate service for drought management. *In:* Wilhite, D.A. (ed), *Drought: A global assessment.* Ed., Routledge.

Köppen, W. 1900. Versuch einer Klassifikation der Klimate, vorzugsweise nach ihren Beziehungen zur Pflanzenwelt. *Geografische Zeitschrift*, **6**, 593 – 611, 657 – 679.

Kottek, M., Grieser, J., Beck, C., Rudolf, B, & Rubel, F. 2006. World Map of the Köppen-Geiger climate classification updated. *Meteorologische Zeitschrift*, **15**, 259 – 263.

Lee, S.H. 1998. Flood simulation with the variation of runoff coefficient in tank model. *Journal of Korea Water Resource Association*, **31**, 3 – 12. (In korean).

McKee, T.B., Doesken, N.J., & Kleist, J. 1993. The relationship of drought frequency and duration to time scales. *In: Eighth Conference on Applied Climatology.* 17-22 January, Anaheim, California.

Mekis, E., & Vincent, L.A. 2005. Precipitation and temperature related climate indices for Canada. *In: Proceedings of the 16th Symposium on Global Change and Climate Variations. Preprints of the 85th AMS Annual Meeting, San Diego, California.*

Mendicino, G., Senatore, A., & Versace, P. 2008. A Groundwater Resource Index for drought monitoring and forecasting in a mediterranean climate. *Journal of Hydrology*, **357**, 282 – 302.

Mitchell, T.D., & Jones, P.D. 2005. An improved method of constructing a database of monthly climate observations and associated high-resolution grids. *International Journal of Climatology*, **25**, 693 – 712.

Narasimhan, B., & Srinivasan, R. 2005. Development and evaluation of Soil Moisture Deficit Index (SMDI) and Evapotranspiration Deficit Index (ETDI) for agricultural drought monitoring. *Agricultural and Forest Meteorology*, **133**(July), 69 – 88.

Naresh Kumar, M., Murthy, C.S., Sesha Sai, M.V.R., & Roy, P.S. 2009. On the use of Standardized Precipitation Index (SPI) for drought intensity assessment. *Meteorological applications*, **16**, 381 – 389.

National Drought Mitigation Centre. 2009. *Historical Maps of the Palmer Drought Index*. http://drought.unl.edu/whatis/palmer/pdsihist.htm, viewed on 10-02-2009.

Niemeijer, S. 2008 (12 - 14 June). *New drought indices*. Presentation on 1^{st} international conference on drought management: Scientific and technological innovations, Zaragoza.

Oladipo, E.O. 1985. A comparative performance analysis of three meteorological drought indices. *Journal of Climatology*, **5**, 655 – 664.

Palmer, W.C. 1965. Meteorological drought. *U.S. Weather Bureau Research Paper*, **No. 45**, 58 pp.

Palmer, W.C. 1968. Keeping track of moisture conditions, nationwide: The new Crop Moisture Index. *Weatherwise*, **21**, 156 – 161.

Peel, M.C., Finlayson, B.L., & McMahon, T.A. 2007. Updated world Köppen-Geiger climate classification map. *Hydrology and Earth System Sciences*, **11**, 1633 – 1644.

Peters, E., & van Lanen, H.A.J. 2005. Separation of base flow from streamflow using groundwater levels - illustrated for the Pang catchment (UK). *Hydrological Processes*, **19**(4), 921 – 936.

Peters, E., Torfs, P.J.J.F., van Lanen, H.A.J., & Bier, G. 2003. Propagation of drought through groundwater - a new approach using linear reservoir theory. *Hydrological Processes*, **17**, 3023 – 3040.

Peterson, T.C., & Vose, R.S. 1997. An overview of the Global Historical Climatology Network temperature database. *Bulletin of the American Meteorological Society*, **12**, 2837 – 2849.

Redmond, K. 2000. Monitoring Drought Using the Standardized Precipitation Index. *Pages 145 – 158 of:* Wilhite, D.A. (ed), *Drought: A global assessment (vol. 1)*. Routledge.

Ritzema, H.P. 1994. Subsurface Flow to Drains. *Pages 263 – 303 of:* Ritzema, H.P (ed), *Drainage Principles and Applications*, second edn. International Institute for Land Reclamation and Improvement.

Rubel, F., & Kottek, M. 2010. Observed and projected climate shifts 1901-2100 depicted by worldmaps of the Köppen-Geiger climate classification. *Meteorologische Zeitschrift*, **19**, acepted.

Rudolf, B., & Schneider, U. 2005. Calculation of gridded precipitation data for the global land-surface using in-situ gauge observations. *In:* 2^{nd} *Workshop of the International Precipitation Working Group*. Global Precipitation Climatology Centre (GPCC). available at: reports and publications section of the GPCC homepage - gpcc.dwd.de.

Schenka, H.J, & Jackson, R.B. 2005. Mapping the global distribution of deep roots in relation to climate and soil characteristics. *Geoderma*, **126**, 129 – 140.

Schneider, U., Fuchs, T., Meyer-Christoffer, A., & Rudolf, B. 2008. *Global precipitation analysis products of the GPCC*. Global Precipitation Climatology Centre (GPCC). available at: reports and publications section of the GPCC homepage - gpcc.dwd.de.

Seibert, J. 2005 (November). *HBV light version 2 Users Manual*. Stockholm University, Department of Physical Geography and Quaternary Geology.

Shafer, B.A., & Dezman, L.E. 1982. Development of a Surface Water Supply Index (SWSI) to assess the severity of drought conditions in snowpack runoff areas (Colorado). *Pages 164 – 175 of: Product of 50th Western Snow Conference*.

Sheffield, J., & Wood, F. 2007. Characteristics of global and regional drought, 1950 - 2000: Analysis of soil moisture data from off-line simulation of the terrestrial hydrologic cycle. *Journal of Geophysical Research*, **112**, D17115.

Sheffield, J., Andreadis, K.M., Wood, E.F., & Lettenmaier, D.P. 2009. Global and continental drought in the second half of the twentieth century: Severity-Area-Duration analysis and temperol variability of large-scale events. *Journal of Climate*, **22**, 1962 – 1981.

Shim, S.B., Kim, M.S., & Shim, K.C. 1998. Flood inflow forecasting on multipurpose reservoir by neural network. *Journal of Korea Water Resource Association*, **31**, 45 – 57.

Simmers, I. 2003. *Understanding Water in a Dry Environment: Hydrological Processes in Arid and Semi-Arid Zones*. International association of hydrogeologists. Balkema Publishers. Lisse, The Netherlands.

Smakhtin, V.U. 2001. Low flow hydrology: a review. *Journal of Hydrology*, **240**, 147 – 186.

Smakhtin, V.U, & Hughes, D.A. 2007. Automated estimation and analyses of meteorological drought characteristics from monthly rainfall data. *Environmental Modelling & Software*, **22**, 880 – 890.

Soul, P.T. 1992. Spatial patterns of drought frequency and duration in the contiguous USA based on multiple drought event definitions. *International Journal of Climatology*, **12**, 11 – 24.

Stahl, K., & Hisdal, H. 2004. Hydroclimatology. *Pages 19 – 52 of:* Tallaksen, L.M, & Lanen, H.A.J. (eds), *Hydrological Drought: Processes and estimation methods for streamflow and groundwater*. Development in water science, no. 48. Elsevier.

Steinemann, A, Hayes, M.J, & Cavalcanti, L. 2005. Drought Indicators and Triggers. *In:* Wilhite, D.A. (ed), *Drought and Water Crises: Science, Technology, and Management Issues*. CRC Press.

Stull, R. 2000. *Meteorology for scientists and engineers*. 2^{nd} edn. Brooks/Cole Thomson learning. pg 99.

Tallaksen, L.M, & van Lanen, H.A.J. 2004. *Hydrological Drought: Processes and estimation methods for streamflow and groundwater*. Development in water science, no. 48. Elsevier.

Tallaksen, L.M., Madsen, H., & Clausen, B. 1997. On the definition and modelling of streamflow drought duration and deficit volume. *Hydrological Sciences*, **42**(1), 15 – 33.

Tallaksen, L.M., Hisdal, H., & van Lanen, H.A.J. 2009. Space-time modelling of catchment scale drought characteristics. *Journal of Hydrology*, **375**, 363 – 372.

Thornthwaite, C.W. 1948. An Approach toward a Rational Classification of Climate. *Geographical Review*, **38**, 54–94.

Uppala, S. M., Kallberg, P. W., Simmons, A. J., Andrae, U., Bechtold, V. Da Costa, Fiorino, M., Gibson, J. K., Haseler, J., Hernandez, A., Kelly, G. A., Li, X., Onogi, K., Saarinen, S., Sokka, N., Allan, R. P., Andersson, E., Arpe, K., Balmaseda, M. A., Beljaars, A. C. M., Berg, L. Van De, Bidlot, J., Bormann, N., Caires, S., Chevallier, F., Dethof, A., Dragosavac, M., Fisher, M., Fuentes, M., Hagemann, S., Hólm, E., Hoskins, B. J., Isaksen, L., Janssen, P. A. E. M., Jenne, R., McNally, A. P., Mahfouf, J. F., Morcrette, J. J., Rayner, N. A., Saunders, R. W., Simon, P., Sterl, A., Trenberth, K. E., Untch, A., Vasiljevic, D., Viterbo, P., & Woollen, J. 2005. The ERA-40 re-analysis. *Quarterly Journal of the Royal Meteorological Society*, **131**, 2961–3012.

Van Lanen, H.A.J., & Tallaksen, L.M. 2007. Hydrological drought, climate variability and changes. *Pages 488 – 493 of:* Heinonen, M. (ed), *Climate and Water. Proceding of the third international conference on climate and water*. Helsinki, Finland, 3-6 september 2007. SYKE.

Van Lanen, H.A.J., & Tallaksen, L.M. 2008. Drought in Europe. *Pages 98 – 108 of:* Lambert, M., Daniell, T., & Leonard, M. (eds), *Procedings Water Down Under*. Adelaide, Australia, 14-17 April 2008. Engineers Australia.

Van Lanen, H.A.J., Weerts, A.H., Kroon, T., & Dijksma, R. 1996. Estimation of groundwater recharge in areas with deep groundwater tables using transient groundwater flowing modelling. *Proceedings of the International Conference on 'Calibration adn Reliability in Groundwater Modelling'*, **Golden, USA**(September 1996), Pages 307 – 316.

Van Lanen, H.A.J., M., Fendeková, Kupczyk, E., Kasprzyk, A., & Pokojski, W. 2004. Flow generating processes. *Pages 53 – 98 of:* Tallaksen, L.M, & van Lanen, H.A.J. (eds), *Hydrological Drought: Processes and estimation methods for streamflow and groundwater*. Development in water science, no. 48. Elsevier.

Van Lanen, H.A.J., Wanders, N, Tallaksen, L.M., & van Loon, A.F. 2010a. *Drought analysis on a global scale using a synthetic hydrological model*. Tech. rept. EU WATCH (Water and global Change) project. (in progress).

Van Lanen, H.A.J., Wanders, N, & van Loon, A.F. 2010b. *Synthetic hydrological model - illustrated with drought using Watch Forcing Data*. Tech. rept. EU WATCH (Water and global Change) project. (in progress).

Van Loon, A.F., van Lanen, H.A.J., van Hisdal, H., Tallaksen, L.M., Fendeková, M., Oosterwijk, J., Horvát, O., & Machlica, A. 2010. Understanding hydrological winter drought in Europe. *IAHS Publ*, **accepted**.

Van Rooy, M.P. 1965. A Rainfall anomaly index (RAI) independent of time and space. *Notos*, **14**, 43 – 48.

Van Stiphout, T.P.J., van Lanen, H.A.J., Boersma, O.H., & Bouma, J. 1987. The effect of bypass flow and internal catchment of rain on the water regime in a clay loam grassland soil. *Journal of Hydrology*, **95**, 1 – 11.

Vincente-Serrano, S.M., Gonzalez-Hidalgo, J.C., Luis, M., & Raventos, J. 2004. Drought pattern in the Mediterranean area: the Valencia region (eastern Spain). *Climate Research*, **26**, 5 – 15.

Weber, L., & Nkemdirim, L. 1998. Palmer's drought indices revisited. *Geografiska Annaler*, **80A**, 153 – 172.

Weedon, G.P., Gomes, S., Viterbo, P., Österle, H., Adam, J.C., Bellouin, N., Boucher, O., & Best, M. 2010. *The WATCH Forcing Data 1958-2001: A Meteorological forcing dataset for land surface- and hydrological models.* Tech. rept. 22. EU WATCH (Water and global Change) project.

Wells, N., Goddard, S., & Hayes, M.J. 2004. A Self-Calibrating Palmer Drought Severity Index. *Journal of Climate*, **17**, 2335 – 2351.

Wilhite, D.A. 2000. *Drought: A global assessment*. Ed., Routledge.

Wilhite, D.A., Svoboda, M.D., & Hayes, M.J. 2005. Monitoring drought in the United States: status and trends. *Pages 121 – 131 of:* Boken, K, Cracknell, A.P., & Heathcote, R.L. (eds), *Monitoring and Predicting Agricultural Drought: A Global Study*. Oxford University Press.

Willeke, G., Hosking, J.R.M., Wallis, J.R., & Guttman, N.B. 1994. The National Drought Atlas. *Institute for water resources report*, **Report No 94-NDS-4**, U.S. Army Corps of Engineers.

World Meteorological Organization. 2009 (December). *Experts agree on a universal drought index to cope with climate risks*. Press release No. 872.

World Meteorological Organization. 2010. *Climate Variability and Extremes*. http://www.wmo.int/pages/themes/climate/climate_variability_extremes.php, viewed on 12-03-2010.

Wösten, J.H.M., Veerman, G.J., de Groot, W.J.M., & Stolte, J. 2001. *Waterretentie,- en doorlatendheidskarakteristieken van boven,- en ondergronden in Nederland: de Staringreeks*. Tech. rept. 153. Alterra - Wageningen University.

Wu, H., Svoboda, M.D., Hayes, M.J., Wilhite, D.A., & Fujiang, W. 2006. Approproate application of the standardized precipitation index in arid locations and dry seasons. *International Journal of Climatology*, **27**, 65 – 79.

Yevjevich, V. 1967. An objective approach to definition and investigation of continental hydrological droughts. *Hydrology papers*, **23**, Colorado state university, Fort Collins, USA.

Yirdaw, S.Z, Snelgrove, K.R., & Agboma, C.O. 2008. GRACE satellite observations of terrestrial moisture changes for drought characterization in the Canadian Prairie. *Journal of Hydrology*, **356**, 84 – 92.

Appendices

I Drought indicators found in literature

1 Aggregate Drought Index (ADI)
2 Agricultural Drought Index (DTx)
3 Anomaly of Normalized Difference Vegetation Index (NDVIA)
4 Base Flow Index (BFI)
5 Bhalme and Mooly Drought Index (BMDI)
6 Consecutive Dry Days (CDD)
7 Corn Drought Index (CDI)
8 Crop Moisture Index (CMI)
9 Crop Specific Drought Index (CSDI)
10 Cumulative Precipitation Anomaly (CPA)
11 Cumulative Streamflow Anomaly (CSA)
12 Deciles (DECILES)
13 Drought Area Index (DAI)
14 Drought Frequency Index (DFI)
15 Drought Severity Index (DSI)
16 Effective Drought Index (EDI)
17 Evapotranspiration Deficit Index (ETDI)
18 Global Vegetation Water moisture Index (GVWI)
19 Groundwater Resource Index (GRI)
20 Keetch-Byam Drought Index (KBDI)
21 Leaf Water Content Index (LWCI)
22 Low Flow Index (Q90)
23 Modified Perpendicular Drought Index (MPDI)
24 Normalized Burn Ratio (NBR)
25 Normalized Difference Infrared Index (NDII)
26 Normalized Difference Vegetation Index (NDVI)
27 Normalized Difference Water Index (NDWI)
28 Normalized Multi-band Drought Index (NMDC)
29 Palfai Aridity Index (PAI)
30 Palmer Drought Severity Index (PDSI)
31 Palmer Hydrological Drought Index (PHDI)
32 Palmer Modified Drought Index (PMDI)
33 Palmer Z-index (Z-index)
34 Percentage of Normal (PN)
35 Perpendicular Drought Index (PDI)
36 Rainfall Anomaly Index (RAI)
37 Reclamation Drought Index (RDI)
38 Reconnaissance Drought Index (RDI)
39 Regional Streamflow Deficiency Index (RSDI)
40 Remote Sensing Drought Risk Index (RDRI)
41 Simple Ratio Water Index (SRWI)
42 Soil Moisture Deficit Index (SMDI)
43 Soil Moisture Drought Index (SMDI)
44 Soybean Drought Index (SCI)
45 Sperling Drought Index (SDI)
46 Standardized Anomaly Index (SAI)
47 Standardized Precipitation Index (SPI)
48 Standardized Vegetation Index (SVI)
49 Surface Water Supply Index (SWSI)
50 Temperature Condition Index (TCI)
51 Total Storage Deficit Index (TSDI)

52 Vegetation Condition Albedo Drought Index (VCADI)
53 Vegetation Condition Index (VCI)
54 Vegetation Drought Response Index (VegDRI)
55 Vegetation Health Index (VHI)
56 Water Index (WI)

Reference	Indicator(s)
Hayes (1999)	8, 12, 30, 34, 36, 47, 49
Hayes (2006)	8, 12, 30, 34, 36, 47, 49
Hayes (2007)	8, 28, 30, 33, 32, 47, 49
Heim (2002)	8, 18, 28, 29, 45, 47, 51
Keyantash & Dracup (2002)	8, 10–12, 12, 28, 29, 31, 34, 47, 49
Keyantash & Dracup (2004)	1
Mekis & Vincent (2005)	6
Mendicino *et al.* (2008)	18
Narasimhan & Srinivasan (2005)	42, 51
Niemeijer (2008)	2–5, 7–19, 21–41, 43–50 ,52–56
Oladipo (1985)	5, 30, 36
Steinemann *et al.* (2005)	34, 47

II Köppen-Geiger map of the world

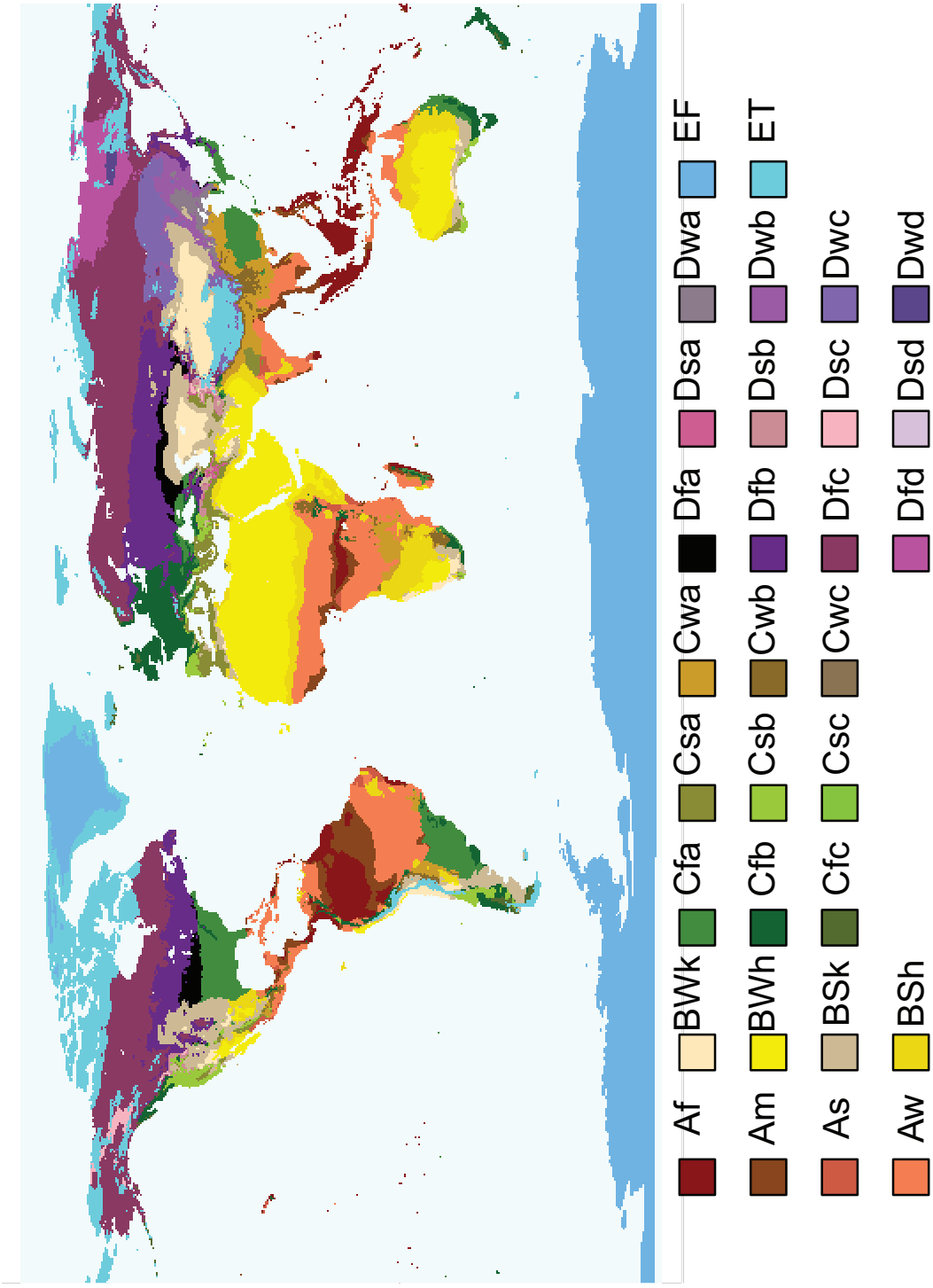

Figure II.1: World map of Köppen-Geiger based upon WATCH Forcing Data.

III Intercorrelation of selected drought indicators (Table 4.1)

Table III.1: Correlations of all selected indicators for a location in Brazil.

	SPI	EDI	MAPVT	CDD	PDSI	Z-Index	SMDI	SVT	ASSM	TSDI	GRI	SSI	QVT	ADI
SPI	1	0.33	0.43	-0.14	0.46	0.92	0.58	0.28	0.27	0.39	0.33	0.31	0.3	-0.03
EDI	0.33	1	0.53	-0.25	0.54	0.37	0.56	0.7	0.7	0.58	0.56	0.72	0.76	0.11
MAPVT	0.43	0.53	1	-0.4	0.3	0.45	0.55	0.82	0.82	0.27	0.23	0.19	0.2	0
CDD	-0.14	-0.25	-0.4	1	-0.071	-0.12	-0.39	-0.44	-0.44	-0.059	-0.044	-0.033	-0.048	0.12
PDSI	0.46	0.54	0.3	-0.071	1	0.55	0.4	0.22	0.21	0.85	0.84	0.79	0.77	0.1
Z-Index	0.92	0.37	0.45	-0.12	0.55	1	0.54	0.27	0.26	0.42	0.37	0.34	0.33	0.1
SMDI	0.58	0.56	0.55	-0.39	0.4	0.54	1	0.67	0.67	0.43	0.34	0.36	0.35	0.12
SVT	0.28	0.7	0.82	-0.44	0.22	0.27	0.67	1	1	0.23	0.18	0.25	0.26	0.09
ASSM	0.27	0.7	0.82	-0.44	0.21	0.26	0.67	1	1	0.23	0.18	0.25	0.25	0.1
TSDI	0.39	0.58	0.27	-0.059	0.85	0.42	0.43	0.23	0.23	1	0.99	0.9	0.9	0.1
GRI	0.33	0.56	0.23	-0.044	0.84	0.37	0.34	0.18	0.18	0.99	1	0.9	0.91	-0.08
SSI	0.31	0.72	0.19	-0.033	0.79	0.34	0.36	0.25	0.25	0.9	0.9	1	0.96	-0.02
QVT	0.3	0.76	0.2	-0.048	0.77	0.33	0.35	0.26	0.25	0.9	0.91	0.96	1	0.01
ADI	-0.03	0.11	0	0.12	0.1	0.1	0.12	0.09	0.1	0.1	-0.08	-0.02	0.01	1

Table III.2: Correlations of all selected indicators for a location in Papua New Guinea.

	SPI	EDI	MAPVT	CDD	PDSI	Z-Index	SMDI	SVT	ASSM	TSDI	GRI	SSI	QVT	ADI
SPI	1	0.64	0.01	-0.15	0.47	0.39	0.35	0.38	0.38	0.49	0.49	0.37	0.47	0.26
EDI	0.64	1	0.22	-0.18	0.74	0.71	0.23	0.34	0.34	0.82	0.82	0.75	0.9	0.29
MAPVT	0.01	0.22	1	-0.08	0.02	0.02	-0.2	0.12	0.12	0	0	0	0.08	0
CDD	-0.15	-0.18	-0.08	1	-0.07	-0.06	-0.49	-0.53	-0.53	-0.09	-0.08	-0.05	-0.09	-0.37
PDSI	0.47	0.74	0.02	-0.07	1	0.89	0.15	0.21	0.21	0.87	0.88	0.86	0.84	0.17
Z-Index	0.39	0.71	0.02	-0.06	0.89	1	0.13	0.19	0.19	0.92	0.93	0.93	0.89	0.15
SMDI	0.35	0.23	-0.2	-0.49	0.15	0.13	1	0.68	0.68	0.18	0.16	0.1	0.12	0.62
SVT	0.38	0.34	0.12	-0.53	0.21	0.19	0.68	1	1	0.22	0.21	0.18	0.21	0.52
ASSM	0.38	0.34	0.12	-0.53	0.21	0.19	0.68	1	1	0.22	0.21	0.18	0.21	0.52
TSDI	0.49	0.82	0	-0.09	0.87	0.92	0.18	0.22	0.22	1	1	0.98	0.95	0.18
GRI	0.49	0.82	0	-0.08	0.88	0.93	0.16	0.21	0.21	1	1	0.98	0.96	0.17
SSI	0.37	0.75	0	-0.05	0.86	0.93	0.1	0.18	0.18	0.98	0.98	1	0.94	0.12
QVT	0.47	0.9	0.08	-0.09	0.84	0.89	0.12	0.21	0.21	0.95	0.96	0.94	1	0.17
ADI	0.26	0.29	0	-0.37	0.17	0.15	0.62	0.52	0.52	0.18	0.17	0.12	0.17	1

Table III.3: Correlations of all selected indicators for a location in Australia.

	SPI	EDI	MAPVT	CDD	PDSI	Z-Index	SMDI	SVT	ASSM	TSDI	GRI	SSI	QVT	ADI
SPI	1	0.1	0.02	-0.01	0.07	0.06	0.07	0.06	0.06	0.06	0.06	0.05	0.06	-0.03
EDI	0.1	1	-0.08	-0.28	0.67	0.67	0.48	0.6	0.6	0.64	0.59	0.53	0.61	-0.16
MAPVT	0.02	-0.08	1	-0.17	0.02	0.02	0.01	-0.03	-0.03	0	0	0	-0.04	0
CDD	-0.01	-0.28	-0.17	1	-0.12	-0.11	-0.67	-0.24	-0.24	-0.05	-0.02	0	-0.02	0.09
PDSI	0.07	0.67	0.02	-0.12	1	0.96	0.28	0.24	0.24	0.82	0.82	0.77	0.81	-0.11
Z-Index	0.06	0.67	0.02	-0.11	0.96	1	0.24	0.22	0.22	0.86	0.86	0.82	0.86	-0.11
SMDI	0.07	0.48	0.01	-0.67	0.28	0.24	1	0.52	0.52	0.23	0.17	0.12	0.17	-0.18
SVT	0.06	0.6	-0.03	-0.24	0.24	0.22	0.52	1	1	0.3	0.2	0.13	0.21	-0.19
ASSM	0.06	0.6	-0.03	-0.24	0.24	0.22	0.52	1	1	0.3	0.2	0.13	0.21	-0.19
TSDI	0.06	0.64	0	-0.05	0.82	0.86	0.23	0.3	0.3	1	0.99	0.97	0.99	-0.12
GRI	0.06	0.59	0	-0.02	0.82	0.86	0.17	0.2	0.2	0.99	1	0.99	1	-0.1
SSI	0.05	0.53	0	0	0.77	0.82	0.12	0.13	0.13	0.97	0.99	1	0.98	-0.08
QVT	0.06	0.61	-0.04	-0.02	0.81	0.86	0.17	0.21	0.21	0.99	1	0.98	1	-0.1
ADI	-0.03	-0.16	0	0.09	-0.11	-0.11	-0.18	-0.19	-0.19	-0.12	-0.1	-0.08	-0.1	1

Table III.4: Correlations of all selected indicators for a location in Germany.

	SPI	EDI	MAPVT	CDD	PDSI	Z-Index	SMDI	SVT	ASSM	TSDI	GRI	SSI	QVT	ADI
SPI	1	0.65	0	-0.25	0.38	0.26	0.62	0.49	0.46	0.23	0.19	0.11	0.19	0.28
EDI	0.65	1	0.04	-0.21	0.68	0.62	0.5	0.49	0.46	0.55	0.52	0.46	0.56	0.22
MAPVT	0	0.04	1	-0.06	-0.01	0	0.03	0.15	0.16	0	0	0	-0.04	0
CDD	-0.25	-0.21	-0.06	1	-0.13	-0.09	-0.41	-0.32	-0.31	-0.06	-0.03	-0.01	-0.04	-0.24
PDSI	0.38	0.68	-0.01	-0.13	1	0.82	0.36	0.35	0.33	0.68	0.66	0.62	0.64	0.16
Z-Index	0.26	0.62	0	-0.09	0.82	1	0.23	0.24	0.23	0.89	0.88	0.86	0.85	0.1
SMDI	0.62	0.5	0.03	-0.41	0.36	0.23	1	0.72	0.64	0.17	0.12	0.05	0.11	0.39
SVT	0.49	0.49	0.15	-0.32	0.35	0.24	0.72	1	0.96	0.18	0.11	0.08	0.16	0.33
ASSM	0.46	0.46	0.16	-0.31	0.33	0.23	0.64	0.96	1	0.17	0.1	0.07	0.14	0.33
TSDI	0.23	0.55	0	-0.06	0.68	0.89	0.17	0.18	0.17	1	1	0.99	0.97	0.07
GRI	0.19	0.52	0	-0.03	0.66	0.88	0.12	0.11	0.1	1	1	0.99	0.97	0.04
SSI	0.11	0.46	0	-0.01	0.62	0.86	0.05	0.08	0.07	0.99	0.99	1	0.97	0.02
QVT	0.19	0.56	-0.04	-0.04	0.64	0.85	0.11	0.16	0.14	0.97	0.97	0.97	1	0.04
ADI	0.28	0.22	0	-0.24	0.16	0.1	0.39	0.33	0.33	0.07	0.04	0.02	0.04	1

Table III.5: Correlations of all selected indicators for a location in Russia.

	SPI	EDI	MAPVT	CDD	PDSI	Z-Index	SMDI	SVT	ASSM	TSDI	GRI	SSI	QVT	ADI
SPI	1	0.49	0	-0.2	0.14	0.11	0.36	0.24	0.19	0.32	0.15	0.06	0.12	0.17
EDI	0.49	1	0.36	-0.19	0.33	0.29	0.4	0.46	-0.24	0.58	0.47	0.41	0.7	0.15
MAPVT	0	0.36	1	-0.01	0	0	0.22	0.59	-0.76	0	0	0	0.53	0.01
CDD	-0.2	-0.19	-0.01	1	-0.05	-0.04	-0.17	-0.18	-0.04	-0.08	-0.03	-0.02	-0.05	-0.13
PDSI	0.14	0.33	0	-0.05	1	0.9	0.12	0.08	0.07	0.68	0.64	0.64	0.48	0.05
Z-Index	0.11	0.29	0	-0.04	0.9	1	0.09	0.05	0.06	0.68	0.65	0.66	0.48	0.03
SMDI	0.36	0.4	0.22	-0.17	0.12	0.09	1	0.71	-0.18	0.28	0.32	0.18	0.37	-0.02
SVT	0.24	0.46	0.59	-0.18	0.08	0.05	0.71	1	-0.5	0.17	0.17	0.08	0.54	0.06
ASSM	0.19	-0.24	-0.76	-0.04	0.07	0.06	-0.18	-0.5	1	0.18	-0.09	-0.08	-0.62	0.18
TSDI	0.32	0.58	0	-0.08	0.68	0.68	0.28	0.17	0.18	1	0.85	0.81	0.63	0.11
GRI	0.15	0.47	0	-0.03	0.64	0.65	0.32	0.17	-0.09	0.85	1	0.94	0.75	-0.06
SSI	0.06	0.41	0	-0.02	0.64	0.66	0.18	0.08	-0.08	0.81	0.94	1	0.7	-0.08
QVT	0.12	0.7	0.53	-0.05	0.48	0.48	0.37	0.54	-0.62	0.63	0.75	0.7	1	-0.04
ADI	0.17	0.15	0.01	-0.13	0.05	0.03	-0.02	0.06	0.18	0.11	-0.06	-0.08	-0.04	1

Table III.6: Correlations of all selected indicators for a location in Canada.

	SPI	EDI	MAPVT	CDD	PDSI	Z-Index	SMDI	SVT	ASSM	TSDI	GRI	SSI	QVT	ADI
SPI	1	0.55	-0.01	-0.16	NA	NA	0.24	0.25	0.31	0.35	0.25	0.23	0.24	-0.15
EDI	0.55	1	0.25	-0.21	NA	NA	0.44	0.43	0.22	0.58	0.45	0.42	0.52	-0.26
MAPVT	-0.01	0.25	1	-0.29	NA	NA	0	0.03	-0.44	0	0	0	0.11	0
CDD	-0.16	-0.21	-0.29	1	NA	NA	-0.08	-0.08	0.01	-0.09	-0.07	-0.07	-0.1	0.06
PDSI	NA	NA	NA	NA	NA	NA	NA	NA	NA	NA	NA	NA	NA	NA
Z-Index	NA	NA	NA	NA	NA	NA	NA	NA	NA	NA	NA	NA	NA	NA
SMDI	0.24	0.44	0	-0.08	NA	NA	1	0.96	0.53	0.57	0.39	0.36	0.38	-0.44
SVT	0.25	0.43	0.03	-0.08	NA	NA	0.96	1	0.49	0.54	0.36	0.33	0.36	-0.4
ASSM	0.31	0.22	-0.44	0.01	NA	NA	0.53	0.49	1	0.51	0.31	0.29	0.17	-0.29
TSDI	0.35	0.58	0	-0.09	NA	NA	0.57	0.54	0.51	1	0.94	0.92	0.92	-0.4
GRI	0.25	0.45	0	-0.07	NA	NA	0.39	0.36	0.31	0.94	1	0.99	0.98	-0.34
SSI	0.23	0.42	0	-0.07	NA	NA	0.36	0.33	0.29	0.92	0.99	1	0.97	-0.33
QVT	0.24	0.52	0.11	-0.1	NA	NA	0.38	0.36	0.17	0.92	0.98	0.97	1	-0.33
ADI	-0.15	-0.26	0	0.06	NA	NA	-0.44	-0.4	-0.29	-0.4	-0.34	-0.33	-0.33	1

IV Meteorological drought indicators

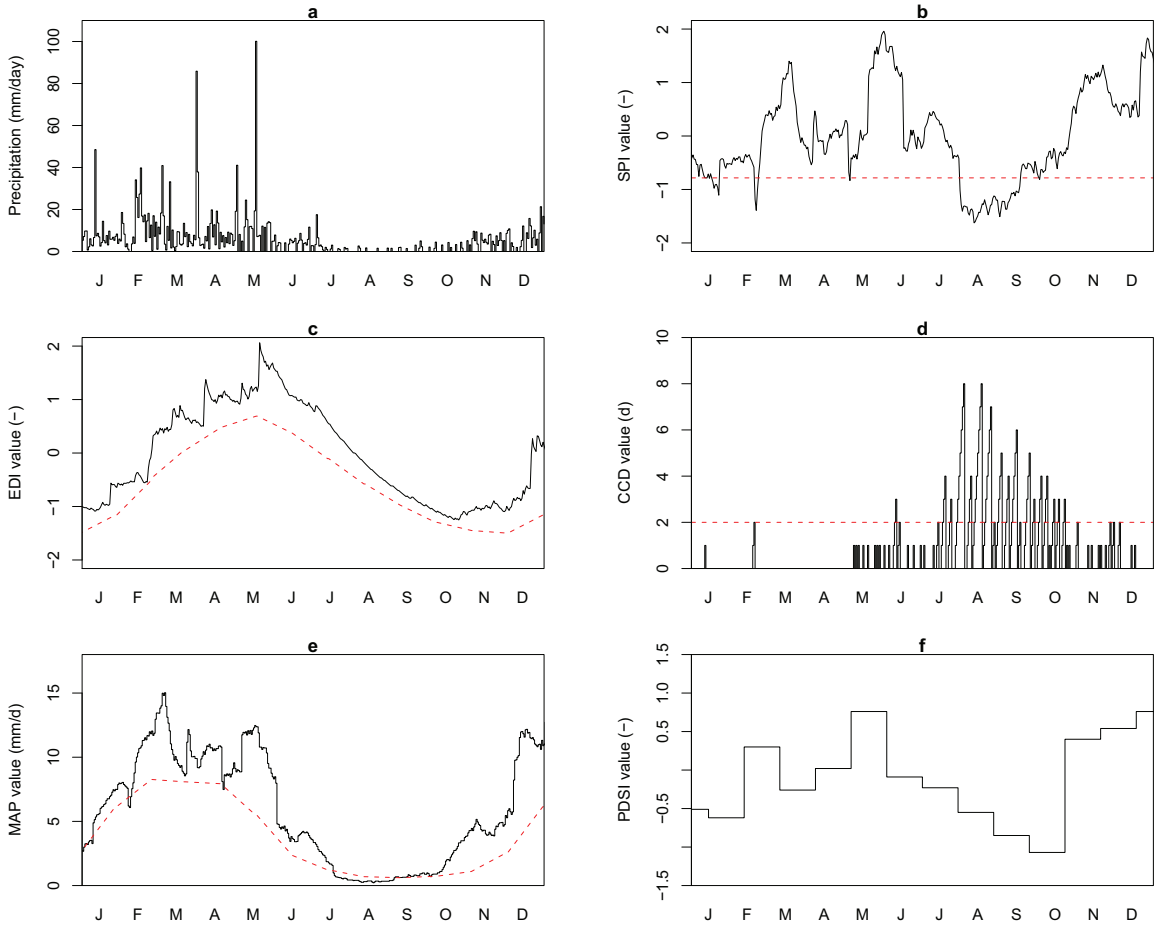

Figure IV.1: Indicator performance for January till December for a representative year (1995) for a location in Brasil (Table 4.1). Figure **a** shows the precipitation rate extracted from the WATCH Forcing Data. In figure **b** the values of the Standardized Precipitation Index (SPI) are indicated for the daily SPI. Figure **c** shows the performance of the Effective Drought Index (EDI) with a lag time of 365 days. The Number of Consecutive Dry Days (CDD) is shown in figure **d**. The performance of the Moving Average Precipitation with a Variable Threshold (MAPVT) for a 30-day moving average can be found in figure **e**. Finally the Palmer Drought Severity Index (PDSI) is described in figure **f**. For all figures the dotted red line gives the threshold, below this threshold the indicator a drought events will occur. Only for the PDSI no threshold is visible, this is due to the fact that the threshold of the PDSI is lower than the values for the selected representative year.

Table IV.1: Number of droughts per selected meteorological drought indicator for all five major climate types.

	Major climate type				
Indicator	A	B	C	D	E
SPI	207	110	236	283	302
EDI	93	69	159	251	123
CDD	662	100	892	799	427
MAPVT	189	149	226	271	230
PDSI	11	19	17	13	NA

Table IV.2: Average duration of droughts per meteorological drought indicator in days, for all five major climate types.

	Major climate type				
Indicator	A	B	C	D	E
SPI	15.52	143.3	13.61	11.35	10.64
EDI	33.42	45.26	19.82	12.61	25.41
CDD	21.07	129.2	14.79	17.11	30.22
MAPVT	16.35	29.62	14.09	11.75	14.07
PDSI	287.8	169.8	186.2	245.8	NA

Table IV.3: Average deficit volumes of droughts per meteorological drought indicator for all five major climate types.

	Major climate type				
Indicator	A	B	C	D	E
SPI (d)	10.37	1.84	9.434	6.675	5.493
EDI (d)	10.12	8.091	10.36	3.501	6.293
CDD (d)	35.64	3569	23.93	27.84	157.1
MAPVT (mm)	13.46	0.5038	8.661	3.165	1.797
PDSI (d)	2409	955.5	1571	2041	NA

V Soil moisture drought indicators

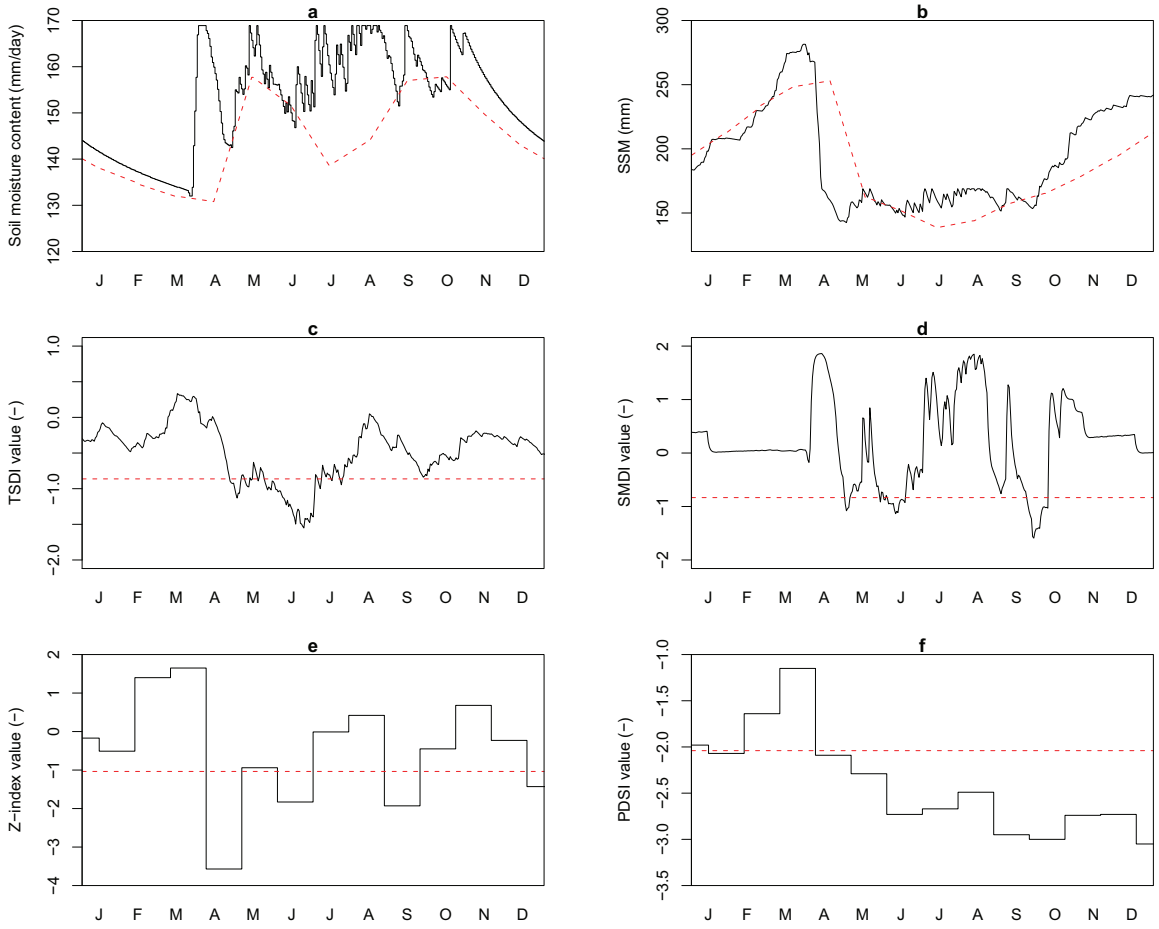

Figure V.1: Indicator performance for January till December for a representative year (1995) for a location in Russia (Table 4.1). Figure **a** soil moisture content, where the red line gives the variable threshold of the soil moisture content (SVT). Figure **b** indicates the soil moisture content plus the snow content, including the variable threshold for this indicator (ASSM). The Total Storage Deficit Index (TSDI) is presented in figure **c** and the Soil Moisture Deficit Index (SMDI) in figure **d** with a fixed threshold (red line). In figure **e** the Z-index is given, with one value per month, the Palmer Drought Severity Index PDSI is shown in figure **f**, is also given per month, for both indicators a fixed threshold is plotted.

Table V.1: Number of droughts per soil moisture drought indicator for all five major climate types.

	Major climate type				
Indicator	A	B	C	D	E
TSDI	79	59	39	109	67
SMDI	555	107	207	151	30
Moisture cont.	766	141	269	191	37
Snow + moisture cont.	766	141	314	255	71
PDSI	9	19	17	13	NA
Z-Index	70	69	70	66	NA

Table V.2: Average duration of droughts per soil moisture drought indicator in days for all five major climate types.

	Major climate type				
Indicator	A	B	C	D	E
TSDI	40.66	54.46	82.38	29.47	47.96
SMDI	5.789	30.03	15.52	21.28	107.7
Moisture cont.	4.172	28.11	11.64	15.88	87.92
Snow + moisture cont.	4.172	28.11	9.936	13.31	46.07
PDSI	351.9	169.8	186.2	245.8	NA
Z-Index	44.77	45.87	45.23	47.51	NA

Table V.3: Average deficit volumes of droughts per soil moisture drought indicator for all five major climate types.

	Major climate type				
Indicator	A	B	C	D	E
TSDI (d)	24.12	28.66	39.47	11.05	10.03
SMDI (d)	3.256	0.2457	9.000	11.52	43.08
Moisture cont. ($mm\ d$)	29.04	0.4324	187.3	85.94	941.8
Snow + moisture cont. ($mm\ d$)	29.04	0.4324	158.8	146.4	1062
PDSI (d)	387.8	78.35	130.9	170.1	NA
Z-Index (d)	17.74	7.548	12.93	9.935	NA

VI Hydrological drought indicators

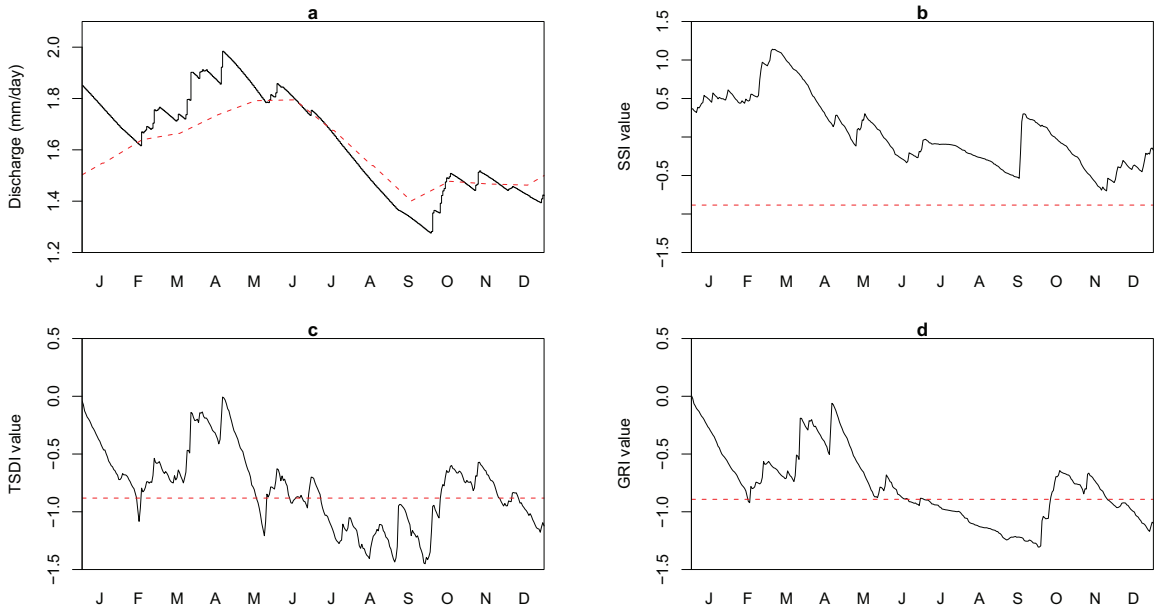

Figure VI.1: Indicator performance for January till December for a representative year (1964) for a location in Germany (Table 4.1). In figure **a** the discharge is plotted, including the variable threshold (QVT)(red dashed line). The Standardized Streamflow Index (SSI) is depicted in figure **b** with the fixe threshold as a red dashed line. In figure **c** the performance of the Total Storage Deficit Index (TSDI) can be found, including the fixe threshold of the TSDI. The Groundwater Resource Index (GRI) is presented in figure **d** with the fixe threshold of the GRI.

Table VI.1: Number of droughts per hydrological drought indicator for all five major climate types.

	Major climate type				
Indicator	A	B	C	D	E
TSDI	79	59	39	109	67
GRI	57	17	20	57	13
Q	64	19	23	51	28
SSI	56	15	11	31	11

Table VI.2: Average duration of droughts per hydrological drought indicator in days for all five major climate types.

	Major climate type				
Indicator	A	B	C	D	E
TSDI	40.66	54.46	82.38	29.47	47.96
GRI	56.37	189.0	160.7	56.37	247.2
Q	50.05	170.5	140.0	62.35	111.3
SSI	57.38	214.2	292.1	103.6	292.1

Table VI.3: Average deficit volumes of droughts per hydrological drought indicator for all five major climate types.

	Major climate type				
Indicator	A	B	C	D	E
TSDI (d)	24.12	28.66	39.47	11.05	10.03
GRI (d)	31.74	102.1	74.55	15.40	45.50
Q (mm)	31.98	8.030	14.75	3.735	2.232
SSI (d)	38.08	162.8	144.5	34.12	82.54

VII Combined drought indicators

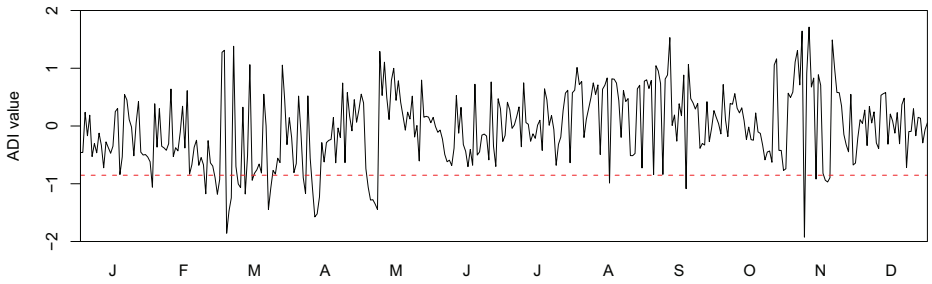

Figure VII.1: Indicator performance for January till December for a representative year (1964) for a location in Germany (Table 4.1). The performance of the Aggregated Drought Index (ADI) is given, including the threshold of the ADI (red dashed line).

Table VII.1: Number of droughts per combined drought indicator for all five major climate types.

	Major climate type				
Indicator	A	B	C	D	E
ADI	1595	1137	1380	1016	488

Table VII.2: Average duration of droughts per combined drought indicator in days for all five major climate types.

	Major climate type				
Indicator	A	B	C	D	E
ADI	2.014	2.826	2.328	3.161	6.584

Table VII.3: Average deficit volumes of droughts per combined drought indicator for all five major climate types.

	Major climate type				
Indicator	A	B	C	D	E
ADI (d)	0.617	1.896	0.612	1.437	4.634

VIII Map with locations selected on the world

Figure VIII.1: World map with selected locations for the analysis of the performance of drought indicators in different hydroclimatic regions.

IX The performance of the finally selected drought indicators for all hydroclimatic regions

Table IX.1: Mean number of droughts in days, for six selected drought indicators, all climate types, average soil and a j-factor of 250 days (1958-2002).

Climate type	# of locations	SPI	EDI	TSDI	MAPVT	SVT	QVT
Af	49	256	152	71	242	421	49
Am	38	289	183	71	266	437	44
As	20	238	116	86	210	221	23
Aw	50	249	144	92	217	259	30
BWk	37	179	91	224	173	131	2
BWh	50	64	43	202	101	87	3
BSk	50	275	129	138	201	155	8
BSh	50	224	118	147	198	228	8
Cfa	50	305	185	108	245	293	24
Cfb	48	271	199	99	249	285	36
Cfc	20	271	220	109	274	473	80
Csa	23	265	136	80	214	181	29
Csb	20	266	152	89	206	189	16
Csc	11	373	246	221	302	267	11
Cwa	30	287	162	74	247	302	35
Cwb	20	299	168	93	251	301	45
Cwc	10	268	156	102	253	293	17
Dfa	20	302	176	123	235	196	18
Dfb	50	302	217	102	266	179	28
Dfc	50	280	195	79	255	130	31
Dfd	28	279	184	74	249	89	10
Dsa	20	278	156	81	224	162	20
Dsb	20	273	148	68	221	139	21
Dsc	20	275	162	59	239	105	17
Dsd	0	NA	NA	NA	NA	NA	NA
Dwa	20	298	163	139	252	231	12
Dwb	20	306	169	127	263	177	12
Dwc	26	301	165	96	260	136	11
Dwd	20	300	212	77	259	95	18
EF	40	297	141	4	221	5	1
ET	50	276	145	53	226	87	21

Table IX.2: Mean deficit volumes of droughts, for six selected drought indicators, all climate types, average soil and a j-factor of 250 days (1958-2002).

Climate type	SPI (d)	EDI (d)	TSDI (d)	MAPVT (mm)	SVT ($mm\ d$)	QVT (mm)
Af	8.06	8.32	22.1	14.2	104	31.1
Am	6.84	4.83	20.7	10	66.6	23.5
As	7.87	6.31	15.6	6.1	76.5	14.8
Aw	7.39	4.94	14.8	6.57	91.4	16.4
BWk	7.05	7.11	3.57	0.55	9.81	$1.47 * 10^{-6}$
BWh	0.0549	9.46	2.5	0.0429	2.93	$3.6 * 10^{-5}$
BSk	7.11	6.61	6.95	1.77	89.9	0.47
BSh	7.72	5.65	3.74	3.32	36.5	2.21
Cfa	6.27	5.81	11.7	6.55	119	15.4
Cfb	7.43	6.05	13.6	5.74	100	10.3
Cfc	7.11	5.51	13.8	9.77	33.4	10.1
Csa	8.25	5.74	15.9	3.91	123	12.5
Csb	8.25	5.98	15.1	3	114	10.2
Csc	5.65	5.33	3.97	4.44	90.3	8.17
Cwa	6.48	4.02	19.3	5.54	81.5	19.4
Cwb	6.58	3.62	18	4.72	68.4	11.6
Cwc	7.38	4.36	10.1	3.22	74.5	11.1
Dfa	6.28	6.4	9.76	3.75	138	9.84
Dfb	6.39	5.53	14.7	4.03	187	9.42
Dfc	6.66	5.33	19.5	2.83	261	7.68
Dfd	6.85	4.85	14	1.71	304	3.42
Dsa	7.61	6.13	17	2.68	164	9.67
Dsb	7.8	5.97	22.2	3.37	213	11.5
Dsc	6.71	7.37	24.3	1.97	307	7.24
Dsd	NA	NA	NA	NA	NA	NA
Dwa	6.58	3.61	5.66	2.79	68.1	8.16
Dwb	5.95	3.52	8.13	2.55	133	4.78
Dwc	6.27	3.66	11.7	1.92	180	5.08
Dwd	.55	2.99	18.5	1.61	270	6.09
EF	6.42	8.04	229	1.86	893	0.0951
ET	6.73	6.66	29	1.49	216	6.73

X The performance of the finally selected drought indicators for different groundwater system response - j-factors

Table X.1: Mean number of droughts, for two selected drought indicators, all climate types, an average soil and different values of the j-factor (1958-2002).

	TSDI			QVT		
Climate type	j=100	j=250	j=1000	j=100	j=250	j=1000
Af	110	71	36	70	49	27
Am	131	71	41	62	44	26
As	135	86	46	35	23	16
Aw	137	92	50	41	30	18
BWk	258	224	192	2	2	2
BWh	230	202	168	3	3	2
BSk	181	138	91	10	8	5
BSh	192	147	93	13	8	6
Cfa	164	108	65	30	24	13
Cfb	136	99	57	48	36	21
Cfc	180	109	62	112	80	38
Csa	113	80	38	41	29	19
Csb	128	89	52	22	16	12
Csc	263	221	97	18	11	7
Cwa	119	74	42	53	35	18
Cwb	128	93	41	58	45	21
Cwc	154	102	47	24	17	8
Dfa	148	123	77	22	18	12
Dfb	135	102	59	38	28	20
Dfc	97	79	49	39	31	22
Dfd	90	74	62	20	10	6
Dsa	119	81	45	29	20	12
Dsb	100	68	41	31	21	13
Dsc	75	59	42	24	17	14
Dsd	NA	NA	NA	NA	NA	NA
Dwa	201	139	53	17	12	7
Dwb	160	127	57	18	12	6
Dwc	113	96	61	16	11	8
Dwd	90	77	43	23	18	10
EF	4	4	4	2	1	1
ET	65	53	39	33	21	13

Table X.2: Mean deficit volumes of droughts, for two selected drought indicators, all climate types, an average soil and different values of the j-factor (1958-2002).

	TSDI			QVT		
Climate type	j=100	j=250	j=1000	j=100	j=250	j=1000
Af	13.9	22.1	51.3	25.3	31.1	27.3
Am	10.7	20.7	36.6	20.9	23.5	24.1
As	8.68	15.6	27.9	12.9	14.8	16.2
Aw	8.1	14.8	26.5	13.7	16.4	17.8
BWk	3.23	3.57	3.35	$4.99 * 10^{-15}$	$1.47 * 10^{-6}$	0.00123
BWh	2.93	2.5	2.3	$1.54 * 10^{-10}$	$3.6 * 10^{-5}$	0.0135
BSk	5.52	6.95	8.2	0.0248	0.47	3.05
BSh	2.82	3.74	10.7	0.281	2.21	7.24
Cfa	6.91	11.7	19.6	12.2	15.4	13.3
Cfb	10.3	13.6	22.8	10.1	10.3	10
Cfc	9.57	13.8	18.7	10.7	10.1	8.92
Csa	10.8	15.9	31.5	11	12.5	10.2
Csb	7.96	15.1	29.3	7.56	10.2	10.6
Csc	3.83	3.97	7.59	1.43	8.17	6.13
Cwa	11.4	19.3	32.5	16.8	19.4	18.3
Cwb	12.2	18	38.1	10.2	11.6	13.4
Cwc	8.51	10.1	24.2	11.2	11.1	14.2
Dsa	7.26	9.76	16.2	7.35	9.84	9.62
Dsb	11.4	14.7	24.1	9.21	9.42	8.64
Dsc	15.4	19.5	27.7	6.99	7.68	5.91
Dsd	14.3	14	20.9	1.29	3.42	5.48
Dfa	10.6	17	31.6	7.02	9.67	9.51
Dfb	12.8	22.2	44.1	10.5	11.5	11.1
Dfc	20	24.3	31.3	5.88	7.24	4.88
Dfd	NA	NA	NA	NA	NA	NA
Dwa	4.48	5.66	22.5	1.24	8.16	17.4
Dwb	7.87	8.13	21.7	2.16	4.78	10.1
Dwc	12.7	11.7	17.9	2.44	5.08	7.86
Dwd	16.4	18.5	41.2	4.94	6.09	8.52
EF	238	229	218	0.0925	0.0951	0.167
ET	22.8	29	33.4	5.33	6.73	6.71

XI The performance of the finally selected drought indicators for different soil types

Table XI.1: Mean number of droughts, for three selected drought indicators, all climate types, j-factor of 250 days and different soil types, Coarse Sand (CS), Light Silty Loam (LSL), Sandy Loam (SL)(1958-2002).

	TSDI			SVT			QVT		
Climate type	CS	LSL	SL	CS	LSL	SL	CS	LSL	SL
Af	70	71	71	678	421	413	58	49	48
Am	78	71	77	719	437	421	54	44	43
As	77	86	81	329	221	199	35	23	22
Aw	88	92	92	439	259	233	43	30	28
BWk	372	224	218	1	131	125	7	2	2
BWh	242	202	194	1	87	84	6	3	3
BSk	118	138	145	226	155	151	17	8	6
BSh	112	147	163	210	228	219	19	8	8
Cfa	106	108	107	487	293	256	47	24	22
Cfb	102	99	99	485	285	266	58	36	34
Cfc	113	109	108	726	473	505	92	80	80
Csa	84	80	75	278	181	154	46	29	29
Csb	93	89	91	289	189	180	34	16	16
Csc	171	221	248	439	267	232	28	11	8
Cwa	75	74	71	490	302	298	45	35	34
Cwb	92	93	89	512	301	294	55	45	46
Cwc	95	102	95	400	293	263	33	17	14
Dfa	111	123	120	424	196	173	36	18	15
Dfb	111	102	94	375	179	165	54	28	30
Dfc	87	79	70	242	130	105	43	31	29
Dfd	90	74	73	207	89	81	32	10	10
Dsa	87	81	82	250	162	151	44	20	16
Dsb	72	68	66	218	139	115	41	21	18
Dsc	73	59	65	223	105	88	33	17	14
Dsd	NA	NA	NA	NA	NA	NA	NA	NA	NA
Dwa	118	139	149	414	231	210	26	12	9
Dwb	118	127	114	372	177	162	27	12	9
Dwc	107	96	89	302	136	119	29	11	8
Dwd	89	77	70	129	95	84	39	18	17
EF	4	4	4	7	5	10	2	1	1
ET	59	53	52	97	87	81	32	21	19

Table XI.2: Mean deficit volumes of droughts, for three selected drought indicators, all climate types, j-factor of 250 days and different soil types, Coarse Sand (CS), Light Silty Loam (LSL), Sandy Loam (SL)(1958-2002).

	TSDI			SVT			QVT		
Climate type	CS	LSL	SL	CS	LSL	SL	CS	LSL	SL
Af	22.8	22.1	21.9	23.7	104	128	26	31.1	31.9
Am	19.9	20.7	20.5	14.5	66.6	77.8	19.5	23.5	26.2
As	15.2	15.6	15.8	13	76.5	102	12.9	14.8	15.4
Aw	14.5	14.8	14.9	13.3	91.4	120	11.9	16.4	16
BWk	1.01	3.57	4.09	0	9.81	14.9	0.0492	$1.47 * 10^{-6}$	$7.2 * 10^{-9}$
BWh	0.759	2.5	2.84	0	2.93	4.26	0.0772	$3.6 * 10^{-5}$	$9.72 * 10^{-7}$
BSk	8.21	6.95	6.22	12.2	89.9	103	3.23	0.47	0.14
BSh	8.32	3.74	3.52	0.193	36.5	44.6	7.01	2.21	0.957
Cfa	12.6	11.7	10.9	11.9	119	161	10.1	15.4	15.7
Cfb	13.4	13.6	15.8	21.2	100	112	7.72	10.3	10.7
Cfc	12.8	13.8	13.7	15.5	33.4	30.8	8.32	10.1	9.88
Csa	15.2	15.9	16.6	29.5	123	168	8.54	12.5	13.5
Csb	15.1	15.1	14.3	22.7	114	142	6.91	10.2	9.72
Csc	5.46	3.97	3.73	10.9	90.3	114	5.69	8.17	5.99
Cwa	19.1	19.3	19	18.5	81.5	97	14.2	19.4	21.3
Cwb	17.8	18	17.7	16.4	68.4	81.4	8.7	11.6	11
Cwc	12.5	10.1	9.97	15.5	74.5	84.7	9.29	11.1	9.34
Dfa	11.3	9.76	9.54	15.4	138	180	6.16	9.84	10.9
Dfb	12.9	14.7	16.2	28.7	187	280	6.02	9.42	10.4
Dfc	17.2	19.5	20.8	49.1	261	344	5.2	7.68	7.86
Dfd	15.5	14	17.8	42.1	304	416	3	3.42	3.33
Dsa	15.7	17	15	33.8	164	208	6.47	9.67	9.92
Dsb	20.1	22.2	20	39.6	213	272	7.25	11.5	10.9
Dsc	21.5	24.3	26.4	53.9	307	449	4.88	7.24	7.51
Dsd	NA	NA	NA	NA	NA	NA	NA	NA	NA
Dwa	9.01	5.66	5.18	1.2	68.1	97.5	7.14	8.16	5.52
Dwb	10.1	8.13	8.01	6.23	133	173	5.85	4.78	4.1
Dwc	10.7	11.7	11.4	12.3	180	235	4.8	5.08	3.98
Dwd	13.6	18.5	21.3	129	270	430	2.93	6.09	6.97
EF	205	229	239	149	893	377	0.0881	0.0951	0.164
ET	23.9	29	30.8	114	216	262	4.91	6.73	7.21

XII Acronyms

ADI	Aggregate Drought Index
ASSM	Accumulated Snow and Moisture Content
BFI	Base Flow Index
CAFEC	Climatically Appropriate For Existing Conditions
CDD	Consecutive Dry Days
CMI	Crop Moisture Index
CPA	Cumulative Precipitation Anomaly
EDI	Effective Drought Index
FT	Fixed Threshold
GHCN	Global Historical Climatology Network
GRACE	Gravity Recovery And Climate Experiment
GRI	Groundwater Resource Index
MAPVT	Moving Average Precipitation with a Variable Threshold
NUT_DAY	Name of the synthetic model
PDSI	Palmer Drought Severity Index
PHDI	Palmer Hydrological Drought Index
Q	Discharge
QVT	Discharge with a Variable Threshold
RAI	Rainfall Anomaly Index
SMDI	Soil Moisture Deficit Index
SPI	Standardized Precipitation Index
SSI	Standardized Streamflow Index
SVT	Soil moisture Content with a Variable Threshold
SWSI	Surface Water Supply Index
TSDI	Total Storage Deficit Index
VIC	Variable Infiltration Capacity
VT	Variable Threshold
WFD	WATCH Forcing Data
Z-index	Palmer Moisture Anomaly Z-index